Flow and Salt Transport in the Suwannee River Estuary, Florida, 1999–2000: Analysis of Data and Three-Dimensional Simulations

By Jerad D. Bales, Stewart A. Tomlinson, and Gina Tillis

Prepared in cooperation with the
Suwannee River Water Management District

Professional Paper 1656-B

U.S. Department of the Interior
U.S. Geological Survey

U.S. Department of the Interior
Gale A. Norton, Secretary

U.S. Geological Survey
P. Patrick Leahy, Acting Director

U.S. Geological Survey, Reston, Virginia: 2006

For product and ordering information:
World Wide Web: http://www.usgs.gov/pubprod
Telephone: 1-888-ASK-USGS

For more information on the USGS--the Federal source for science about the Earth, its natural and living resources, natural hazards, and the environment:
World Wide Web: http://www.usgs.gov
Telephone: 1-888-ASK-USGS

Suggested citation:
Bales, J.D., Tomlinson, S.A., and Tillis, G, 2006, Flow and Salt Transport in the Suwannee River Estuary, Florida, 1999–2000, Analysis of Data and Three-Dimensional Simulations: U.S. Geological Survey Professional Paper 1656-B, 66 p.

Library of Congress Cataloging-in-Publication Data

Bales, Jerad
Flow and Salt Transport in the Suwannee River Estuary Florida, 1999–2000, Analysis of Data and Three-Dimensional Simulations/ Author List
p. cm. –(U.S. Geological Survey professional paper ; 1656-B)
Includes bibliographic references.
1. Subject heading. 2. Subject heading. 3. Subject heading. I. Main entries.
II.Main entries. III. Main entries.
TN24.M9 M55 2002
553'.09786'6—dc21

2001051109

ISBN 0-607-97815-9 (Set)

Preface

Many areas of the United States have experienced water shortages as a consequence of increased water use due to population pressures, industrial growth, and changes in agricultural irrigation practices. As a result of these increasing demands on water resources, many states have established, or are considering, instream-flow protection programs to ensure that the water requirements for ecosystem maintenance will be met. The State of Florida in 1972 adopted legislation directing the water management districts to establish minimum flows and levels (MFLs)for all watercourses, and minimum levels for aquifers and surface waters, in their respective regions. Section 373.042 of the Florida Statutes specifies that a minimum flow for a watercourse is the flow at which further withdrawals would be significantly harmful to the water resources or ecology of the area. Similarly, the Statute defines the minimum level as the level of water in an aquifer, or level of surface water, at which further withdrawals would be significantly harmful to the water resources of the area. The Statute also allows the development of minimum flows and levels using the "best information available" and the recognition of seasonal variation in setting the flows and levels.

The Suwannee River Water Management District (SRWMD) in the north-central part of the State is one of five regional water management districts in Florida. The District's first priority is to set MFLs for the lower Suwannee River, from its confluence with the Santa Fe River to the Gulf of Mexico. The SRWMD began the process for setting MFLs in 1994 with a series of long-term cooperative studies with the U.S. Geological Survey that included data collection, analysis, and interpretation. The USGS program culminated in the completion of three major studies which were conducted to understand the effects that reduced flow in the river could have on the forested floodplain and the mixing of freshwater and saltwater in the estuary, as well as the effects that ground-water withdrawals could have on flows in the river. These studies are reported in Chapters A, B, and C of this Professional Paper 1656 series; additionally, a summary of the program is presented in Chapter D, which includes a discussion of how the results from these three studies can be used collectively by the water management district.

Chapter A of the series describes the hydrology, vegetation, and soils of the forested floodplain of the lower Suwannee River. The chapter goes on to describe the relation of forest types and other floodplain characteristics to long-term river flow, and to estimate potential impacts on the floodplain if river flows were reduced. Chapter B focuses on flow and the mixing of freshwater and saltwater in the lower river and estuary. Salinity and other hydrologic data collected during a period of unusually low flow were used to calibrate a three-dimensional hydrodynamic and transport model that simulates time-varying water levels, currents (lateral, longitudinal, and vertical), and salinity conditions. This chapter includes important discussions of modeled scenarios and hydrologic changes that could result from a reduction of flow in the river. Reductions in streamflow could come from changes in climatic conditions or from direct withdrawal, but may also come from ground-water pumpage adjacent to or many miles from the river. Chapter C presents a discussion of hydrologic conditions governing the interaction between ground water and surface water, an evaluation of the magnitude and timing of water exchanges between the lower Suwannee River and the Upper Floridan aquifer using historical data, and the models that were used to simulate the exchanges. Also presented in this chapter is a discussion of how a hydrologic model could be used to evaluate hypothetical water-use scenarios, and the ground-water and surface-water exchanges that could result from these hypothetical conditions. Chapter D summarizes the cooperative program and highlights the importance of this multidisciplinary program to our understanding of the hydrology in the lower Suwannee Basin – an understanding borne out of an extensive data collection program and complex interpretive studies. Chapter D provides a "roadmap" for water managers to make better use of the integrated results of these studies.

Contents

Figures

Tables

Conversion Factors and Datum

Multiply	By	To obtain
meter (m)	3.281	foot
square kilometer (km^2)	0.3861	square mile
meter squared per second (m^2/s)	10.7639104	foot squared per second
cubic meters per second (m^3/s)	3.281	cubic foot per second

Vertical coordinate information is referenced to the North American Vertical Datum of 1988 (NAVD 88).

Horizontal coordinate information is referenced to the North American Datum of 1983 (NAD 83).

Specific conductance is given in microseiemens per centimeter at 25 degrees Celsius (µS/cm at ˚25 C).

In this report, "sea level" refers to the National Geodetic Vertical Datum of 1929 (NGVD of 1929)—a geodetic datum derived from a general adjustment of the first-order level nets of the United States and Canada, formerly called Sea Level Datum of 1929.

Abbreviations

ADCP	acoustic Doppler current profiler
AVMs	acoustic velocity meters
EDL	electronic data logger
EFDC	Environmental Fluid Dynamic Code model
FDEP	Florida Department of Environmental Protection
FIM	Fisheries-Independent Monitoring program
MLLW	mean lower low water
NDBC	National Data Buoy Center
NGDC	National Geophysical Data Center
NOS	National Ocean Service
psu	practical salinity unit
rkm	river kilometer
RMS	root mean square

Data-Collection Sites

AGR	above Gopher River
WM	West Pass Suwannee River near mouth site
WP	West Pass site
EP	East Pass site
EM	East Pass Suwannee River near mouth site
RB	Gulf of Mexico at Red Bank Reef site
CK	Cedar Key site
KB	Keaton Beach site

Flow and Salt Transport in the Suwannee River Estuary, Florida, 1999–2000: Analysis of Data and Three-Dimensional Simulations

By Jerad D. Bales, Stewart A. Tomlinson, and Gina Tillis

Abstract

A three-dimensional numerical model was developed to assist in the evaluation of the effects of changes in freshwater flow on the salinity regime of the lower Suwannee River, its estuary, and Suwannee Sound. Hydrodynamic and salt-transport modeling were supported by data from a comprehensive data-collection network operated in the lower Suwannee River during 1998–2000. The study area included all of the downstream-most 12 kilometers of the Suwannee River, Suwannee Sound, and part of the Gulf of Mexico. Development, calibration, and application of the hydrodynamic and salt-transport model were completed by using data primarily collected during October 1999–September 2000.

Streamflows at Wilcox, Florida, during much of the study period were at record low levels. New record low monthly mean streamflows were established during 11 months of the 24-month data-collection period. Monthly mean flow was above average only during the first 2 months of the study. During water year 2000, monthly mean flows averaged 35 percent of normal, or about 191 cubic meters per second (m^3/s) lower than normal.

At above Gopher River streamgage, measured flows ranged from 558 to -368 m^3/s (negative indicates flood, or upstream flow) during October 1999 to September 2000. Flows at above Gopher River gage were downstream about two-thirds of the time during October 1999–September 2000, a period of extended and record low flows. Total flows were consistently greater at the West Pass streamgage than at the East Pass streamgage, probably because West Pass has greater storage than East Pass, thereby resulting in a greater tidal prism in West Pass. Net flows were much less variable than total flow. For example, net flows at the East Pass streamgage were between 40 and 70 m^3/s 70 percent of the time during October 1999–September 2000. In contrast to total flows, net flows generally were higher at the East Pass streamgage than at the West Pass streamgage.

Net freshwater flow increased on average 30 m^3/s between Wilcox and above Gopher River streamgage, a reach representing only about 3 percent of the total basin drainage area. This increase was fairly consistent from month to month. An increase in flow downstream from Wilcox where additional drainage is small likely indicates the presence of a substantial contribution of ground water to the river in this reach. The sum of net flows at the East Pass streamgage and the West Pass streamgage (downstream from above Gopher River streamgage) generally was less than the net flow at above Gopher River streamgage, with the average difference during the study period equal to 13 m^3/s. It is possible that some of the flow at above Gopher River streamgage flows south across the marshlands to the Gulf of Mexico rather than returning to the channel during falling tides.

Salinity near the surface (top) at the East Pass gage was less than 1 practical salinity unit (psu) 86 percent of the time during October 1999–September 2000, and was less than 1 psu 77 percent of the time near the bottom. In contrast, salinity at the East Mouth gage (both top and bottom) was greater than 1 psu at least 70 percent of the time. Median salinities at the East Pass, West Pass, and West Mouth gages were less than 2 psu, whereas median salinity at East Mouth gage near the bottom was about 9 psu. Much less difference was noted in salinity between the two sites in West Pass than between the two sites in East Pass. Higher ebb velocities in East Pass, more direct connections between the Gulf and West Pass, and channel geometry likely contributed to the lower upstream migration of salt in East Pass compared to West Pass.

The Environmental Fluid Dynamics Code three-dimensional hydrodynamic and transport model was applied to the study area. The total area encompassed by the model is 1,038.6 square kilometers. The model domain contains 2,385 computational cells in each of 6 horizontal layers, giving a total of 14,310 computational cells.

Measured streamflow at above Gopher River streamgage was used as the upstream boundary condition for the model. A constant flow of 15 m^3/s was added at the east side of East Pass to represent inflows from Dan May Creek and other possible sources. Tidal data collected by the National Ocean Service at Cedar Key were used to construct tidal boundary conditions at all open-water computational cells. Cedar Key tides were shifted in time around the model domain such that the time difference in the arrival of high water at boundary cells between Cedar Key and Horseshoe Point gradually varied from 0 to 15 minutes. Cedar Key tides also were adjusted by -0.05 meter to improve agreement between measured and simulated water levels. Salinity-boundary conditions along the northwestern and southeastern boundaries were assumed to be time-invariant, but did vary horizontally, from 36 psu at the seaward-most computational cell to 20 psu at the shore.

Monthly mean differences between measured and simulated water levels generally were less than 0.2 meter. Measured and simulated amplitudes of the principal diurnal (O1 and K1) and semidiurnal (M2 and S2) harmonics differed by no more than 0.065 meter, and most differed by less than 0.02 meter.

The streamflow amplitude generally was simulated accurately at the East Pass streamgage, but simulated ebb flows were less than measured flows and simulated flood flows were greater than measured. The mean difference between measured and simulated flows was less than 5 percent of the total flow range at the East Pass streamgage during October 1999–September 2000. Simulated streamflows at the West Pass streamgage were less than measured values for both ebb and flood flows. The mean absolute difference between measured and simulated flows for November–December was 6 percent of the total flow range at the site during October 1999–September 2000. Streamflows were simulated quite accurately at site E6, located just upstream from the East Pass-West Pass split, and there was no tendency to over or under simulate flows. There also was good agreement between measured and simulated flows at Wadley Pass and Northern Pass.

Simulated monthly mean salinities at the East Pass gage typically were greater than measured values, with larger differences evident in June and July 2000 than during November–December, 1999. Top simulated salinities agreed more closely with measured values than did bottom salinities. Simulated monthly mean salinities at the East Mouth site agreed very closely with measured values, except for bottom salinities in June–July 2000. Top and bottom simulated maximum salinities that occurred during a tidal cycle were typically less than measured values at both the West Pass and the West Mouth gages, whereas top simulated minimum tidal-cycle salinities were typically greater than measured values. Differences between monthly mean measured and simulated salinities at the Red Bank Reef site were 1 psu or less for November–December 1999, and less than 3 psu for June–July 2000.

The sensitivity of model simulations to changes in selected boundary conditions and model parameters was evaluated by using simulation results from November–December 1999. Simulated flows were unaffected by changes in salinity and wind boundary conditions. Simulated flows and salinities were most sensitive to changes in the bed elevation. Changes in the salinity-boundary conditions did not, however, affect simulated salinities as much as changes in the resistance coefficient or changes in bathymetry.

Bottom elevations for the computational grid near the shore were estimated from navigation charts because digital data were unavailable for these shallow areas. The results of these sensitivity tests indicate the need for accurate bathymetric data, particularly in these shallow regions near the shore where tides, flow, and salinity are strongly affected by bathymetry. Greater resolution of the computational grid in Suwannee Sound might improve salinity simulations in this area, but such refinement would be dependent on better bathymetric data, and computer run times would increase as the number of computational cells increase. Additional improvements in simulations, particularly in Suwannee Sound, require time-varying salinity data on salinity along the model boundaries, and probably data on tidal creek freshwater flows. Inclusion of the saltmarsh area east of East Pass should improve flow and salinity simulations, as well as provide insight into the functioning of the saltmarsh.

Introduction

Estuaries are partially enclosed water bodies that are a transition zone between the freshwater of a river and the saline, tidal environment of the ocean. Estuaries and their associated wetlands provide an extremely productive ecosystem for finfish, shellfish, birds, and other wildlife. For example, more than 95 percent of the commercial fisheries harvested in the Gulf of Mexico are estuarine-dependent (U.S. Environmental Protection Agency, 1999). Estuaries also support human uses, including water supply, wastewater assimilation, recreation, and commercial and sport fishing.

The Suwannee River (fig. 1) is a valuable resource for Florida and supports an estuary of national importance. Water resources of the Suwannee River are under increasing stress from growing water demands and from introduction of nutrients and other contaminants associated with human activities (Berndt and others, 1998). It is reasonable to anticipate that demand for surface- and ground-water in the Suwannee River Basin water will continue to increase, so there is a need to anticipate the effects of changes in riverflow on the river system. In fact, Florida law (Chapter 373.042, Florida Statutes) directs water management districts to establish minimum streamflows and water levels for rivers within their jurisdiction as a tool for managing water withdrawals. This study was conducted by the U.S. Geological Survey (USGS), in cooperation with the Suwannee River Water Management District, to

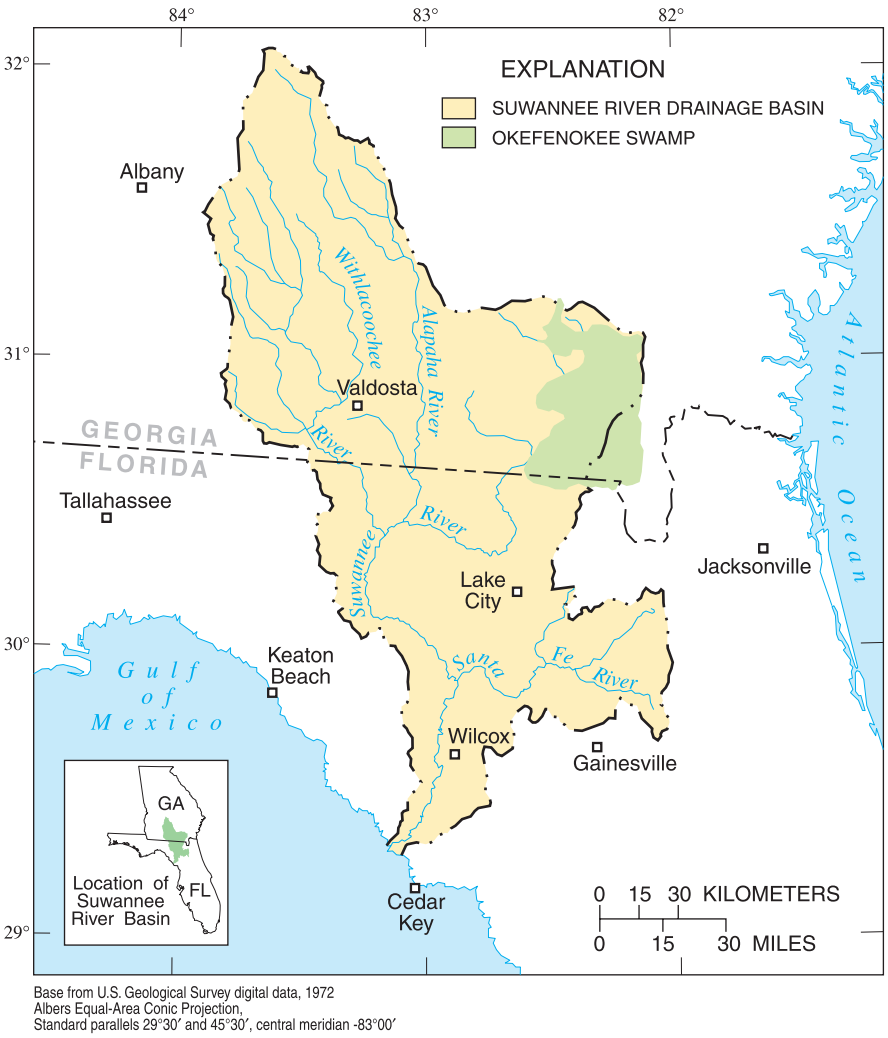

Figure 1. Suwannee River Basin, Florida and Georgia.

provide tools and information that can be used to assist in the establishment of minimum streamflows and water levels for the Suwannee River.

One of the most sensitive areas to changes in flow in the Suwannee River is its estuary, where the balance of fresh and saline water has resulted in a productive ecosystem. The relation between salinity and streamflow in an estuary is difficult to quantify because of variable factors affecting salinity levels. At any given point in the estuary, salinity varies temporally with rising and falling tides, with seasonal changes in sea level and ocean salinity, with regional weather conditions that can generate onshore or offshore flows, and with the natural variations in freshwater flow driven by weather. Salinity at an instant in time also varies from place to place in the estuary. The strongest gradients occur in the longitudinal (upstream to downstream) and vertical (water surface to streambed) directions, but lateral gradients also occur, particularly in wide estuaries.

Humans can influence salinity distributions in an estuary in two primary ways: alterations to the freshwater flow regime and modifications to estuarine morphometry, including channel deepening and construction of structures, such as jetties and groins. Some channel deepening has occurred in the Suwannee River estuary in the past, but the Suwannee is not a major shipping route and little future deepening, other than maintenance of the existing channel, is anticipated. Changes in salinity in response to abrupt alterations in freshwater management (Lepage and Ingram, 1986; Bradley and others, 1990) and in response to gradual increases in freshwater withdrawals (Kjerfve and others, 1996; Boyer and others, 1999) have been documented in numerous other estuaries. The effect of similar changes in freshwater inflows on the Suwannee River salinity regime are unknown, but such changes could have a measurable effect on the ecosystem.

Credible methods are needed for estimating the effects of changes in freshwater flow to the Suwannee River estuary to effectively manage freshwater withdrawals from the river system and to protect the living resources of the Suwannee River estuary. Several approaches have been used in other estuarine systems to predict salinity distributions. Statistical approaches, both regression techniques (Hammett, 1992; Tillis, 2000) and sophisticated time series models (Huang and Foo,

2002), have been used with some success. Statistical models are relatively simple to develop if a good dataset exists, but the models may have poor predictive power, particularly for conditions outside the range of those used to generate the model.

Numerical models that solve the equations of motion and transport for the estuary also have been used to investigate the relation between freshwater flow and salinity. One-dimensional steady (Knowles, 2002) and unsteady (de Vries and Weiss, 2001) models have been used, as have two-dimensional laterally-averaged models (Kurup and others, 1998), two-dimensional depth-averaged models (Goodwin, 1987), and three-dimensional models (Suscy and Morris, 1998; Huang and Spaulding, 2002). Numerical models can be complex to develop and properly calibrate, but a carefully constructed model can be applied to conditions other than those used to develop the model. In addition, a numerical model developed to evaluate effects of changes in flow or salinity can also be used for other purposes, such as estimating flushing times, describing circulation and flow patterns, evaluating effects of bathymetric changes, and providing a foundation for contaminant transport models.

A numerical modeling approach was selected to evaluate the effects of changes in freshwater flow on the salinity regime of the lower Suwannee River and Suwannee Sound. Because the model was to extend from the river out into the Gulf of Mexico, a three-dimensional model was selected. Modeling was supported by data from a fairly comprehensive data-collection network established in the lower Suwannee River.

Purpose and Scope

The purpose of this report is to characterize hydrologic and salinity conditions in the Suwannee River estuary using data collected during 1998–2000, and to document calibration and testing of a three-dimensional hydrodynamic and salt-transport model developed for the estuary and adjacent areas of the Gulf of Mexico. The study area included all of the downstream-most 12 kilometers (km) of the Suwannee River, Suwannee Sound, and part of the Gulf of Mexico (fig. 2). Data collected during October 1998–September 2000 were used to characterize hydrologic and salinity conditions in the Suwannee River estuary. Data collected primarily during October 1999–September 2000 were used for development, calibration, and application of the hydrodynamic and salt-transport model.

The principal purpose for the hydrologic data collection was for construction and testing of the hydrodynamic and transport model. Data included continuous (15-minute interval) measurements of water level at seven sites in the study area (including one National Ocean Service site), flow calculated from velocity and water level at three locations, wind speed and direction at three sites (including two National Oceanic and Atmospheric Administration sites), near-surface and near-bottom salinity at five locations, and middepth salinity at one location in the study area. In addition, discharge was measured at 21 locations throughout the study area during two sets of 3-day synoptic flow measurements, and 53 vertical profiles of water temperature and salinity were measured under a wide range of flow and tidal conditions at 18 sites located in the study area. These data, as well as selected data collected by others in the study area, were used to describe the hydrologic characteristics and salinity regime of the study reach, and to calibrate and apply the hydrodynamic and salt-transport model.

Tidal characteristics of measured water levels are described and compared to available data at nearby tide gages. Characteristics of flow in the Suwannee River estuary are briefly summarized, and measured flows during the study period are compared to long-term conditions. Spatial and seasonal variations in flow are described, and net freshwater flow through the estuary is estimated. Salinity and salinity stratification (difference between simultaneously measured surface and bottom salinity) were characterized as a function of location, season, flow, and tidal conditions.

Flow and salinity distributions in the channels of the Suwannee River estuary were simulated by using a three-dimensional unsteady flow and transport model. The model was calibrated to simulate water level, velocity, flow, and salinity along the length, across, and throughout the full depth of the estuary. The calibrated model was used to simulate

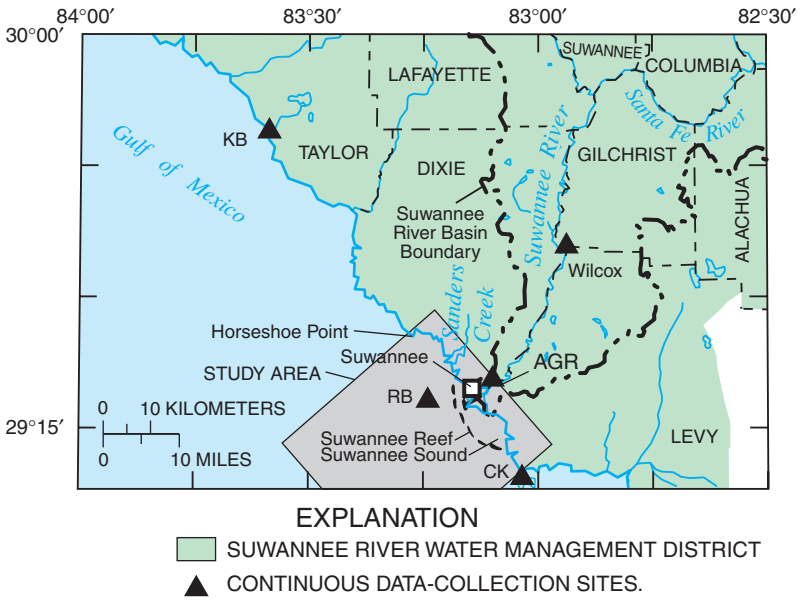

Figure 2. Lower Suwannee River and adjacent areas of Gulf of Mexico, showing selected continuous data-collection sites. Site abbreviations are defined on table 1.

the combined effects of selected freshwater flow, tidal, and meteorological conditions on water level, flow distribution, and salinity.

Results from this investigation have direct relevance to the Suwannee River estuary, a nationally important resource. Understanding gained in this study of the interactions among freshwater flows, tides, and salinity response has relevance to other estuaries throughout the Nation, particularly at a time when competing demands for water are increasing. Resource managers are becoming increasingly sensitive to the need to maintain instream flows and hydrologic variability to protect living aquatic resources.

Setting

The Suwannee River drains a 25,770-square kilometer (km^2) basin in central southern Georgia and central northern Florida. Average streamflow for 1931, 1941–2003 at the downstream-most long-term streamgaging station (Suwannee River near Wilcox, Florida, USGS station number 02323500; fig. 2) is 287 m^3/s; an additional 720 km^2 drains into the river between this streamgaging station and the mouth of the river. Streamflows typically are lowest in November and December, and highest in March and April (fig. 3).

The Suwannee River estuary consists of the lower reach of the Suwannee River, the delta at the mouth of the river, and the coastal area of the Gulf of Mexico between Horseshoe Point and Cedar Key (Orlando and others, 1993). Most of the estuary consists of Suwannee Sound, which is bounded on the seaward side by the Suwannee Reef (Orlando and others, 1993; fig. 2). Mattson and Krummrich (1995) defined the estuary as extending 11–15 km upstream from the mouths of East and West Passes. Orlando and others (1993) defined the upstream terminus of the estuary as being at the head of tide, which has been identified as being 29 and 53 km from the mouth of the river, respectively, by the National Ocean Service, (1985) and Mattson and Rowan (1989). The latter distance (53 km) coincides with the USGS streamgage near Wilcox (fig. 2), where backwater effects from tides affect streamflows at low flows. For this report, the upstream boundary of the Suwannee River estuary is defined as the upstream limit of saltwater intrusion under non-surge conditions, which is about 12 km upstream from the mouth of West Pass, or rkm 12 (river kilometer 12).

A river delta has formed at the mouth of the Suwannee River as a result of the low-slope coastal shelf and freshwater discharge from the river (Siegel and others, 1996); no barrier islands are present offshore from the mouth of the river. East Pass, which meanders in a southerly direction toward the Gulf of Mexico, is about 100 meters (m) wide and typically 6 m deep. West Pass is about 275 m wide and typically 3 m deep. Less than 1.6 km downstream from the town of Suwannee, West Pass subdivides into Northern Pass, Alligator Pass, and Wadley Pass. The width of Alligator Pass ranges between about 250–400 m; water depths are typically 1–2 m at high tide. Northern Pass is about 150 m wide, and 1–2 m deep at high tide; Wadley Pass is only slightly wider than Northern Pass and typically 2 m deep at high tide. A 1.3-m deep channel has been dredged from the seaward side of the Suwannee Reef through Wadley Pass to the confluence of Wadley Pass and West Pass (National Oceanic and Atmospheric Administration, 1998).

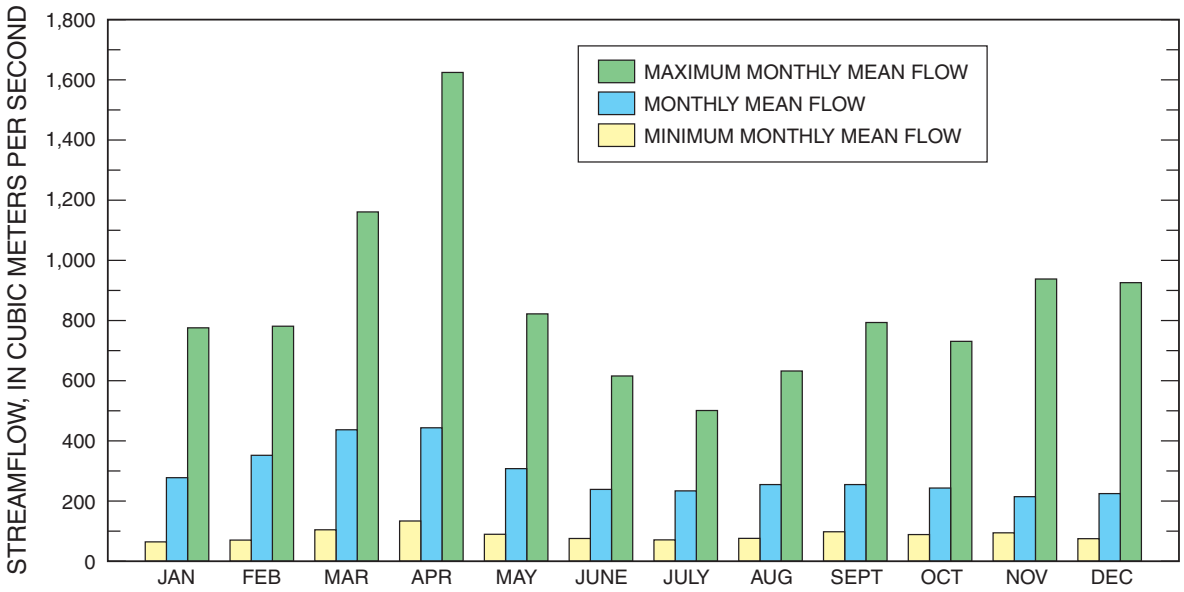

Figure 3. Monthly mean, minimum, and maximum streamflow at Suwannee River near Wilcox, Florida, 1931, 1941–2003.

The seabed in Suwannee Sound is about 0.6–2.1 m below mean lower low water (MLLW; National Oceanic and Atmospheric Administration, 1998), or about 1.5–3 m deep at mean high tide. MLLW elevation is 0.692 m below NAVD 88 at Cedar Key and mean high tide elevation is 0.363 m above NAVD 88 (National Oceanic and Atmospheric Administration, 2003). Seaward of Suwannee Reef, water depths gradually increase, so that 20 km west of West Pass, water depths are about 6–7 m at high tide.

A number of investigations of flow and salinity have been conducted in the lower Suwannee River, with one of the earliest systematic studies reported by Leadon (1979). Important aspects of many of the studies were summarized by Light and others (2002) and Tillis (2000). Results from previous investigations are presented throughout this report for comparison with findings from this study.

Acknowledgments

The authors gratefully acknowledge the data collection, the thoughtful and discerning comments on Suwannee River issues, and the support provided by Mr. John Good, Mr. Rob Mattson, and Mr. Tom Mirti of the Suwannee River Water Management District. Thorough and insightful reviews of the report draft provided by Dr. Earl Hayter, U.S. Environmental Protection Agency; Dr. Pete Sucsy, St. Johns River Water Management District; and Mr. John Good, Suwannee River Water Management District, contributed greatly to the quality of the report and are appreciated. Dr. John Hamrick, Tetra-Tech, provided assistance on initial implementation of EFDC; and Dr. Dudley Benton, Dynamic Solutions, assisted in creation of the computational grid. Support by Tallahassee USGS Water Science Center staff for their data collection, data processing, and report production is thankfully acknowledged.

Methods

This section describes data-collection methods for the study. An overview also is given of the hydrodynamic and salt-transport model that is applied to the Suwannee River estuary. Methods used in the actual implementation of the model are provided in a subsequent section.

Data Collection

The primary purpose of the data collection was to support development and testing of the Suwannee River estuary model. Data collection consisted of continuous hydrologic data (water level, discharge, wind, and salinity) and synoptic measurements of discharge and salinity by the USGS, and continuous water-level and wind measurements by National Oceanographic and Atmospheric Administration (NOAA). Some bathymetric data were collected by the USGS, but most were obtained from NOAA.

Continuous Data Collection

The USGS data-collection network for this study included five fixed sites located in the downstream-most 12 km of the Suwannee River (table 1, fig. 4) and one fixed site in the Gulf of Mexico about 8.5 km west-northwest of the mouth of Alligator Pass (table 1, fig. 4). Data at the USGS sites were collected more or less continuously between October 1998–September 2000, except at the AGR site (table 1, fig. 4) where collection began in June 1999.

At the five fixed sites in the lower Suwannee River, sensors were connected to an electronic data logger (EDL) through a serial-digital interface housed in a metal shelter above the water. The shelter was attached to a 12-m-long concrete piling, which was driven to refusal in the streambed about 6–9 m from the bank (fig. 5) At the Gulf of Mexico Red Bank Reef site (RB, fig. 2), data were collected by an internal EDL in a multiparameter sensor attached to an existing aid-to-navigation marker.

Water-level data were collected by the USGS at six sites (table 1; fig. 4) In this report, these sites are referred to as EP (East Pass), EM (East Pass, Suwannee River, near its mouth), WP (West Pass), WM (West Pass, Suwannee River, near its mouth), AGR (Suwannee River above its confluence with Gopher River), and RB (Red Bank reef in the Gulf of Mexico). Water levels were measured at 15-minute intervals by using a submersible pressure transducer set to an arbitrary datum. At all sites other than RB, which was located offshore, datum corrections were applied during data processing in order to reference water levels to the National Geodetic Vertical Datum (NGVD) of 1929. Datums were determined from standard land surveys and differential global positioning system surveys performed by the USGS and the State of Florida Department of Environmental Protection (FDEP).

Water-level data measured at Cedar Key (National Ocean Service site 8727520) were obtained from the National Ocean Service (NOS) for use in this investigation (National Oceanic and Oceanographic Administration, 2003). Water levels were measured at 6-minute intervals and reported in meters relative to several different datums.

Acoustic velocity meters (AVMs) were used at sites AGR, WP, and EP to measure flow velocity at 15-minute intervals. The AVMs measured the average velocity in a representative volume having the shape of a conical frustum above the face of the instrument. The lower face of the frustum, which was parallel to the face of the AVM and had a diameter of 1.0 m, was located 0.5 m from the face of the AVM, and the upper face with a diameter of 4.0 m was 2.0 m above and parallel to the face of the AVM. The vertical axis of the conical frustum was aligned with the vertical axis of the AVM. The average velocity measured by the AVM is referred to as the “index velocity.”

Ratings were developed to compute discharge at 15-minute intervals from measurements of index velocity and water level. First, a stage- cross-sectional area relation (for example, fig. 6) was developed for each AVM site from channel cross-sectional surveys at the AVM location. The stage-area relation allows continuous measurements of water level to be used to estimate the corresponding flow area. Second, measurements of discharge were made at each site by using an acoustic Doppler current profiler (ADCP) over a range of flows, during both ebbing and flooding flows. Methods for application of the ADCP are described by Simpson (2002). A total of 95 sets of discharge measurements were made at AGR; 72 were made at WP; and 133 were made at EP in order to develop the relation between cross-sectional averaged flow velocity and the index velocity at each site. Measurements were made throughout the tidal cycle (fig. 7).

A cross-sectional mean velocity was then calculated for each discharge measurement, and a relation was developed between cross-sectional mean velocity and the simultaneously measured index velocity for each site (fig. 8). Fifteen-minute interval discharge records were computed by multiplying cross-sectional area (determined from the stage-area relation) by the cross-sectional mean velocity (determined from the mean velocity-index velocity rating). The index velocity method for computing discharge is described by Morlock and others (2002).

Water temperature and specific conductance were measured at 15-minute intervals at all six USGS fixed sites in the study area (fig. 4, table 1). Salinity was calculated from the specific conductance and temperature readings by using published algorithms (American Public Health Association and others, 1992). Instruments were serviced at approximately monthly intervals following protocols similar to those given by Wagner and others (2000). Vertical profiles of water temperature and specific conductance were measured at approximately 1 m intervals at the gage site whenever instruments were serviced. In addition, several sets of measurements were made to define the cross-sectional distribution of salinity under different conditions at selected sites (table 2, sites designated VLP, vertical/lateral profiles).

Table 1. Continuous data-collection sites.

[NGVD 29, National Geodetic Vertical Datum of 1929; USGS; U.S. Geological Survey; WL, water level; V, velocity; Q, discharge; WT, water temperature; SC, specific conductance, WSD, wind speed and direction; NA, not applicable; NDBC, National Data Buoy Center; NOS, National Ocean Service]

Station name	Station abbreviation	Station number (agency)	Latitude	Longitude	Suwannee River kilometer	Period of record	Data	Water-level gage datum (meters; NGVD 29)	Elevation of salinity sensors (meters, NGVD 29)		
									Top	Mid-depth	Bottom
Suwannee River above Gopher River near Suwannee	AGR	02323592 (USGS)	29° 20' 19"	83° 03' 13"	12.2	1999–continuing	WL, V[1], Q, WT, SC	-0.64	-0.59	NA	-3.05
West Pass Suwannee River at Suwannee	WP	291930083082800 (USGS)	29° 19' 30"	83° 08' 28"	4.5	1995–2000	WL, V, Q, WT, SC, WSD	-1.41	-0.85	NA	-4.50
West Pass Suwannee River near mouth near Suwannee	WM	291842083085100 (USGS)	29° 18' 42"	83° 08' 51"	3.1	1995–2000	WL, WT, SC	-1.61	-0.92	-1.58	-1.99
East Pass Suwannee River near Suwannee	EP	291841083070800 (USGS)	29° 18' 41"	83° 07' 08"	6.1	1995–2000	WL, V, Q, WT, SC	-0.81	-0.62	NA	-3.97
East Pass Suwannee River at mouth near Suwannee	EM	291652083064100 (USGS)	29° 16' 52"	83° 16' 41"	1.9	1995–2000	WL, WT, SC	-1.33	-0.49	-1.62	-2.86
Gulf of Mexico at Red Bank Reef	RB	291912083154800 (USGS)	29° 19' 12"	83° 15' 48"	NA	1999–2000	WL[2], WT, SC	NA	NA	NA	NA
Cedar Key	CK	CDRF1 (NDBC)	29° 08' 10"	83° 01' 45"	NA	1995–continuing	WSD	NA	NA	NA	NA
Cedar Key	CK	8727520 (NOS)	29° 08' 06"	83° 01' 54"	NA	1914–continuing	WL	NA	NA	NA	NA
Keaton Beach	KB	KTNF1 (NDBC)	29° 49' 02"	83° 35' 30"	NA	1995–continuing	WSD	NA	NA	NA	NA

[1]Velocity data collection began in 1999.
[2]Water level at this site was not referenced to any datum.

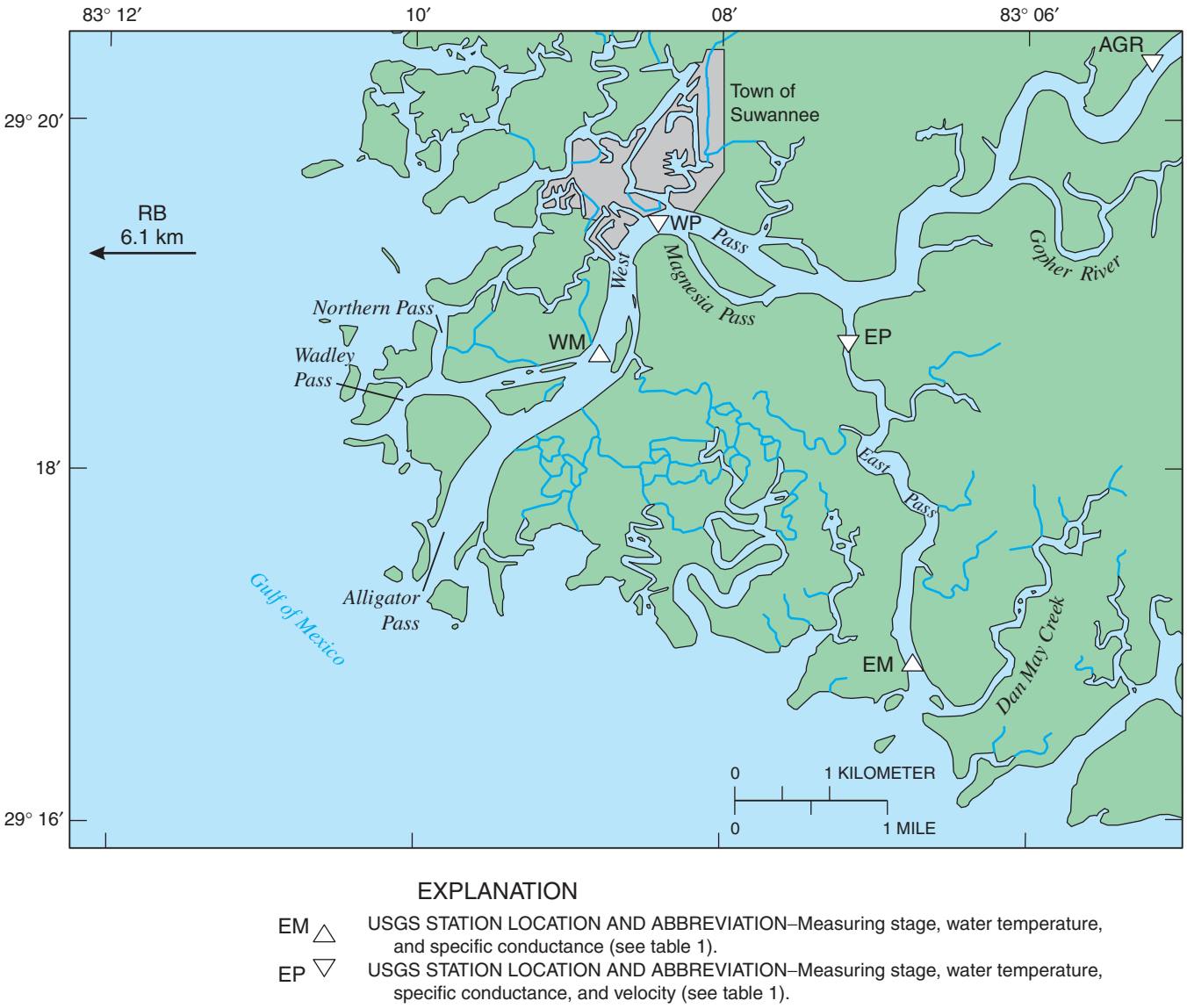

Figure 4. Continuous data-collection sites in the downstream-most 12 kilometers of the Suwannee River.

Water temperature and specific conductance were measured at approximately mid-depth at the two West Pass and the two East Pass sites beginning in 1995. Near-surface and near-bottom sensors were added at EP and WP in March 1999, and the mid-depth sensors were removed in April 1999. Near-surface and near-bottom sensors were added at EM and WM in June 1999, and the mid-depth sensors were left in place through the end of the study (September 2000). Near-surface and near-bottom water temperature and specific conductance were measured at AGR, and water temperature and specific conductance were measured at one location in the water column at RB throughout the respective periods of record at those sites.

Wind speed and direction were measured at WP by the USGS (table 1; fig. 4). The anemometer was about 10 m above the water surface. Average readings over 15-minute intervals were recorded. Hourly wind speed and wind direction also were obtained from sites at Keaton Beach (KB; fig. 1; National Buoy Data Center, 2003a) and Cedar Key (CK; fig. 1; National Buoy Data Center, 2003b). Other meteorological data were available from these sites but were not used in the study.

Figure 5. Data-collection structure at the Suwannee River above Gopher River data-collection site.

Field Measurements

Three general types of field measurements were made by the USGS during the study: measurements made in support of continuous streamgage operation, special measurements made synoptically at multiple sites throughout the downstream-most 12 km of the Suwannee River, and miscellaneous measurements made to address site-specific issues. The field measurements made in support of continuous data collection—vertical profiles of water temperature and conductance at the site, and discharge measurements for streamflow ratings—were previously described.

Vertical profiles of water temperature and specific conductance were measured synoptically at 17 locations in the lower Suwannee River (table 2, sites labeled VP, with exception of WP and EP; fig. 9). A full set of measurements were made on 53 occasions between November 24, 1998, and September 26, 2000. At each site, measurements were made in the deepest part of the channel at about 0.6-m vertical intervals from the channel bottom to the water surface. Standard USGS protocols for field measurements were followed (Wilde and others, 1998). Measurements were made during the full range of tidal conditions (fig. 10).

Synoptic discharge measurements made in December 1999 and May-June 2000 provided "snapshots" of flow distribution in the estuary. A total of 20 sites were measured during the two synoptic discharge measurement periods (table 2). During December 14-16, 1999, a total of 411 discharge measurements at 16 cross sections were made when streamflow at Wilcox (fig. 2) was about 98 m^3/s (fig. 11A).

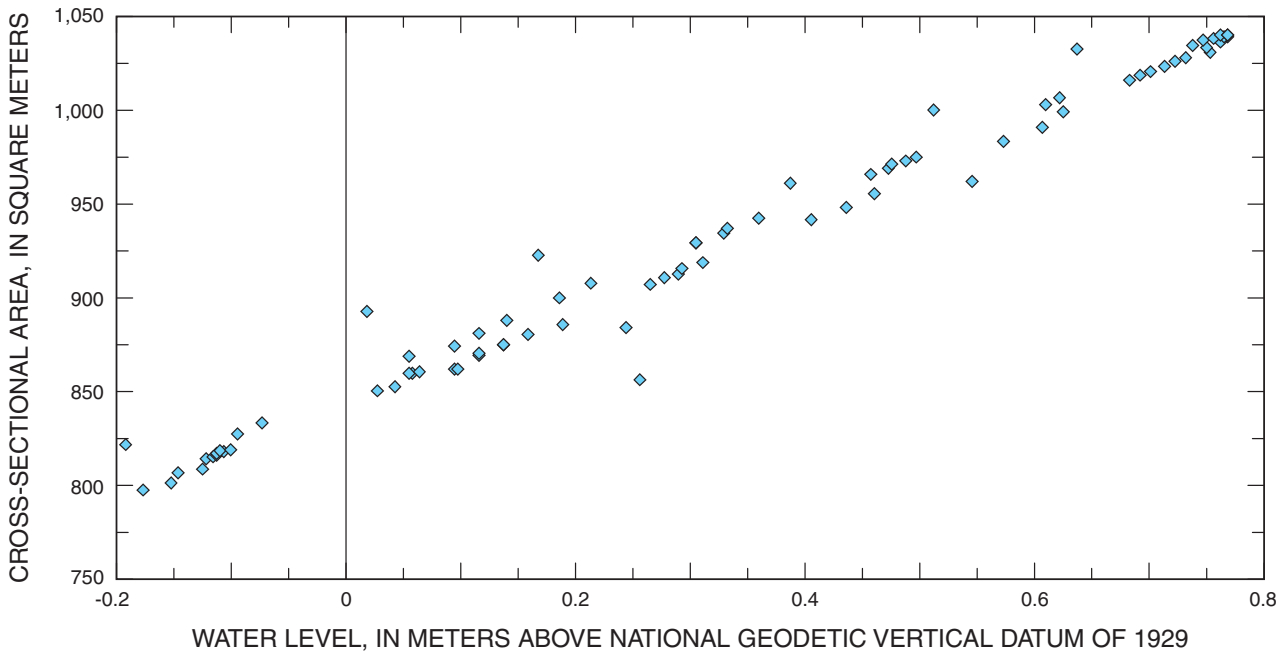

Figure 6. Stage-area data for the Suwannee River above Gopher River site.

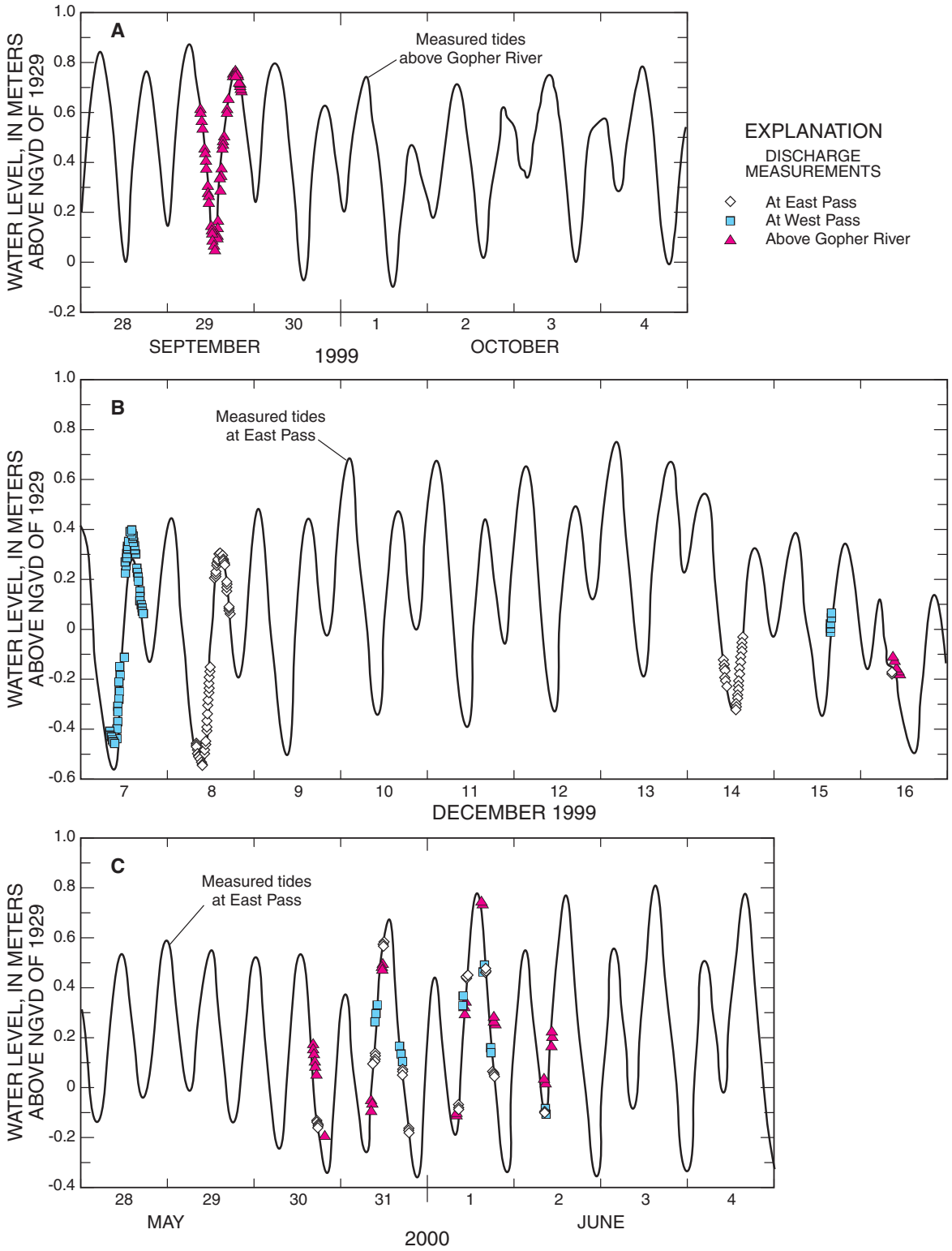

Figure 7. Tidal conditions during which discharge measurements were made from (A) September 28-October 4, 1999; (B) December 7-16, 1999; and (C) May 28-June 4, 2000.

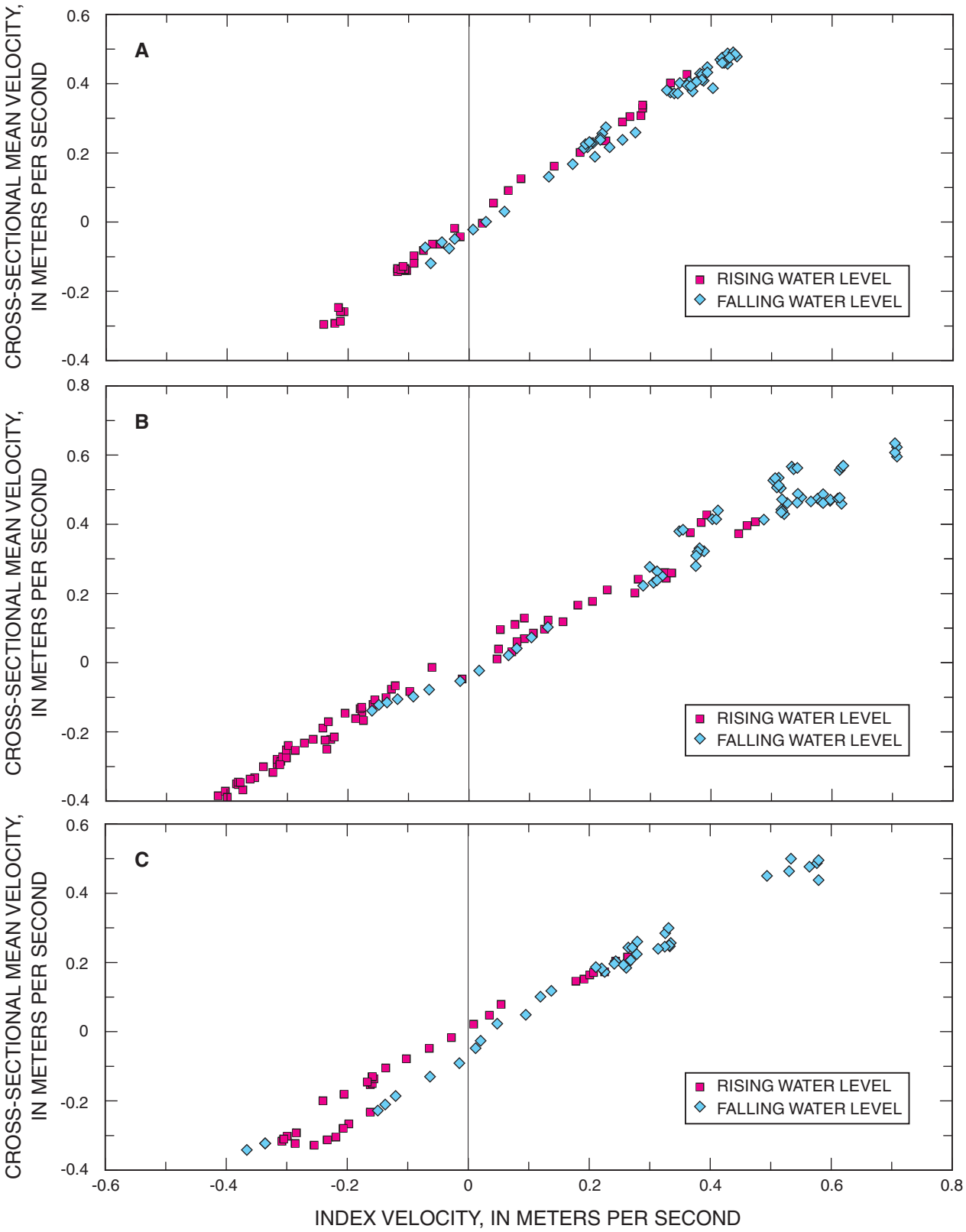

Figure 8. Mean velocity-index velocity ratings for (A) above Gopher River, (B) East Pass, and (C) West Pass sites.

Table 2. Field measurement sites.

[Q, field measurements of discharge, December 1999 and May–June 2000 (sites shown in fig. 11); VP, vertical profiles of temperature and specific conductance, November 1998–September 2000 (sites shown in fig. 9); VLP, vertical and lateral profiles of temperature and specific conductance, March–September 2000 (sites shown in fig. 11)]

Location	Station abbreviation	USGS station number	Latitude	Longitude	Data
Suwannee River above Gopher River	AGR	02323592	29° 20′ 19″	83° 03′ 13″	Q, VLP
Suwannee River at Gopher River	G1	291937083061300	29° 19′ 37″	83° 06′ 13″	Q, VP
Suwannee River above East Pass	E6	291901083070300	29° 19′ 01″	83° 07′ 03″	Q, VP
West Pass, upstream from head of Magnesia Pass	W9	291903083071800	29° 19′ 03″	83° 07′ 18″	Q
West Pass between head and outlet of Magnesia Pass	W8	291911083074800	29° 19′ 11″	83° 07′ 48″	Q, VP
Magnesia Pass near outlet	Q2	291911083081000	29° 19′ 11″	83° 08′ 10″	Q
West Pass above Demory Canal	Q3	291925083081800	29° 19′ 25″	83° 08′ 18″	Q
Demory Canal near head	Q4	29192208383600	29° 19′ 22″	83° 08′ 36″	Q
West Pass, Suwannee River	W7	291919083083500	29° 19′ 19″	83° 08′ 35″	VP
West Pass at gage	WP	291930083082800	29° 19′ 30″	83° 08′ 28″	Q, VP, VLP
West Pass below head of Suwannee Canal	W6	291853083084200	29° 18′ 53″	83° 08′ 42″	Q, VP
West Pass, Suwannee River	W5	291833083085100	29° 18′ 33″	83° 08′ 51″	VP
West Pass at West Mouth gage	WM	291842083085100	29° 18′ 42″	83° 08′ 51″	Q, VP, VLP
Wadley Pass below West Pass	W4	291830083092600	29° 18′ 30″	83° 09′ 26″	Q, VP
Cut between Alligator Pass and Wadley Pass	Q5	291821083093300	29° 18′ 21″	83° 09′ 33″	Q
Cut upstream from Wadley and Northern Pass split	Q6	291827083094300	29° 18′ 27″	83° 09′ 43″	Q
Northern Pass	Q7	291833083093300	29° 18′ 33″	83° 09′ 33″	Q
Wadley Pass	Q8	291826083095900	29° 18′ 26″	83° 09′ 59″	Q
Wadley Pass near mouth	W1	291811083102200	29° 18′ 11″	83° 10′ 22″	VP
Alligator Pass, Suwannee River	W3	291814083091900	29° 18′ 14″	83° 09′ 19″	VP
Alligator Pass, Suwannee River	W2	291739083094300	29° 17′ 39″	83° 09′ 43″	VP
Alligator Pass outlet	Q9	291806083093100	29° 18′ 06″	83° 09′ 31″	Q
East Pass at gage	EP	291841083070800	29° 18′ 41″	83° 07′ 08″	Q, VP, VLP
East Pass, Suwannee River	E5	291828083065900	29° 18′ 28″	83° 06′ 59″	VP
East Pass, Suwannee River	E4	291802083065200	29° 18′ 02″	83° 06′ 52″	VP
East Pass, Suwannee River	E3	291728083064600	29° 17′ 28″	83° 06′ 46″	VP
East Pass, Suwannee River below Bull Creek	Q10	291726083064700	29° 17′ 26″	83° 06′ 47″	Q
East Pass above East Mouth gage	E2	291707083064800	29° 17′ 07″	83° 06′ 48″	VP
East Pass at East Mouth gage	EM	291652083064100	29° 16′ 52″	83° 06′ 41″	Q
Dan May Creek at mouth	Q11	291638083062400	29° 16′ 38″	83° 06′ 24″	Q
East Pass near mouth	E1	291636083064600	29° 16′ 36″	83° 06′ 46″	VP
Gulf of Mexico at Buoy 1	B1	291836083120200	29° 18′ 36″	83° 12′ 02″	VP

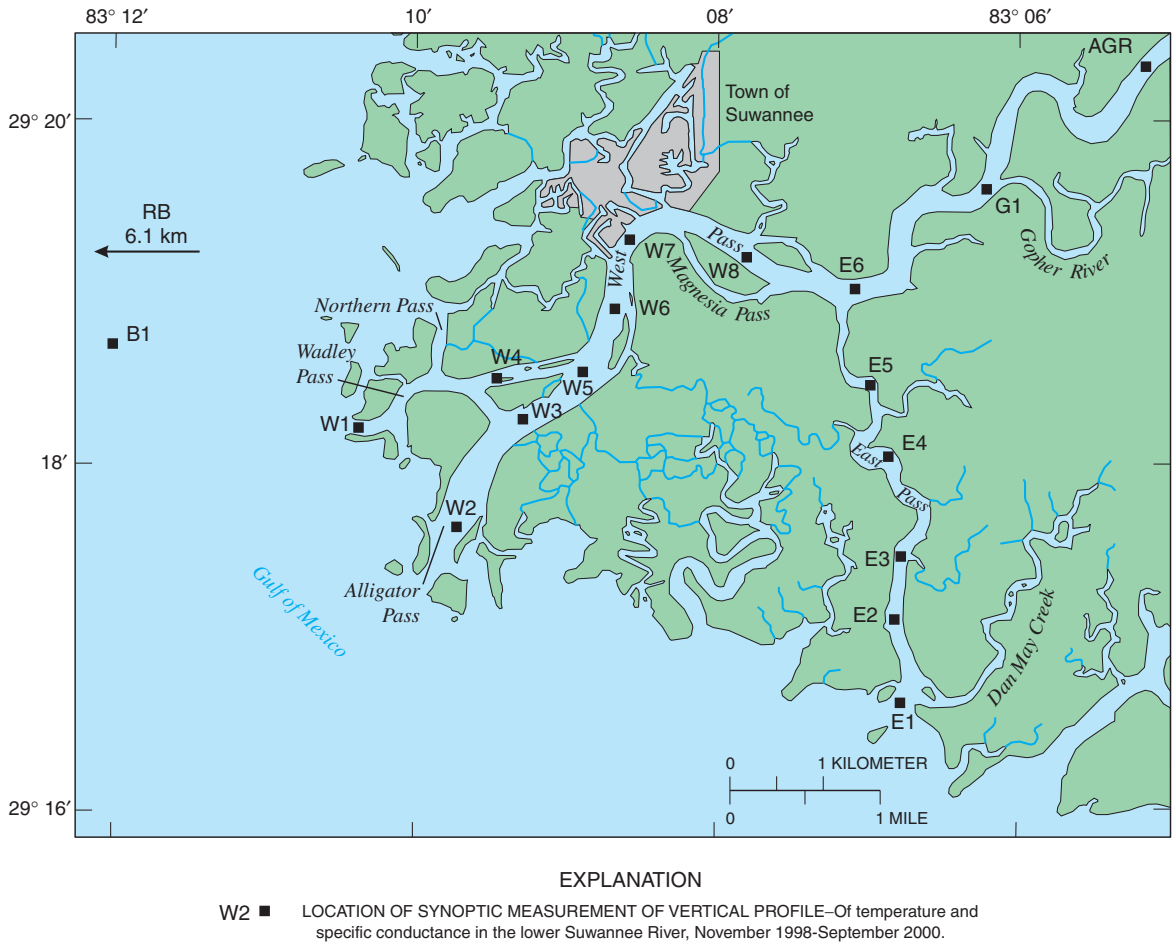

Figure 9. Locations of synoptic measurements of vertical profiles of temperature and specific conductance in the lower Suwannee River, November 1998–September 2000.

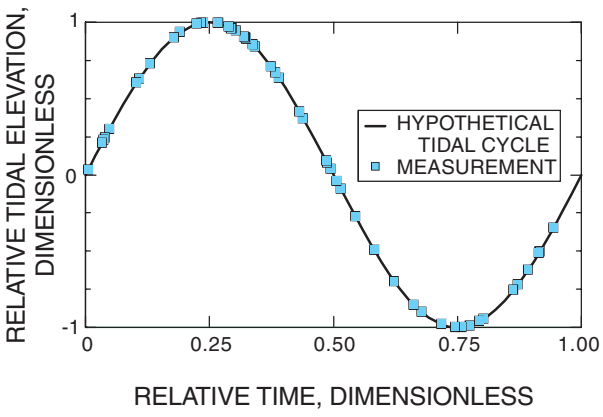

Figure 10. Generalized tidal conditions during which synoptic measurements of specific conductance and water temperature were made in the lower Suwannee River, November 1998–September 2000.

During May 30 to June 2, 2000, a total of 488 measurements were made at 17 cross sections when streamflow at Wilcox was about 73 m^3/s (fig. 11B). Some of these cross sections differed from those measured during December 1999.

Bathymetry

Bathymetric data were obtained from a limited number of USGS measurements in the river and from NOS databases. Water depth was recorded by the USGS during measurement of the vertical profiles of temperature and specific conductance at the 16 mid-channel measurement locations (fig. 9). Water depth also was recorded along the boat path during ADCP discharge measurements (fig. 11); depth was measured by one of the transducers on the ADCP.

Most of the bathymetric data were obtained from NOS databases. Coastline data were obtained from the NOAA National Geophysical Data Center (NGDC) online Coastline

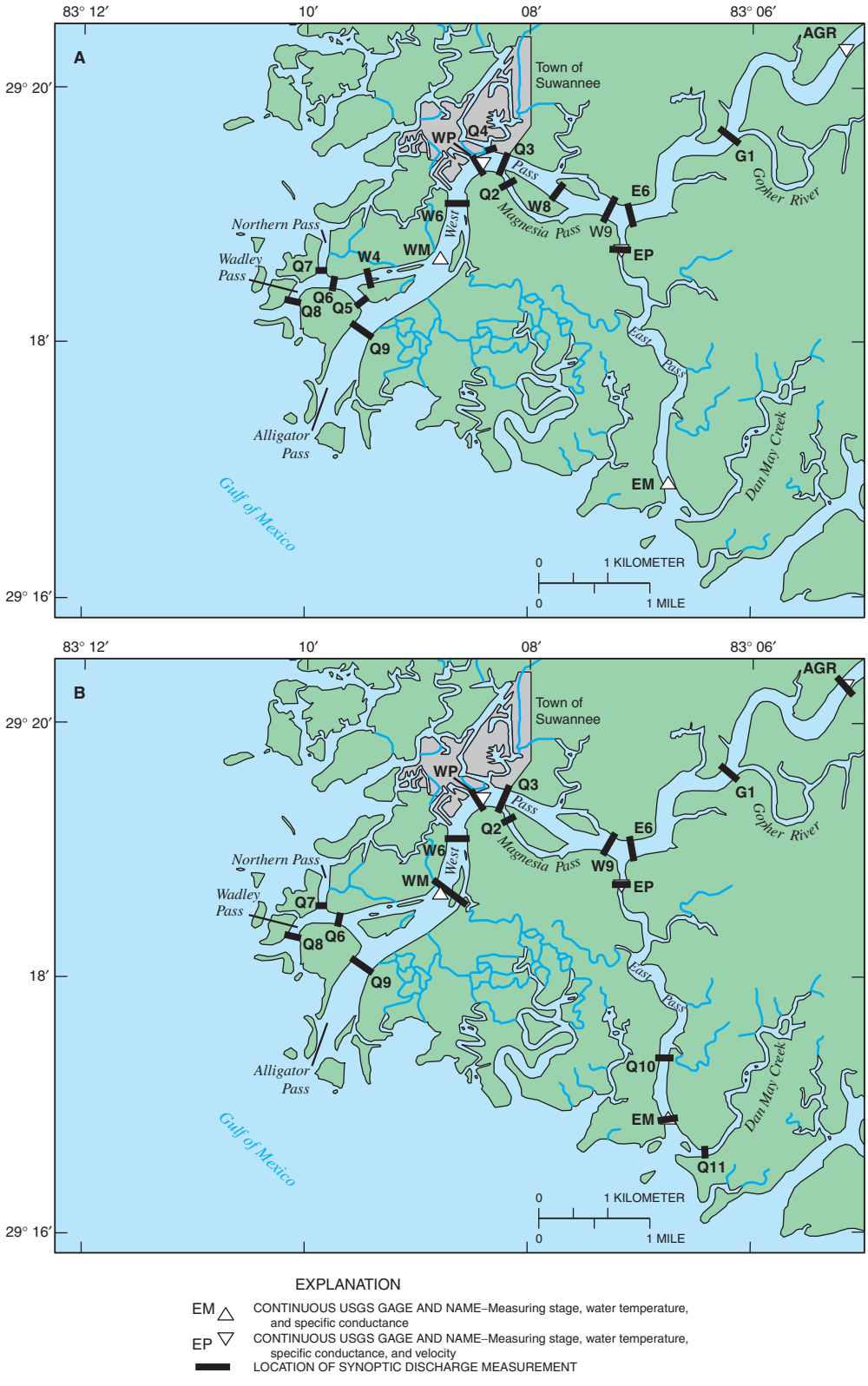

Figure 11. Locations of synoptic measurements of discharge in the lower Suwannee River: (A) December 14–16, 1999; and (B) May 30–June 2, 2000.

Extractor (National Oceanic and Atmospheric Administration, 2001a). Data were provided as horizontal coordinates of the shoreline in the Albers projection. Hydrographic survey data also were obtained online from NGDC (National Oceanic and Atmospheric Administration, 2001b). Horizontal coordinates were provided as both latitude-longitude and horizontal coordinates in the Albers projection. The most recent hydrographic data were from surveys completed in 1976. The NGDC software package GEODAS (National Geophysical Data Center, 2004) was used to view the bathymetric data and to perform some initial processing. A geographic information system was used to create a smooth surface from the bathymetric data points; the surface was subsequently sampled to provide depths at 50-m and 100-m grid spacings.

NOAA surveys did not include much of the shallow areas within 2–5 km of the shoreline. Bathymetric data for these areas were obtained from NOS Chart No. 11408 (National Oceanic and Atmospheric Administration, 1998).

Flow and Transport Modeling

A three-dimensional, unsteady numerical model was used to simulate hydrodynamics and salt transport in the study area. The Suwannee River exhibits large vertical and longitudinal gradients in salinity, although lateral gradients are small. Because the model domain extended into the Gulf of Mexico where longitudinal, vertical, and lateral gradients in salinity and the flow field are present, a fully three-dimensional model was appropriate for this application.

The Environmental Fluid Dynamics Code (EFDC) three-dimensional hydrodynamic and transport model was applied to the study area. This particular model was selected for several reasons. Out of 13 three-dimensional hydrodynamic models that Walton and others (1998) reviewed for potential application to the Duwamish River-Elliott Bay system in Seattle, Washington, the EFDC model was selected primarily because of the comprehensive nature of the model (including the capability for water-quality simulations), open architecture, and nonproprietary availability. All of these attributes also apply to the Suwannee River estuary. Although Walton and others (1998) applied the EFDC model to their study, they noted that the model did not have a Windows-based graphical shell for model setup, execution, and analysis of results. EFDC has been successfully applied to many water bodies, including several in Florida, with applications to wind and thermal-driven circulation in Lake Okeechobee (Jin and others, 2000, 2002), and tidal circulation and salt transport in Indian River Lagoon (Moustafa and Hamrick, 1993; Suscy and Morris, 1998) and Florida Bay (Tetra Tech, Inc., 2003). EFDC also is supported by the U.S. Environmental Protection Agency (2004), and its executable code can be obtained from their Watershed and Water Quality Modeling Technical Support Center website.

The following description of EFDC (Hamrick, 1992) was given by Moustafa and Hamrick (1993):

> "EFDC solves the vertically hydrostatic, free surface, variable density, turbulent averaged equations of motion and transport equations for turbulent kinetic energy and macroscale, salinity and temperature in a stretched, (sigma) vertical coordinate system, and horizontal coordinate systems which may be Cartesian or curvilinear-orthogonal. The code uses a three time level, finite difference scheme with an internal-external mode splitting procedure to separate the internal shear or baroclinic mode from the external free surface gravity wave or barotropic mode..... The implicit external solution allows large time steps which are constrained only by the stability criteria of the explicit advection scheme used for nonlinear accelerations. The vertical diffusion coefficients for momentum, mass, and temperature are determined by the second moment closure scheme of Mellor and Yamada (1982). Other features of the code include additional transport equations for conservative and nonconservative tracers and suspended sediment."

The model also has algorithms to simulate wetting and drying within the model domain (Ji and others, 2001). A graphical user interface, EFDC_Explorer, was recently developed for EFDC (Craig, 2004). The interface has some capabilities for grid construction and offers a graphical user interface to build model input. The post-processor allows model results to be extracted from any computational cell, and for those results to be plotted and saved to external files. EFDC_Explorer was used in this study for post-processing model results, but was not used for pre-processing. Model results extracted by using EFDC_Explorer were compared with results printed directly from EFDC to separate files to ensure compatibility of results.

Hydrologic Conditions, 1998–2000

Flow and salt transport in the Suwannee River estuary are governed by a number of highly variable factors, including flows, tides, wind, and channel morphometry. This section provides an overview of hydrologic conditions in the estuary during the study period. Freshwater delivery to the estuary is first described by using data measured at the long-term streamgage at Wilcox (fig. 2). Tidal conditions in the Gulf of Mexico and the Suwannee River estuary are subsequently described by using data from USGS and NOS water-level gages. Flows in the estuary are characterized by using continuous data from three streamgages and synoptically collected

discharge data at 21 locations in the study area. Finally, salinity conditions in the estuary are summarized using data from six continuous monitors and vertical profiles measured throughout the estuary during the study period, as well as selected data collected by others.

Freshwater Flow

Streamflow has been measured continuously at the Suwannee River at Wilcox since 1941. The drainage area at the Wilcox streamgage is 25,048 km^2, which is 97 percent of the total Suwannee River Basin drainage area. Prior to December 9, 1999, discharge at the streamgage was computed by using a complex relation among stage, water-surface slope, and flow. Subsequently, discharge has been computed by using the index-velocity method that was used at the AGR, EP, and WP sites.

Flows less than about 450 m^3/s at Wilcox are affected by tides in the Gulf of Mexico (fig. 12). Consequently, because tides have a period of about 24.8 hours, daily (24 hour) mean flows should not be calculated directly from measured total flows. Instead, the tidal effects can be removed from the record by using a low-pass filter on the 15-minute data (Godin, 1972; Walters and Heston, 1982; Dijkzeul, 1984), and daily mean net flows can then be calculated from these filtered flows. The following discussion of flows in which total flows during the study period are compared with historical total flows, however, is based on 24-hour mean flows at Wilcox because historical flows at that site have all been calculated as 24-hour means.

Monthly mean discharge at Wilcox for the period of record (October 1930–September 1931; October 1941–September 2000) varied from 216 m^3/s in the dry season (November) to 444 m^3/s in the wet season (April). The maximum monthly mean discharge was 1,623 m^3/s in April 1948, and the lowest monthly mean discharge was 69 m^3/s in July 2000. (A new record low of 61 m^3/s was established in January 2002 after the completion of this study.) The annual mean discharge for the period of record was 287 m^3/s, ranging from 696 m^3/s in 1948 to 96 m^3/s in 2000. The highest recorded daily mean discharge was 2,406 m^3/s (April 14, 1948); the lowest was 56 m^3/s (July 16, 2000), which occurred during this study. (A new record low of 30 m^3/s was established on February 6, 2002, after the completion of this study.)

Streamflows during much of the study period were at record low levels (fig. 13). New record low monthly mean streamflows were established during 11 months of the 24-month data-collection period, with April being the only calendar month for which a new record low was not set. Monthly mean flow was above average only during the first 2 months of the study. During water year 2000, monthly mean flows averaged 35 percent of normal, or about 191 m^3/s lower than normal. The drought of 1999–2000 continued for 2 more years, and new minimum monthly streamflows records were established during 8 months of the 2002 water year.

Water Level and Tides

The Suwannee River estuary experiences mixed semidiurnal tides, typified by two unequal high and two unequal low tides each day. The total range in tidal elevations during October 1999–September 2000 was about 0.5 m greater at the Cedar Key tidal gage than at the Suwannee River sites (table 3). The maximum elevation was about the same at all sites, but the minimum elevation was much lower at Cedar Key. Of the Suwannee River gages, EM, the gage nearest the Gulf of Mexico, had the largest total tidal range, and AGR, the most inland gage, had the smallest.

Clewell and others (1999) reported land-surface elevations along five transects adjacent to channels in the lower Suwannee River (two adjacent to Wadley Pass, one adjacent to West Pass, and two adjacent to East Pass). Top-of-bank elevations at these transects ranged between 0.1–0.2 m above NAVD 88, and swamp elevations generally were 0.05–0.1 m below top-of-bank. Land-surface elevations also were reported by Light and others (2002) for two transects near rkm 5 on the north side of West Pass; top-of-bank elevations ranged between 0.3–0.6 m above NAVD 88, and marsh elevations were about 0.2 m. Assuming that these top-of-bank elevations are representative of conditions near the five water-level gages in the river, water levels were likely above top-of-bank at these locations about 25–30 percent of the time during October 1999–September 2000 (fig. 14). On average, water levels would have been continuously above top-of-bank less than 6 hours (about one half of a tidal cycle) at any given location (fig. 15).

Spectral and harmonic analysis (Pawlowicz and others, 2002) were used to further describe tidal conditions. As expected, most of the tidal energy is associated with the diurnal and semidiurnal frequencies (0.042 and 0.083 cycles per hour, respectively; fig. 16). More tidal energy is associated with the longer periods at AGR than at CK (fig. 16); the tidal energy spectra for EP, EM, WP, and WM are similar to that at AGR.

Harmonic constituents were computed from the water-level records for all five Suwannee River water-level gages and for the CK tide gage (table 4). Harmonic analysis could not be performed on the RB water-level data, because data were not measured relative to a consistent datum throughout the data-collection period. The M2 tidal amplitude computed for CK for October 1999–September 2000 was 0.369 m, and the S2 amplitude for the same period was 0.131 m (table 4). NOAA (National Oceanic and Atmospheric Administration, 2003) reported M2 and S2 amplitudes of 0.386 and 0.135 m, respectively, for the most recent tidal epoch (1983–2001), so the results from the study period are consistent with the more accurate results computed from the 19-year tidal epoch record. The amplitude of the M2 tidal constituent is greatest at CK, and decreases with distance from the Gulf of Mexico, with the lowest amplitude at AGR. According to this analysis, the M2 tide at CK and AGR are out of phase by 4.75 hours (calculated as the difference in phase between the two sites, divided by 360 degrees per tidal period, multiplied by the number of hours per M2 tidal period).

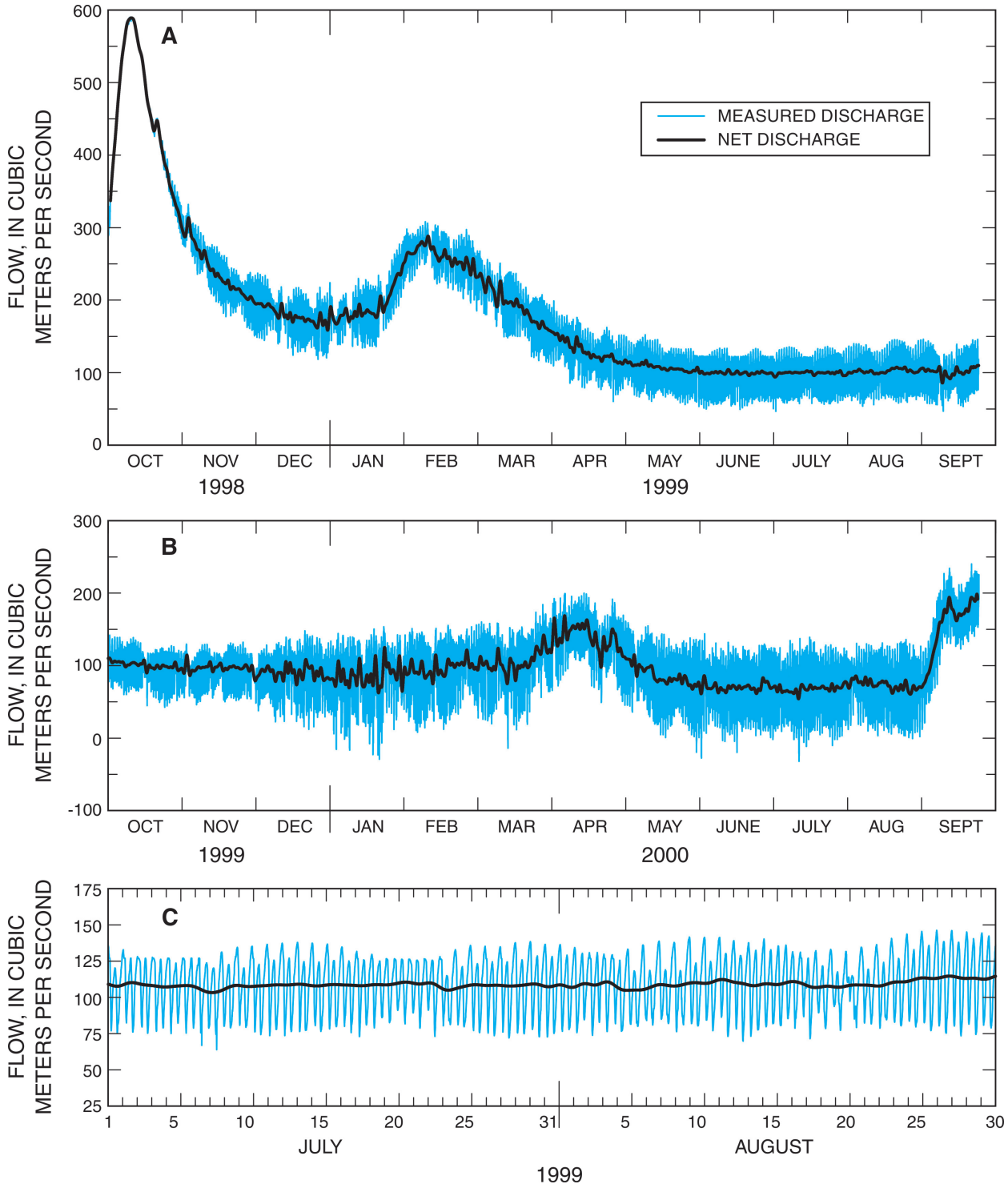

Figure 12. Measured discharge and calculated net flows in the Suwannee River at Wilcox for (A) October 1998–September 1999, (B) October 1999–September 2000, and (C) July–August 1999.

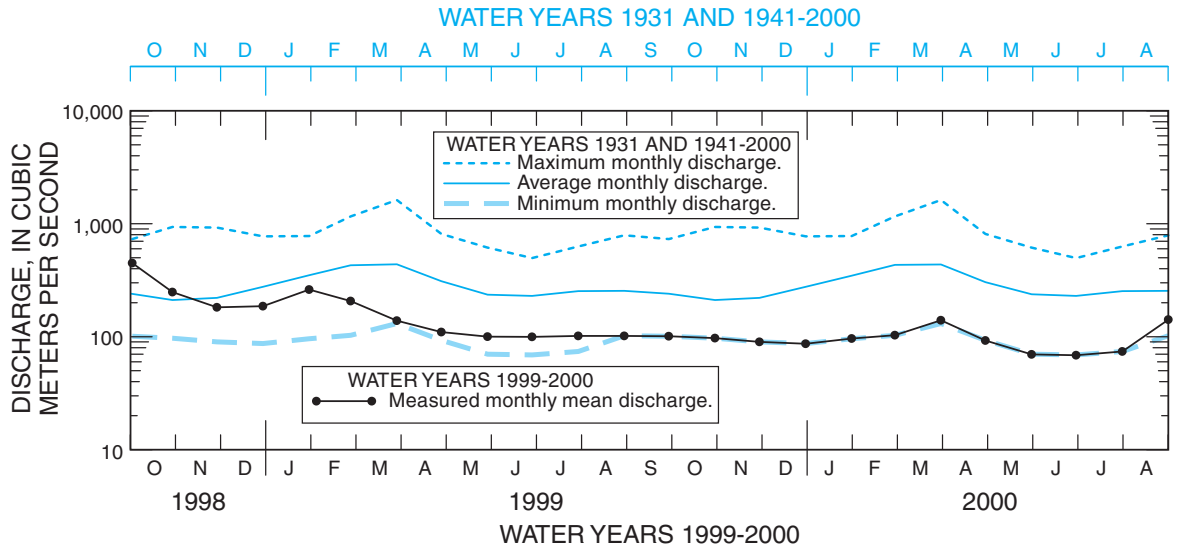

Figure 13. Monthly mean discharge, water years 1999–2000, and maximum, mean, and minimum monthly discharge, water years 1931 and 1941–2000, for the Suwannee River near Wilcox, Florida.

Table 3. Maximum, minimum, median, tidal elevations, and total tidal range at six water-level gages in the study area, October 1999–September 2000.

[Elevation is in meters above North American Vertical Datum of 1988]

Statistic	Above Gopher River (fig. 4)	East Mouth (fig. 4)	East Pass (fig. 4)	West Mouth (fig. 4)	West Pass (fig. 4)	Cedar Key (fig. 2)
Maximum elevation	0.76	0.86	0.82	0.89	0.88	0.85
Minimum elevation	-0.81	-0.98	-0.95	-0.84	-0.83	-1.27
Median elevation	0.07	-0.15	0	-0.05	0	-0.05
Total range (meters)	1.57	1.84	1.77	1.73	1.71	2.12

Astronomical tides at the water-level sites for October 1999–September 2000 were reconstructed from the calculated harmonic constituents for CK (fig. 17A) and EP (fig. 17B). As might be expected, there was better agreement between measured tides and predicted astronomical tides at CK than at EP. Periodicities at approximately diurnal frequencies, however, remained in the detided (difference between measured water level and estimated astronomical tides) record from both sites (fig. 17C). In addition, evidence of weather effects on the water-level record can be seen during February 8–10, 2000, when sustained winds from the northwest were followed by strong southerly winds, often at speeds in excess of 6 m/s.

The energy spectra were recalculated for the detided water levels (fig. 15) at CK and AGR. Most of the diurnal and semidiurnal tidal energy (frequencies of 0.0403 and 0.0805 cycles per hour, respectively) was removed from the CK record after the astronomical tides were subtracted from the measured water level. Substantial energy remained, however, in the AGR detided water-level record. The remaining energy at these frequencies is likely the result of nonlinear frictional effects as the tidal wave moves across the Suwannee Reef and up into the river, and the interaction of the M2 tide with its first harmonic, M4. Water depth at low tide may be only half the depth at high tide in much of the estuary shoreward of the reef. Hence, frictional effects are relatively greater at low tide than at high tide, resulting in tidal distortion and the presence of overtides (Speer and Aubrey, 1985; Friedrichs and Aubrey, 1988).

Because of the nonlinear frictional effects, with higher friction at low water than at high water, the time delay between high water in the Gulf and high water in the Suwannee River is less than the time delay between low water at the two locations. As a result, falling tides are slightly longer in duration than rising tides (fig. 15) and the system may be flood dominant. Extensive intertidal storage typically leads to ebb dominance (Friedrichs and Aubrey, 1988). The fact that the Suwannee River estuary tends to be slightly flood dominant (according to this analysis) indicates that the effects of intertidal storage on tides are small, particularly relative to frictional effects.

Siegel and others (1996) reported that winds blowing from 10–20 degrees west of north (approximately parallel to the orientation of the west Florida shelf) have the greatest effect on sea level shoreward of the Suwannee Reef, but that there was no prevailing wind direction. During this study, winds at WP were predominantly from the northeast during October–November and from the southwest during March–

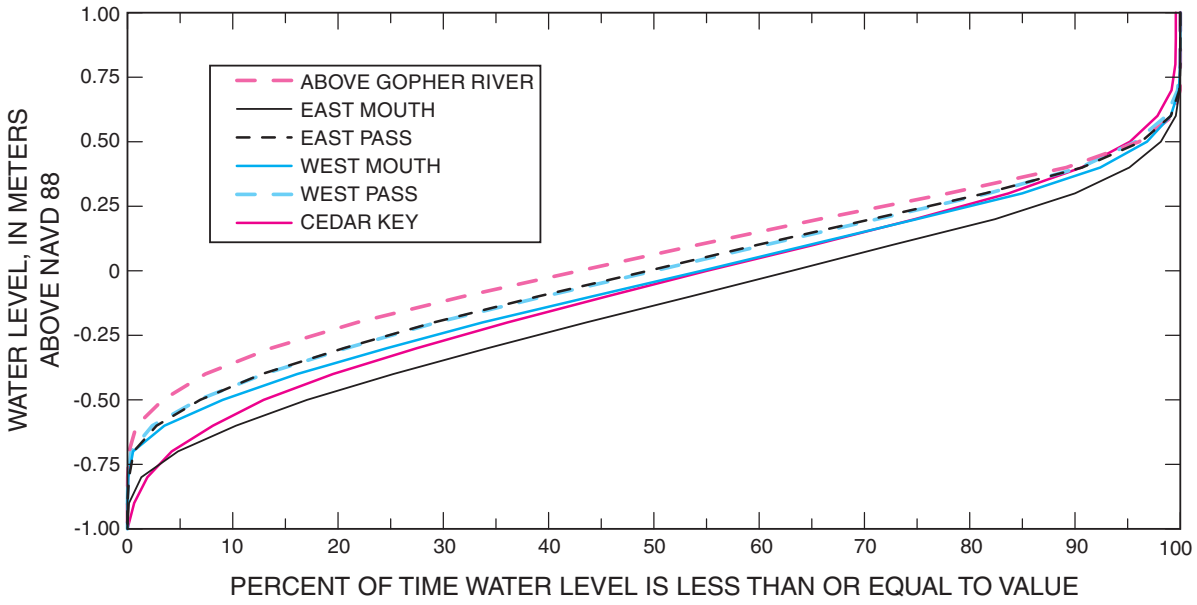

Figure 14. Water-level duration curves for six water-level gages in the study area, October 1999–September 2000.

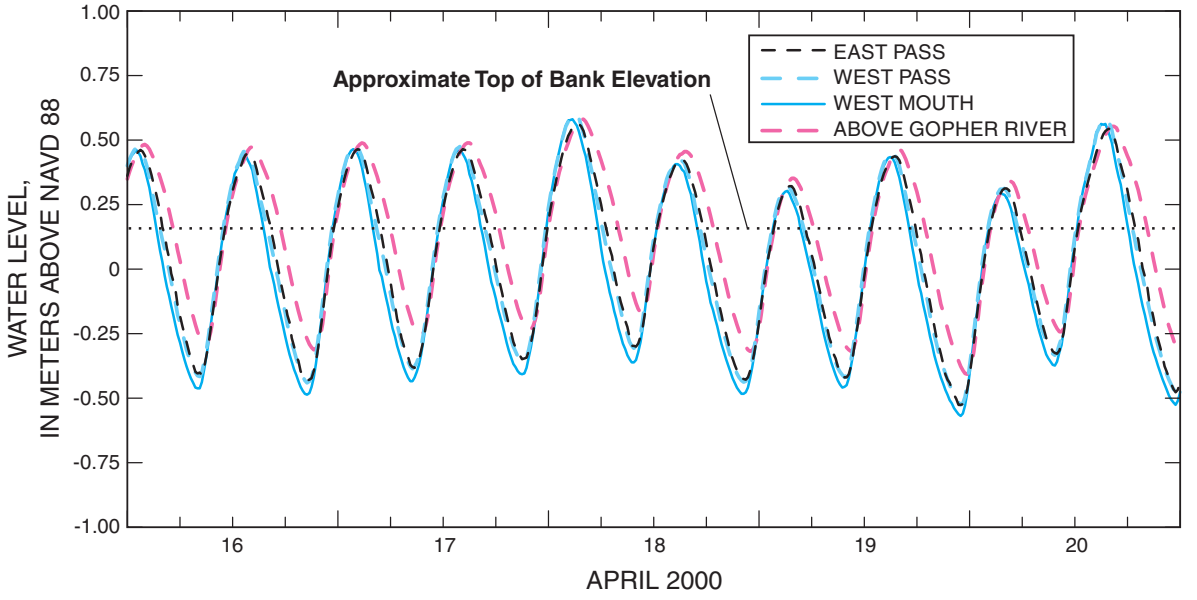

Figure 15. Measured water level at East Pass, West Pass, West Mouth, and above Gopher River, April 16–20, 2000.

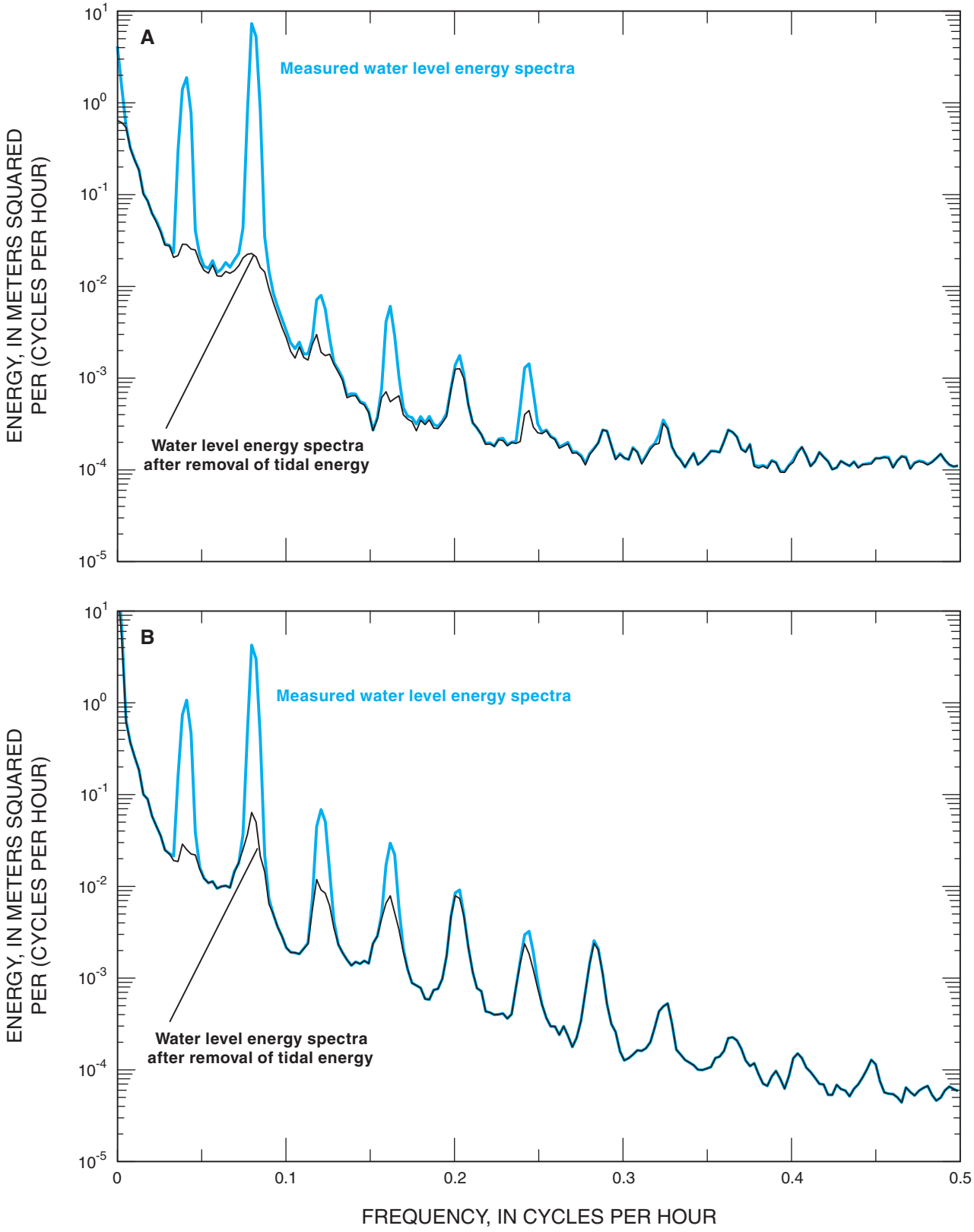

Figure 16. Tidal energy spectrum for (A) Cedar Key and (B) above Gopher River water-level gages, October 1999–September 2000.

Table 4. Tidal amplitude and phase for selected harmonic constituents at Cedar Key, above Gopher River, East Pass, West Pass, East Mouth, and West Mouth water-level gages, October 1999–September 2000.

Name	Symbol	Period (hours)	Amplitude (meters)						Phase (degrees)					
			Cedar Key	Above Gopher River	East Pass	East Mouth	West Pass	West Mouth	Cedar Key	Above Gopher River	East Pass	East Mouth	West Pass	West Mouth
Principal lunar semidiurnal	M2	12.42	0.369	0.257	0.299	0.328	0.297	0.314	230	8	257	340	251	248
Principal solar semidiurnal	S2	12.00	0.131	0.085	0.105	0.118	0.102	0.115	95	115	126	82	120	117
Major lunar elliptical semidiurnal	N2	12.66	0.066	0.041	0.049	0.056	0.050	0.042	181	104	214	70	210	198
Luni-solar diurnal	K1	23.93	0.161	0.113	0.129	0.142	0.130	0.134	112	92	132	70	131	129
M2 overtide, quarter diurnal	M4	6.21	0.009	0.015	0.008	0.012	0.013	0.013	332	259	42	255	64	66
Principal lunar diurnal	O1	26.87	0.142	0.095	0.113	0.124	0.112	0.111	349	172	12	148	11	6
M2–K1 compound tide, third diurnal	MK3	8.18	0.007	0.022	0.019	0.021	0.021	0.022	289	354	305	341	300	302
Solar diurnal	S1	24.00	0.018	0.050	0.042	0.052	0.040	0.037	76	232	101	206	91	84
Solar annual	SA	365.18 (days)	0.123	0.133	0.154	0.161	0.118	0.170	174	318	161	321	165	184
Principal solar diurnal	P1	24.07	0.047	0.024	0.032	0.035	0.029	0.029	203	274	228	251	227	217

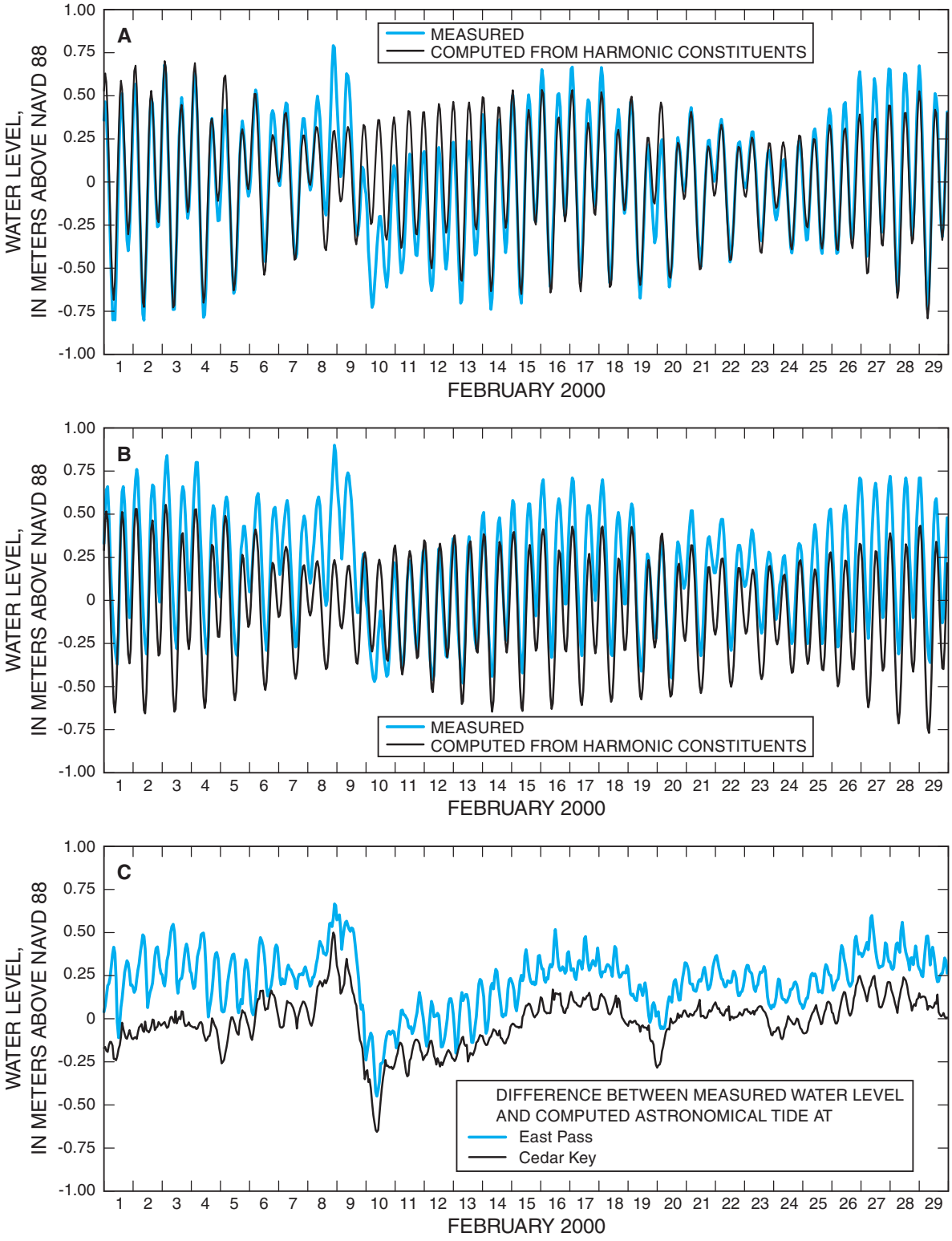

Figure 17. Measured water level and astronomical tides at (A) Cedar Key and (B) East Pass, and (C) the difference between measured water level and computed astronomical tides at Cedar Key and East Pass, February 2000.

May and July. In addition, winds at WP during this study were predominantly from the west to southwest (onshore) between 2:00 a.m. and 10:00 a.m., and from the east-northeast (offshore) between 3:00 p.m. and 1:00 a.m., an indication that the sea-breeze effect (or convection-caused winds) is present well up into the river. Siegel and others (1996) also observed that about 15 percent of the tidal energy at their observation sites was associated with winds at periods greater than diurnal, which is one reason the astronomical and measured tides at CK are not in exact agreement.

Tidal Flows

Measured flood index velocities were very similar at EP and WP (figs. 18 and 19A). (See previous discussion of AVMs in Data Collection Methods section. The index velocity is the velocity measured in a representative, but small, volume of the total flow at the gaging station. The index velocity is not the same as the cross-sectional mean velocity, nor is the vector direction of the index velocity necessarily the same as that of all water parcels at the measurement section.) The maximum flood velocity was about the same at EP and WP (about -70 centimeters per second (cm/s)), but was only about half that at AGR. Index velocity (and thus flow) was negative (flood flow) about 38 percent of the time at EP and WP, and about 32 percent of the time at AGR. In general, flood velocities at AGR were about half those at EP and WP (figs. 18 and 19A).

In contrast to flood currents, ebb velocities at WP were more similar to those at AGR than at EP, whereas ebb velocities at EP were somewhat greater than at the other two sites. The median ebb index velocity at EP was 43 cm/s (fig. 18), compared to a median of about 30 cm/s at both AGR and WP (median based on ebb velocities only). A smaller cross-sectional area and a more direct connection to the Gulf may account for the higher ebb velocities in East Pass relative to West Pass.

Higher ebb velocities relative to flood velocities indicates the likely presence of an ebb-dominant system in estuaries with negligible freshwater inflow (Friedrichs and Aubrey, 1988), which is, of course, not true of the Suwannee River. Recall, also, that the water-level data indicated that the Suwannee River was slightly flood dominant. The higher ebb velocities relative to flood velocities likely reflect the relatively high freshwater discharge through the estuary, particularly relative to the cross-sectional flow area.

Flow typically reverses from flood to ebb at all sites within 1–2 hours after the occurrence of high water (for example, fig. 19B), which is typical of a standing wave. The lag between low water and reversal from ebb to flood typically is slightly longer. Maximum ebb currents typically occur 4–5 hours after high water.

Tidal currents at diurnal to semidiurnal periods and shoreward of Suwannee Reef have been reported to generally be in the east-west direction, and currents seaward of the reef typically are in the north-south direction (Siegel and others, 1996). Currents at periods greater than diurnal are somewhat correlated with wind direction, with greater correlation in the winter than summer (Siegel and others, 1996), probably because winter winds are continuous in direction for longer durations than are summer winds. Winds from the north tend to generate westward currents, and winds from the south generate eastward currents in the deeper waters seaward of the Suwannee Reef (Siegel and others, 1996).

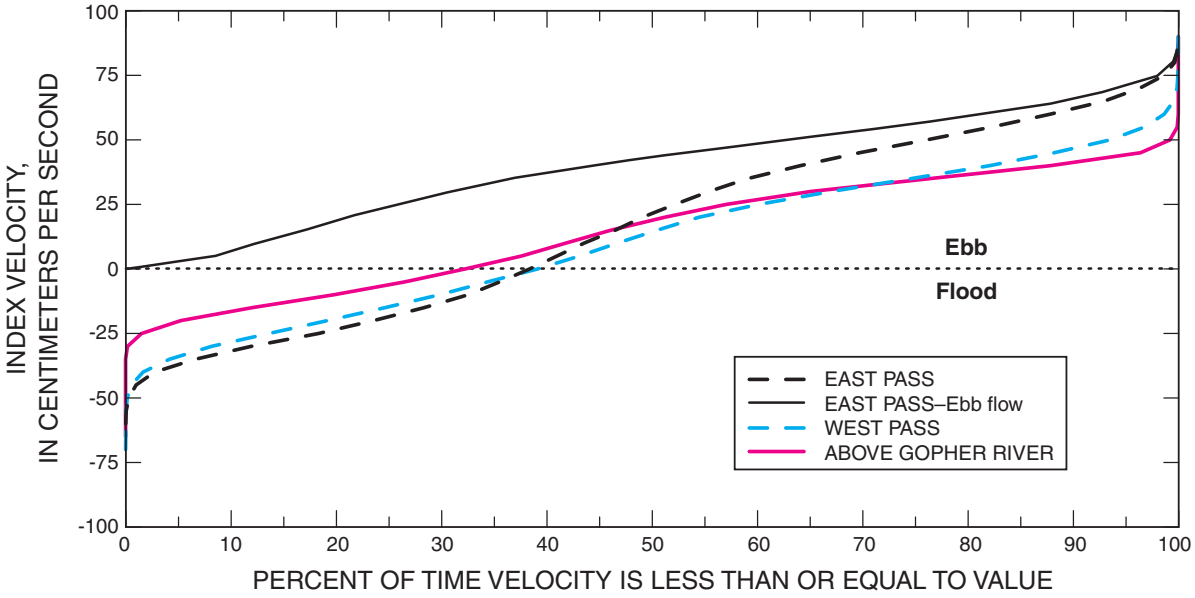

Figure 18. Duration curves for index velocity at East Pass, West Pass, and above Gopher River streamgages, October 1999–September 2000.

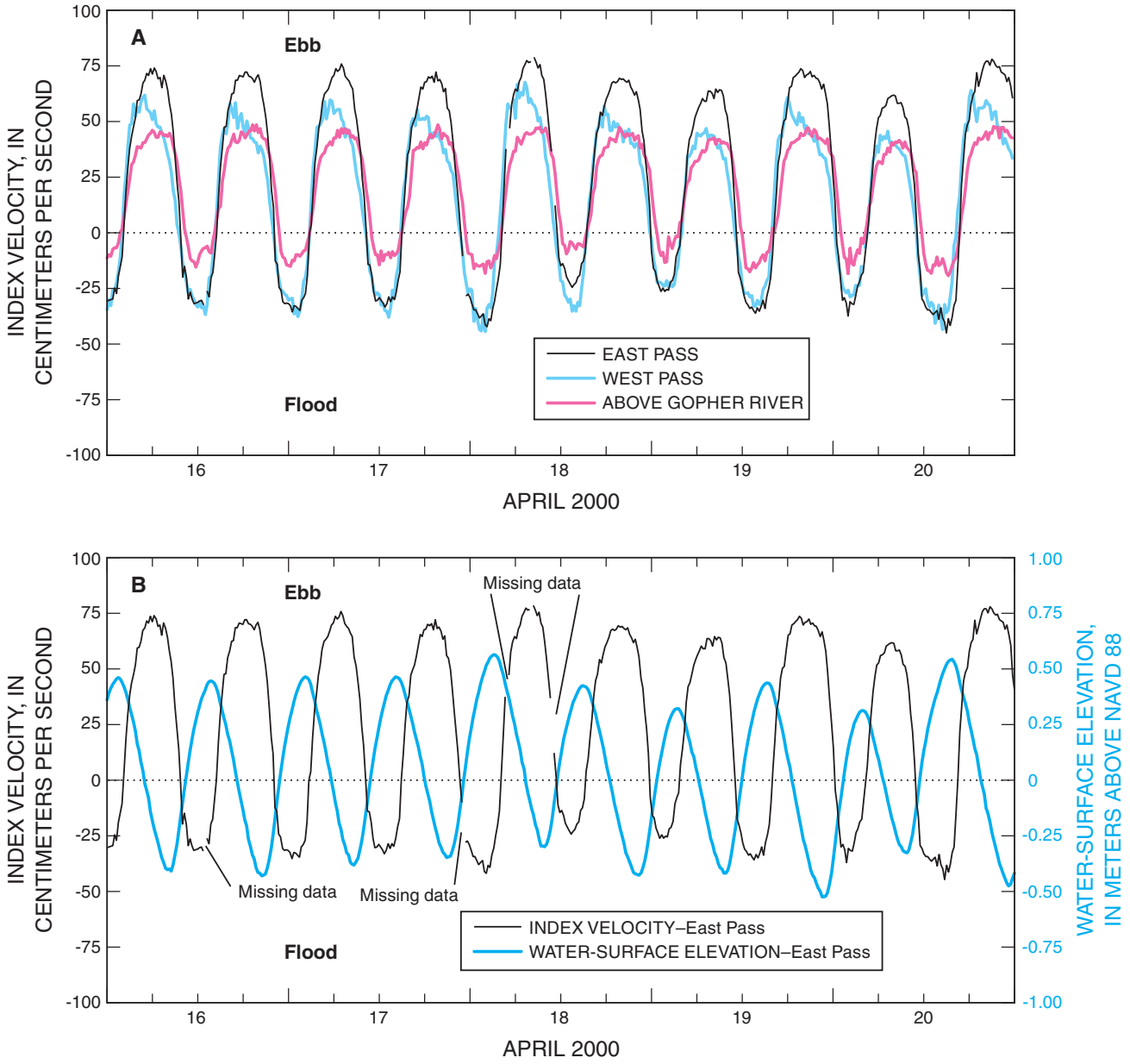

Figure 19. Typical (A) index velocities, East Pass, West Pass, and above Gopher River streamgages, and (B) index velocities and water-surface elevation, East Pass, April 16–20, 2000.

At AGR, measured total flow ranged from 558 to -368 m^3/s (negative indicates flood, or upstream flow) during October 1999 to September 2000. At EP, maximum ebb flow was 351 m^3/s and maximum flood flow was -315 m^3/s. At WP, maximum ebb flow was 655 m^3/s, almost double the maximum at EP, and maximum flood flow was -711 m^3/s. Flows at AGR were downstream about two-thirds of the time (fig. 20A) during October 1999–September 2000, a period of extended and record low flows (fig. 13). Flows were in the downstream direction 55 and 58 percent of the time at EP and WP, respectively (fig. 20A).

Total flows were consistently greater at WP than at EP (fig. 20A), probably because West Pass has greater storage than East Pass, thereby resulting in a greater tidal prism in West Pass. During spring tides, the sum of flows measured at EP and WP was almost twice as large as the flow measured at AGR (fig. 21). The difference between flow at AGR and the sum of flows at EP and WP was much smaller during neap tides, however, probably because of lower storage during neap tides.

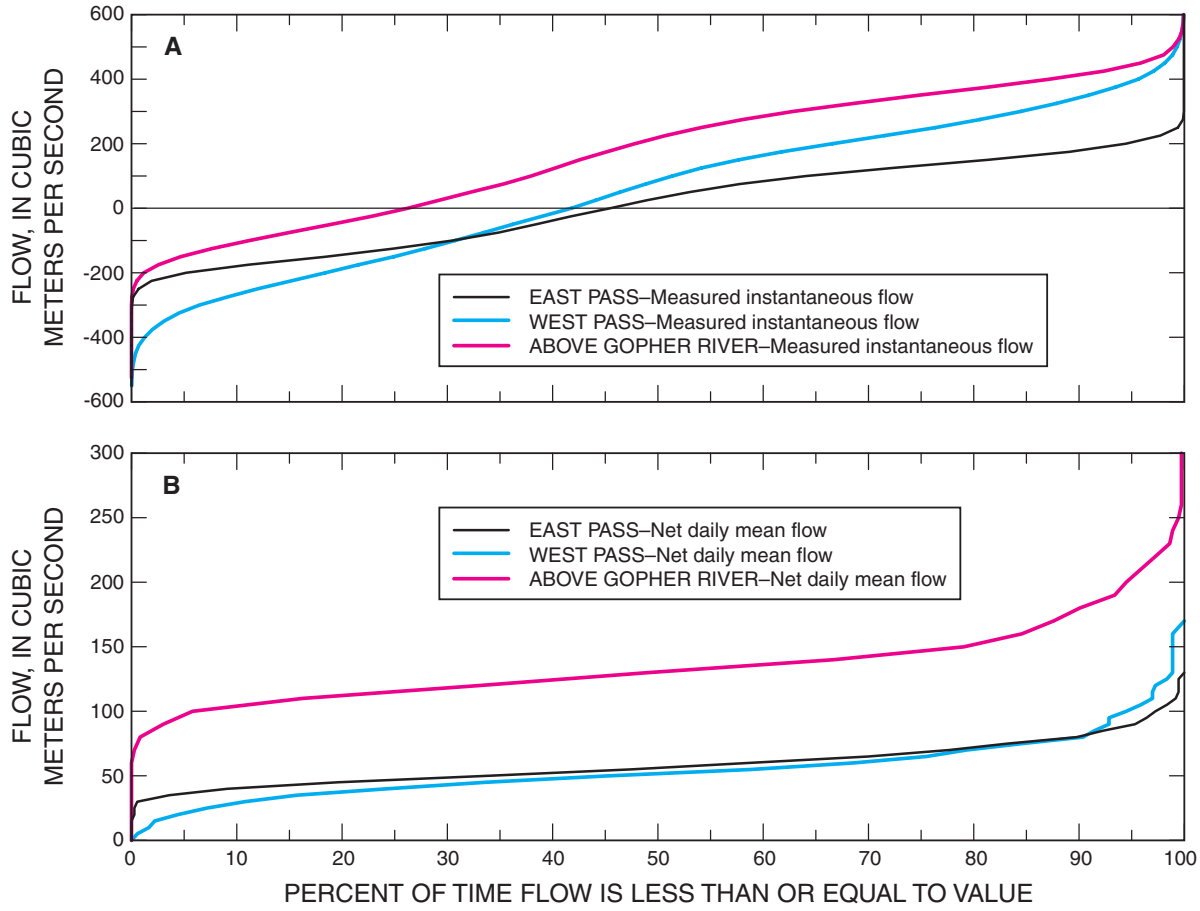

Figure 20. Duration curves for (A) measured instantaneous discharge and (B) net (total flow minus tidal flow) daily mean discharge at East Pass, West Pass, and above Gopher River streamgages, October 1999–September 2000.

A low-pass digital filter (Godin, 1972; Walters and Heston, 1982; Dijkzeul, 1984) was used to separate the tidal flows from the net (freshwater) flow at the three gages. Net flows were much less variable than total flow (figs. 20B and 22); EP net flows were, for example, between 40 and 70 m^3/s 70 percent of the time during October 1999–September 2000. In contrast to total flows, net flows generally were higher at EP than at WP (fig. 20B). Because East Pass has a more direct connection with the Gulf than West Pass and does not have the multiple outlet channels that are present in West Pass, more freshwater enters the Gulf through East Pass than West Pass. Calculated net daily mean flows at WP were negative on two occasions—both times when the instantaneous streamflow amplitude was about one-third the normal amplitude.

Monthly mean net flows were calculated for the Wilcox, AGR, EP, and WP gages (fig. 23). According to this analysis, net freshwater flow increased substantially between Wilcox and AGR, a reach representing only about 3 percent of the total basin drainage area. The average increase in flow between Wilcox and AGR was 30 m^3/s during the study period, and the increase was fairly consistent from month to month. This large and fairly consistent increase in flow downstream from Wilcox, where the contributing drainage area is small, indicates the likely presence of a substantial contribution of ground water to the river in this reach.

The sum of net flows at EP and WP, downstream from AGR, was generally less than the net flow at AGR, with the average difference during the study period equal to 13 m^3/s. It is possible that some of the flow at AGR bypasses the streamgages at WP and EP. If high water spills over the south banks (for example, fig. 15) in the reaches between AGR and the two downstream streamgages, water could flow south to the Gulf of Mexico, rather than returning to the channel during falling tides. Additional, specially designed studies would be required to determine the source of the apparent increase in flow between Wilcox and AGR, and the reason for the loss in flow downstream of AGR.

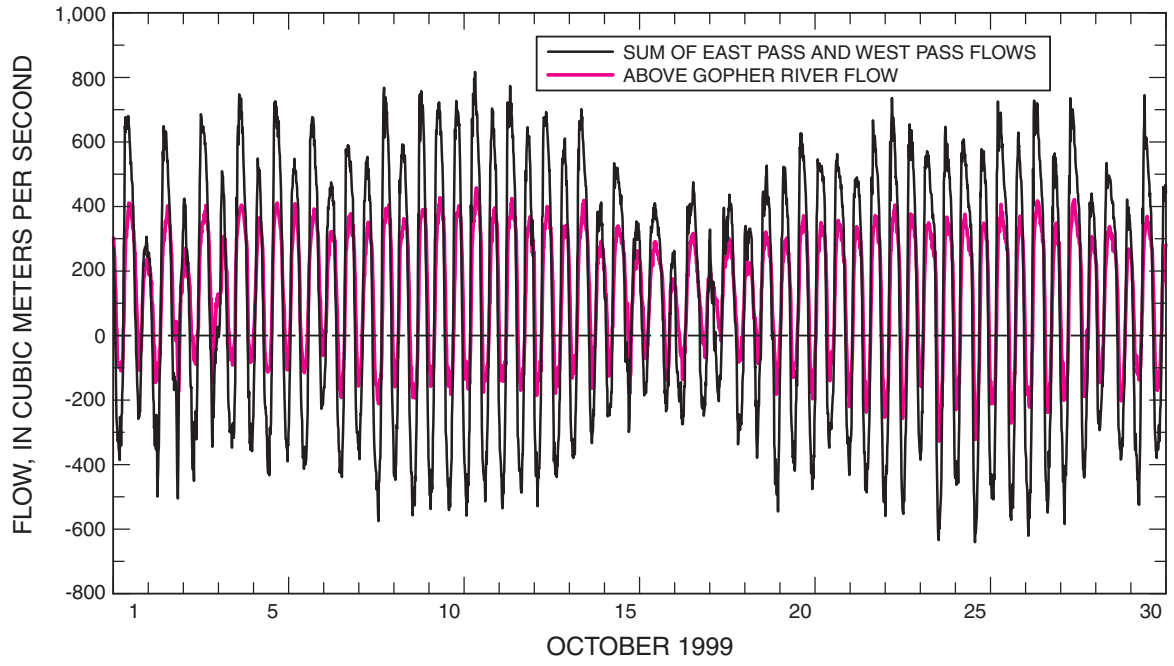

Figure 21. Measured discharge at above Gopher River streamgage and the sum of discharges simultaneously measured at the East Pass and West Pass streamgages, October 1–30, 1999.

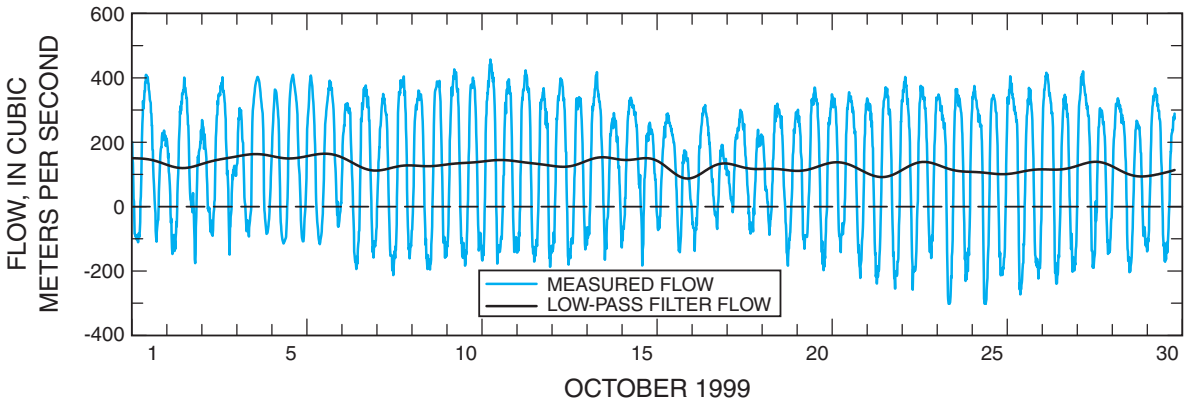

Figure 22. Measured total flow and calculated net flow at above Gopher River streamgage, October 1–30, 1999.

The primary purpose of the discharge measurements made in December 14–16, 1999, was to determine the distribution of flows around the various channel junctions in the study area (figs. 24 and 25). Measurements during May 30–June 2, 2000 (fig. 26) were more distributed throughout the study area, so some of the patterns apparent in the December 1999 data cannot be confirmed from the May–June 2000 data. Nevertheless, some generalizations about flow distributions can be made from the data, as follows.

- Generally, there was little variability in flow within West Pass between WP upstream to the East Pass-West Pass split (fig. 24B, comparison of sites W6, W8, W9, and WP; fig. 26B, comparison of sites W6, W8, and WP).
- Flow in Magnesia Pass was quite low (figs. 24C and 26B) at about 10 m^3/s, or about 5 percent of the concurrent flow in West Pass, during all measurements.
- Flow at WP was approximately equal to the sum of the flows in Alligator Pass, Wadley Pass, and the split between Alligator and Wadley Passes (fig. 25A and 25B).

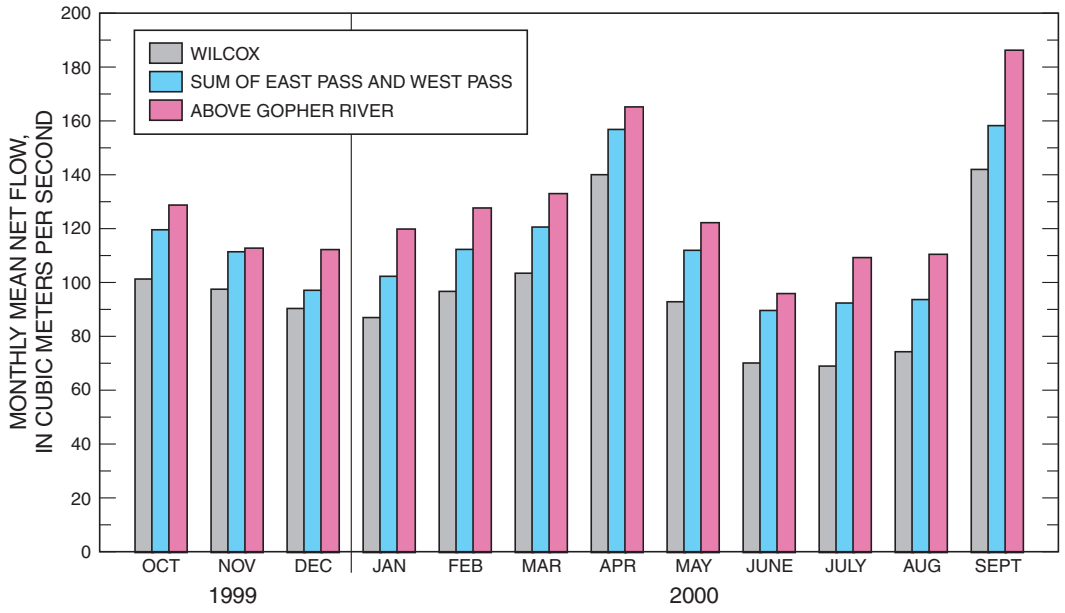

Figure 23. Monthly mean net flow at Wilcox and above Gopher River, and the monthly sum of monthly mean flows at East Pass and West Pass, October 1999–September 2000.

- During flood flows in December 1999, flow magnitude was higher in Wadley Pass than in Alligator Pass (figs. 25C and 26A), but the opposite was true during ebb flows (fig. 25B). This pattern persisted for ebb flows during May–June 2000 (fig. 26), but was not true for flood flows, when Alligator Pass flow magnitudes exceeded those in Wadley Pass.

- Flood flows in Dan May Creek (fig. 11) typically were at least half of concurrent flows at EP (fig. 26). Ebb flows, however, were generally much lower, and usually less than 30 m^3/s. It is possible that some of the discharge (on ebb flow) in Dan May Creek could be water measured at AGR, but which bypassed the EP and WP streamgages by flowing south across the marsh east of the East Pass channel.

These observations illustrate the dynamic nature of flow conditions in the study area.

Salinity

Salinity at AGR was less than 0.2 psu more than 99 percent of the time during October 1999–September 2000. The only time AGR salinity exceeded 0.2 psu during this period was on July 31, 2000, between 9:00 a.m. and 11:00 a.m., when the maximum bottom salinity was 0.5 psu (specific conductance = 1,050 µS/cm at 25 ˚C) and the maximum top salinity was 0.4 psu. Net flow on this date was about 115 m^3/s; minimum net flow during October 1999–September 2000 was 49 m^3/s. Flow was ebbing during the time the salinity was slightly elevated, so it may be that the higher than normal readings were the result of dissolved solids from a source other than the ocean.

On September 19, 1999, bottom salinity at AGR reached a maximum of 3.3 psu; the maximum surface salinity at that time was 0.5 psu. Salinity was elevated above normal levels for 4 hours. High tides during September 15–19 were as much as 0.6 m below normal and the tidal range was about 0.6 m, compared to a typical range of 1.0–1.2 m. Hurricane Irene crossed the southern tip of Florida on September 15, and Tropical Storm Harvey formed in the Gulf of Mexico on September 19. It is likely that these two storms, primarily Hurricane Irene, produced the lower than normal water levels in the Suwannee River, resulting in the elevated salinities in the river at AGR. Except for September, salinities at AGR during June–September 1999 were less than 0.2 psu.

Of the four remaining salinity monitoring gages in the Suwannee River, salinity at EP was the lowest (fig. 27). Salinity near the surface at EP was less than 1 psu 86 percent of the time during October 1999–September 2000, and salinity near the bottom was less than 1 psu 77 percent of the time. In contrast, salinity at EM (both top and bottom) was greater than 1 psu at least 70 percent of the time (fig. 27). Median salinities at EP, WP, and WM were all less than 2 psu, whereas median salinity at EM near the bottom was about 9 psu. There was much less difference in salinity between the WP and WM gages in West Pass than between the EP and EM gages in East Pass. Higher ebb velocities in East Pass, more direct connections to the Gulf and West Pass, and channel geometry all likely contributed to the lower upstream migration of salt in East Pass compared to West Pass.

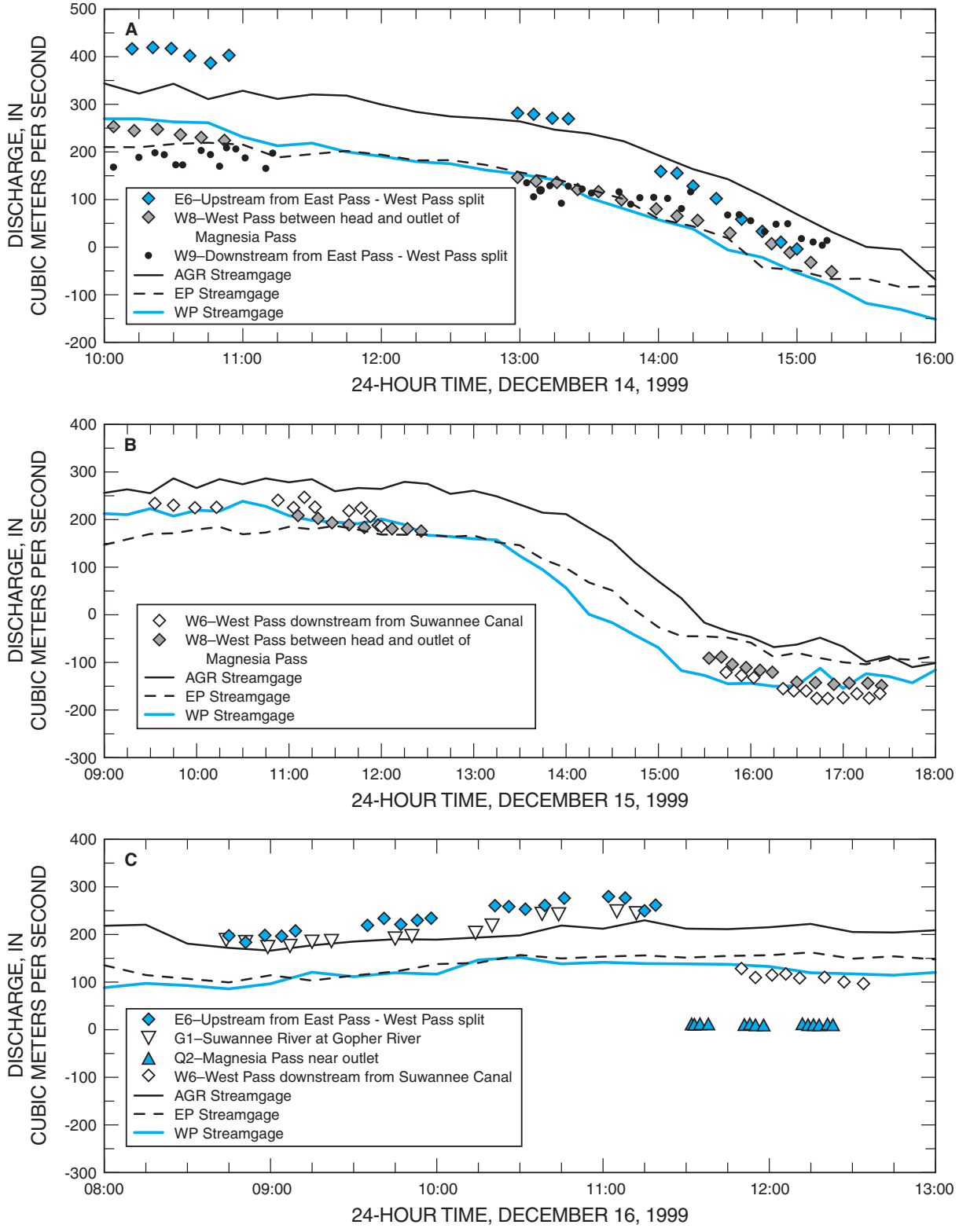

Figure 24. Individual discharge measurements in the vicinity of the East Pass-West Pass split, and flow measured at above Gopher River, East Pass, and West Pass streamgages, (A) December 14, 1999, 10:00–16:00; (B) December 15, 1999, 9:00–18:00; and (C) December 16, 1999, 8:00–13:00.

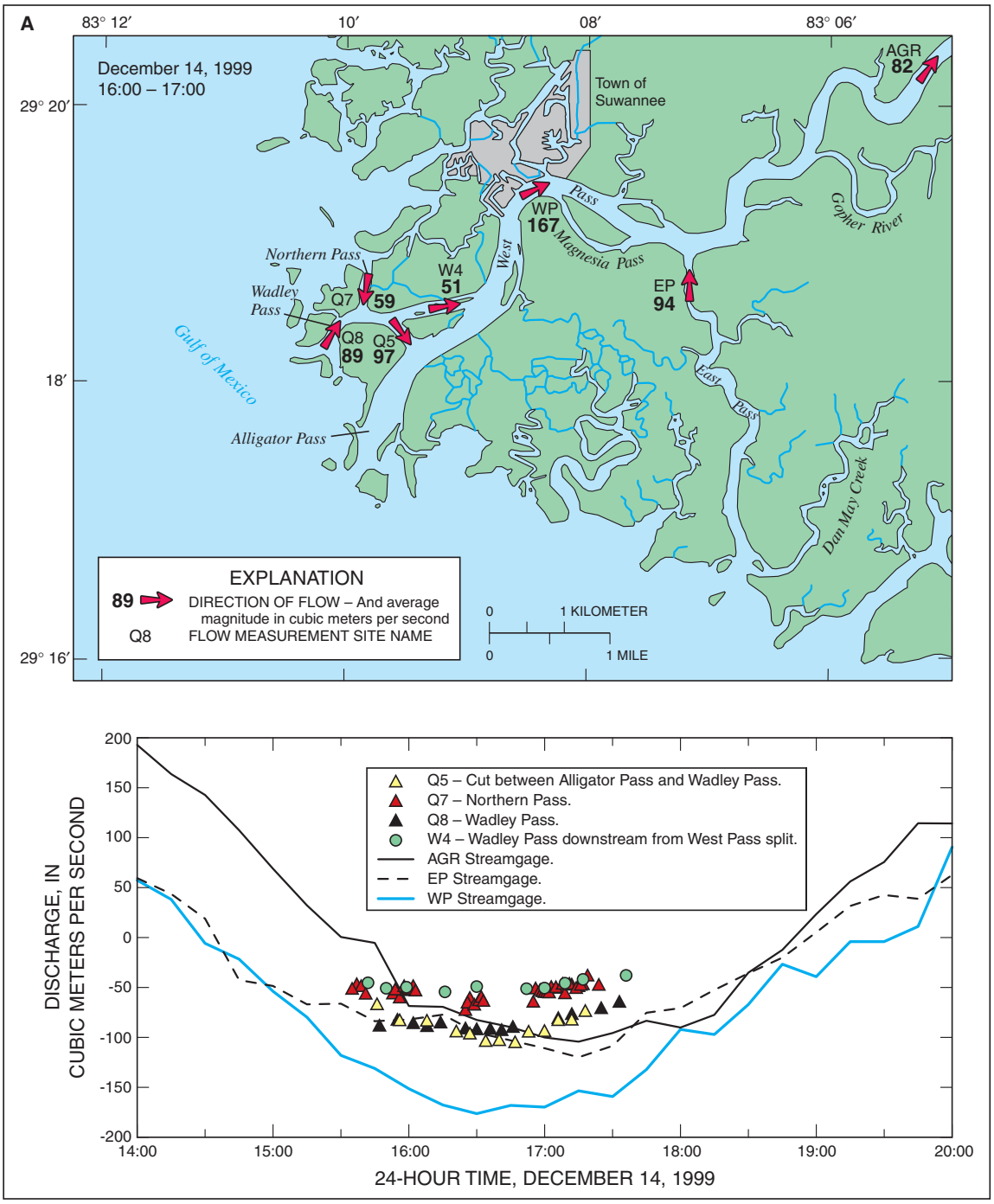

Figure 25. Measured (graph) and average measured (map) discharge for selected locations over three time periods: (A) December 14, 1999, 16:00–17:00; (B) December 15, 1999, 8:00–10:00; and (C) December 15, 1999, 14:30–15:30.

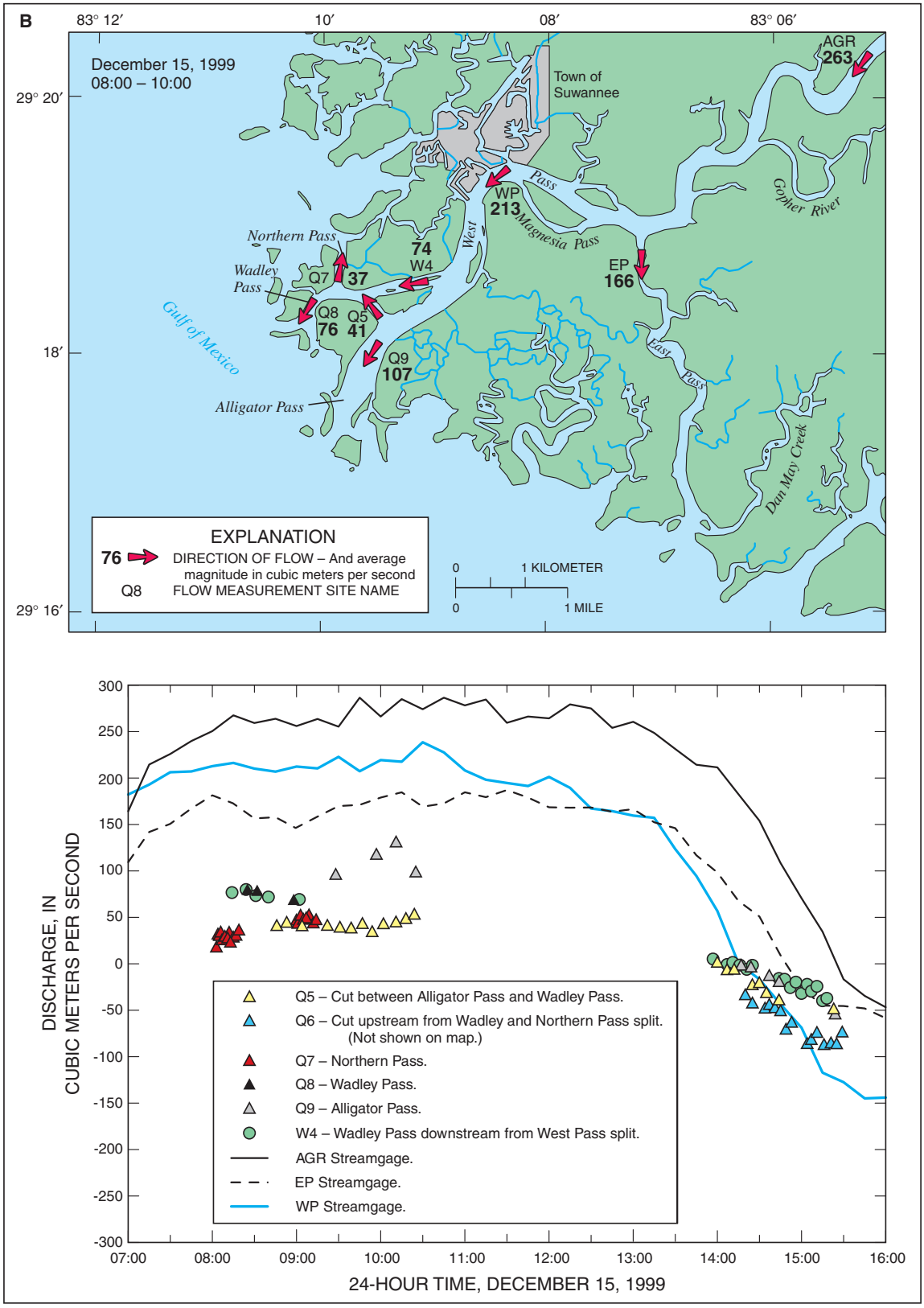

Figure 25. Measured (graph) and average measured (map) discharge for selected locations over three time periods: (A) December 14, 1999, 16:00–17:00; (B) December 15, 1999, 8:00–10:00; and (C) December 15, 1999, 14:30–15:30. —Continued

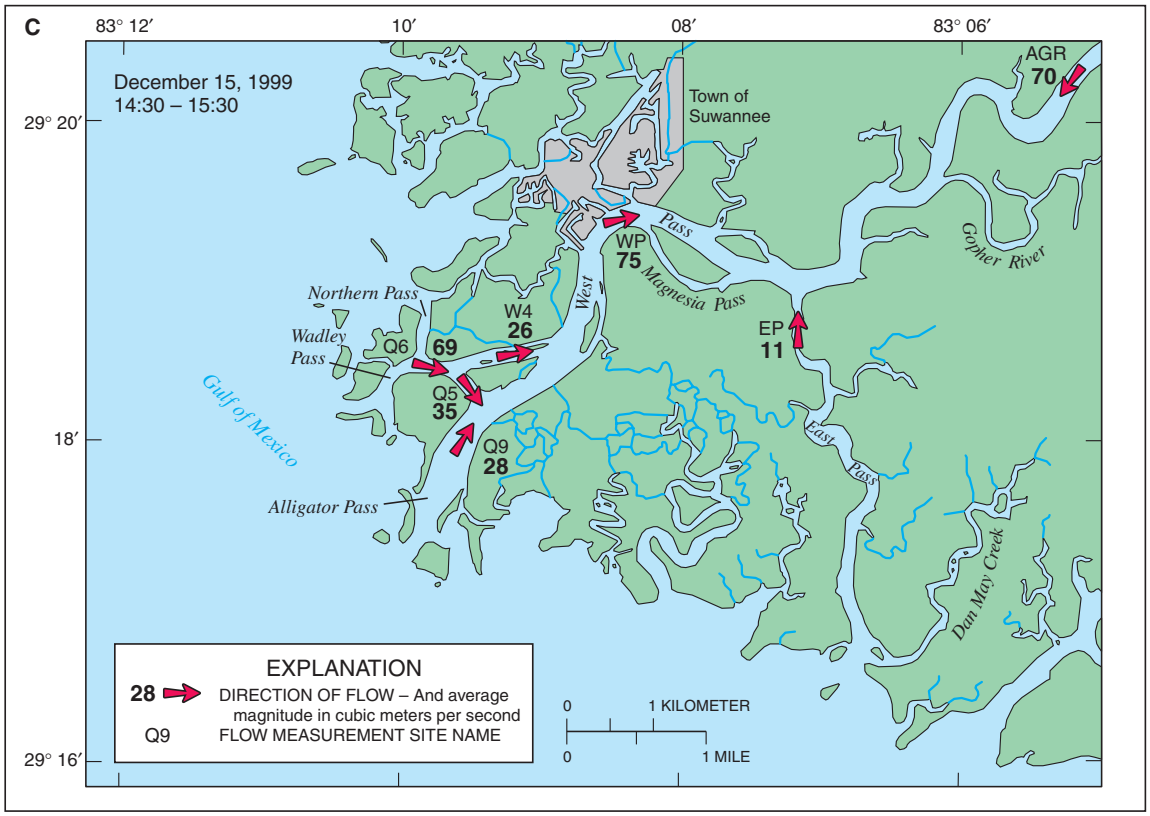

Figure 25. Measured (graph) and average measured (map) discharge for selected locations over three time periods: (A) December 14, 1999, 16:00–17:00; (B) December 15, 1999, 8:00–10:00; and (C) December 15, 1999, 14:30–15:30. [Refer to discharge-measurement graph on p. 30 for the (C) time period.] —Continued

Monthly mean salinities were calculated as the mean of the 15-minute salinities measured from the first low tide of the calendar month to the last low tide of the calendar month in order to avoid aliasing. Lowest monthly mean salinities were in April 2000 (fig. 28), which was the month with the second highest net flow at AGR (fig. 23). Salinities were higher in the fall of 1999, although flows were lower in the summer of 2000 (figs. 23 and 28). A direct correlation between monthly mean flow and monthly mean salinity is not evident. A greater difference also existed between monthly mean top and bottom salinities in the fall of 1999 than the summer of 2000; the reason for this difference is not apparent.

Top-to-bottom differences in salinity (hereafter called stratification) varied with time and location. As indicated by the salinity duration curves (fig. 27), there was much less stratification at EP than at EM, but stratification was similar at WP and WM. Median stratification at EM was 2 psu, and stratification exceeded 5 psu 30 percent of the time. At EP, however, stratification was less than 1 psu 90 percent of the time. At both WP and WM, stratification was less than 4 psu 90 percent of the time.

Stratification was invariably greatest near high tide (fig. 29), but the magnitude varied from location to location, even at a given tidal phase. These variations were primarily due to differences in channel depth. As the flow was ebbing near low tide, little stratification typically occurred in either East Pass or West Pass upstream from the Wadley Pass-Alligator Pass split. Salinities in Alligator Pass often remained high, even as flow was ebbing.

In the same manner as tidal flow at AGR, EP, and WP, salinity is closely related to tidal conditions. Hence, it seems reasonable, as was done with the flow and water-level records, to extract the tidal component of salinity variations from the record, leaving a “detided” salinity that is primarily a function of processes other than tidal conditions. The salinity records at EP and WP were low-pass filtered. These low-pass filtered salinity records were then examined using scatter plots and various statistical relations to determine if any relation existed between net flow at AGR and “detided” salinity (fig. 30). Although on occasion an increase in flow is followed by an obvious decrease in salinity (for example, November 2, 1999, West Pass bottom; fig. 30B), the amount of scatter in the data

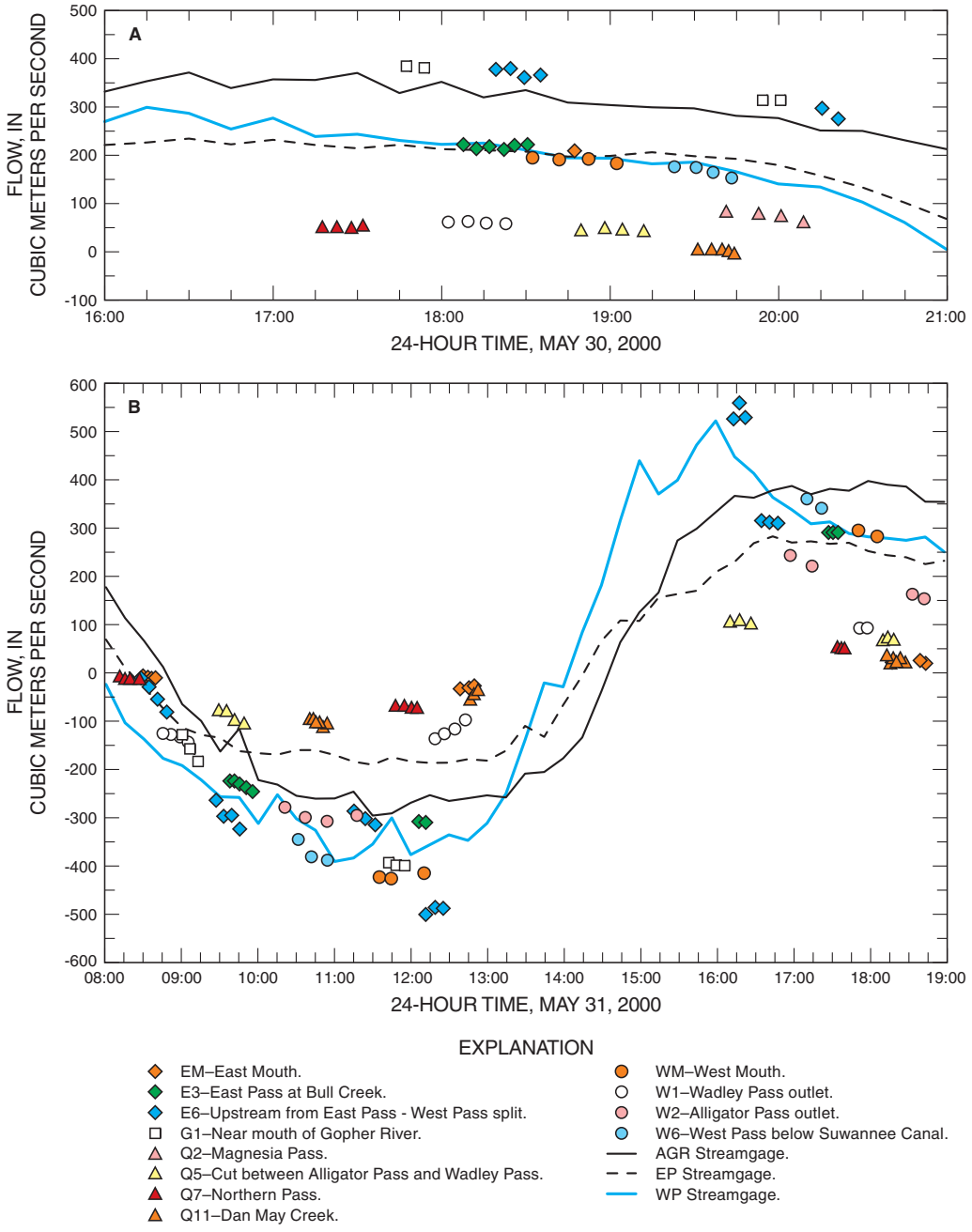

Figure 26. Individual discharge measurements in the lower Suwannee River, and flow measured at above Gopher River, East Pass, and West Pass streamgages, (A) May 30, 2000, 16:00–21:00; (B) May 31, 2000, 8:00–19:00; (C) June 1, 2000, 7:00–20:00; and (D) June 2, 2000, 7:00–12:00.

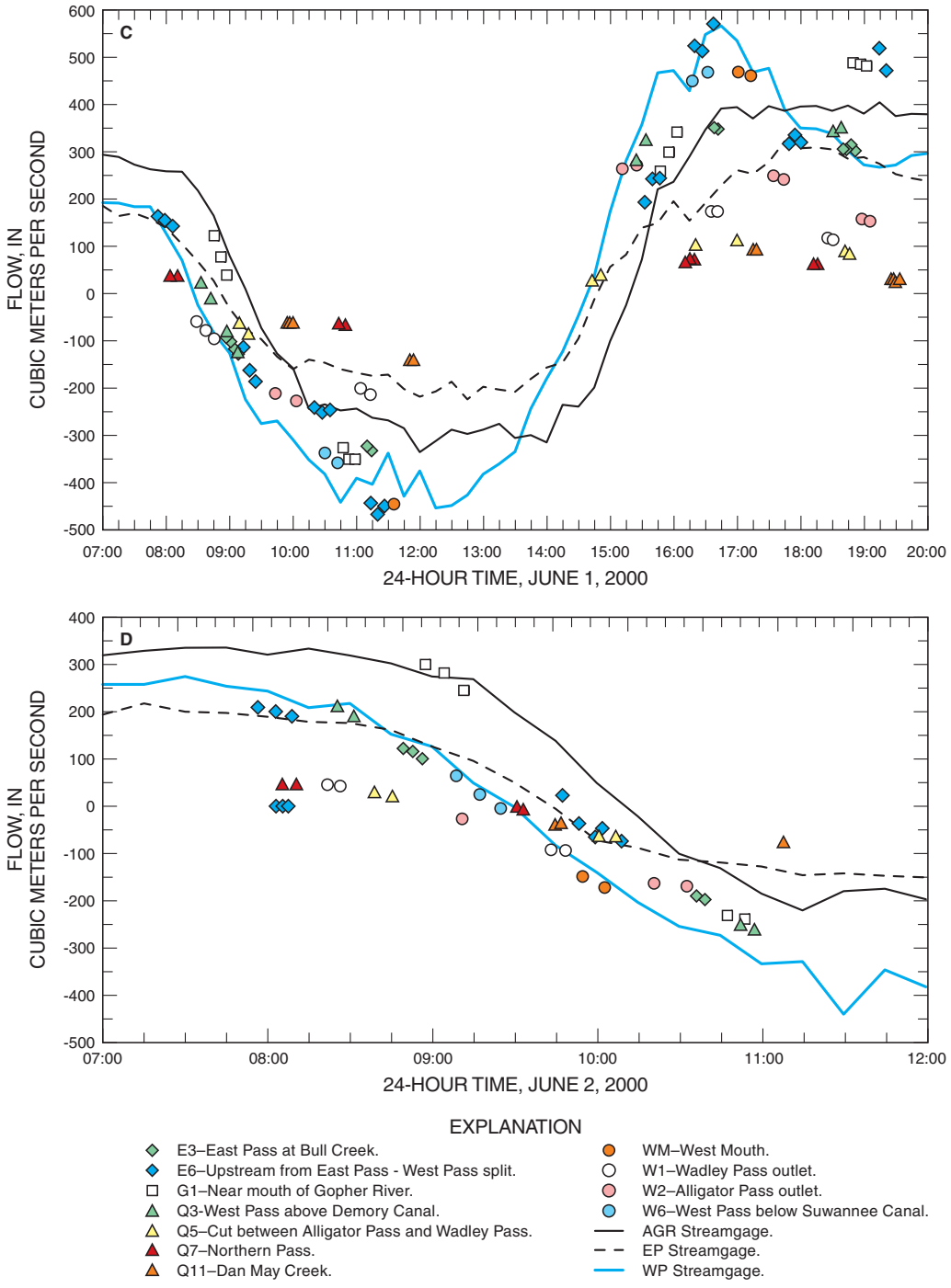

Figure 26. Individual discharge measurements in the lower Suwannee River, and flow measured at above Gopher River, East Pass, and West Pass streamgages, (A) May 30, 2000, 16:00–21:00; (B) May 31, 2000, 8:00–19:00; (C) June 1, 2000, 7:00–20:00; and (D) June 2, 2000, 7:00–12:00. —Continued

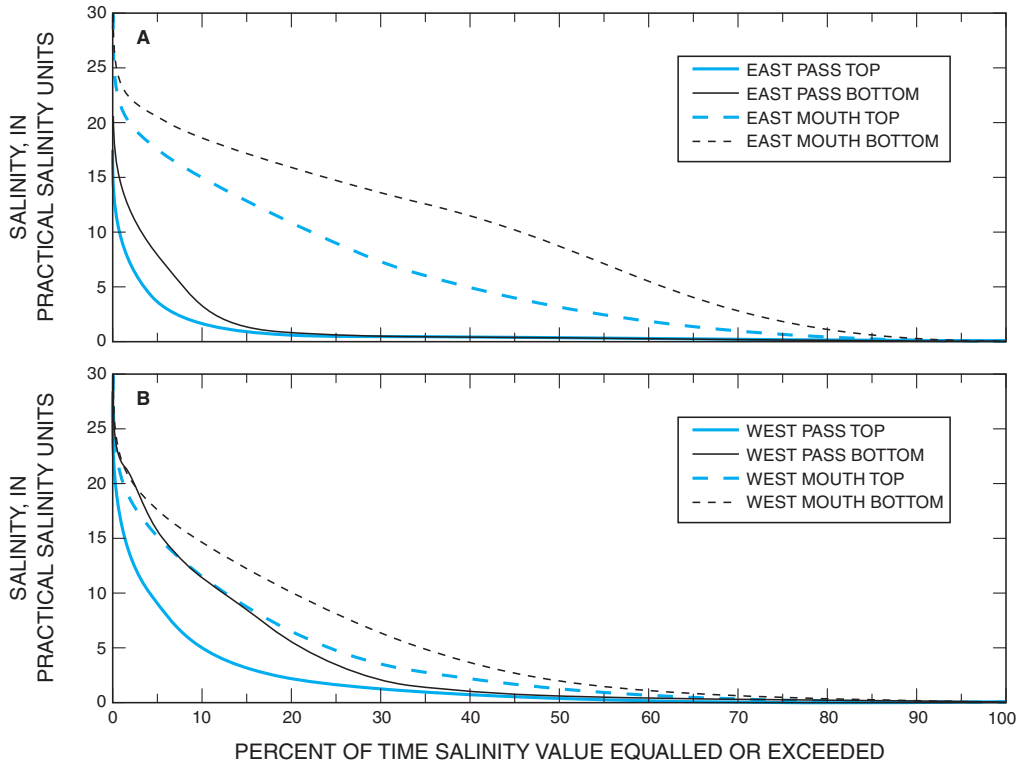

Figure 27. Duration curves for top and bottom salinity at (A) East Pass and East Mouth, and (B) West Pass and West Mouth salinity gages, October 1999–September 2000.

negated identification of a pattern. For example, at WM during October 1999–September 2000, a detided salinity of 2 psu occurred over a range of net flows of 69–298 m^3/s at AGR, and a salinity of 5 psu occurred over a range of net flows of 75–193 m^3/s. Consequently, tidal conditions and flows in the river are not the only factors that control salinity in the lower Suwannee River.

Monthly mean salinity at RB ranged from 27.4 psu in September 2000 to 33.7 psu in November 1999. Monthly maximum salinities exceeded 34 psu for all months except March, July, and August 2000, when monthly maximum values were between 31.3 and 33.8 psu. The median salinity at RB during October 1999–September 2000 was 32.5 psu, and salinity was less than 30 psu only 15 percent of the time. The low monthly mean salinity at RB during September 2000 corresponded with the highest monthly mean flow during October 1999–September 2000 at Wilcox (fig. 13), although the September 2000 monthly mean flow was only slightly higher than the mean flow in April 2000, when the monthly mean salinity at RB was 31.1 psu. In addition, some of the lowest salinities at RB during the study period occurred during July–August 2000, when the monthly mean flows at Wilcox were at a minimum for the study period.

Salinity data from measurements made by Florida State agencies in the Gulf of Mexico near the mouth of the Suwannee River were provided by the Suwannee River Water Management District (John Good, written commun., March 24, 2005). Data from the Shellfish Environmental Assessment Section (SEAS) of the Bureau of Aquaculture Environmental Services were available for 1995–2003 (figs. 31 and 32); most sites were visited multiple times. Data from the Fisheries-Independent Monitoring (FIM) program, conducted by the Florida Fish and Wildlife Resource Institute, were available for 1999–2000, with typically only one or two measurements per site; water depths were generally less than 1 m. No information on data-collection methods and quality-assurance procedures were available. Although data were collected in tidal creeks and embayments, those data are not included in the subsequent discussion. Only data collected seaward of the mouths of creeks and rivers are included (fig. 31).

Data from two SEAS sites are presented to demonstrate salinity variability in the Suwannee Sound. Site 214 is the northernmost of the two sites, and site 245 is seaward of the mouths of East Pass and Wadley Pass (fig. 31). Salinity at these sites, as well as the other SEAS sites, was measured about 10 times per year, without regard to tidal phase or river flow.

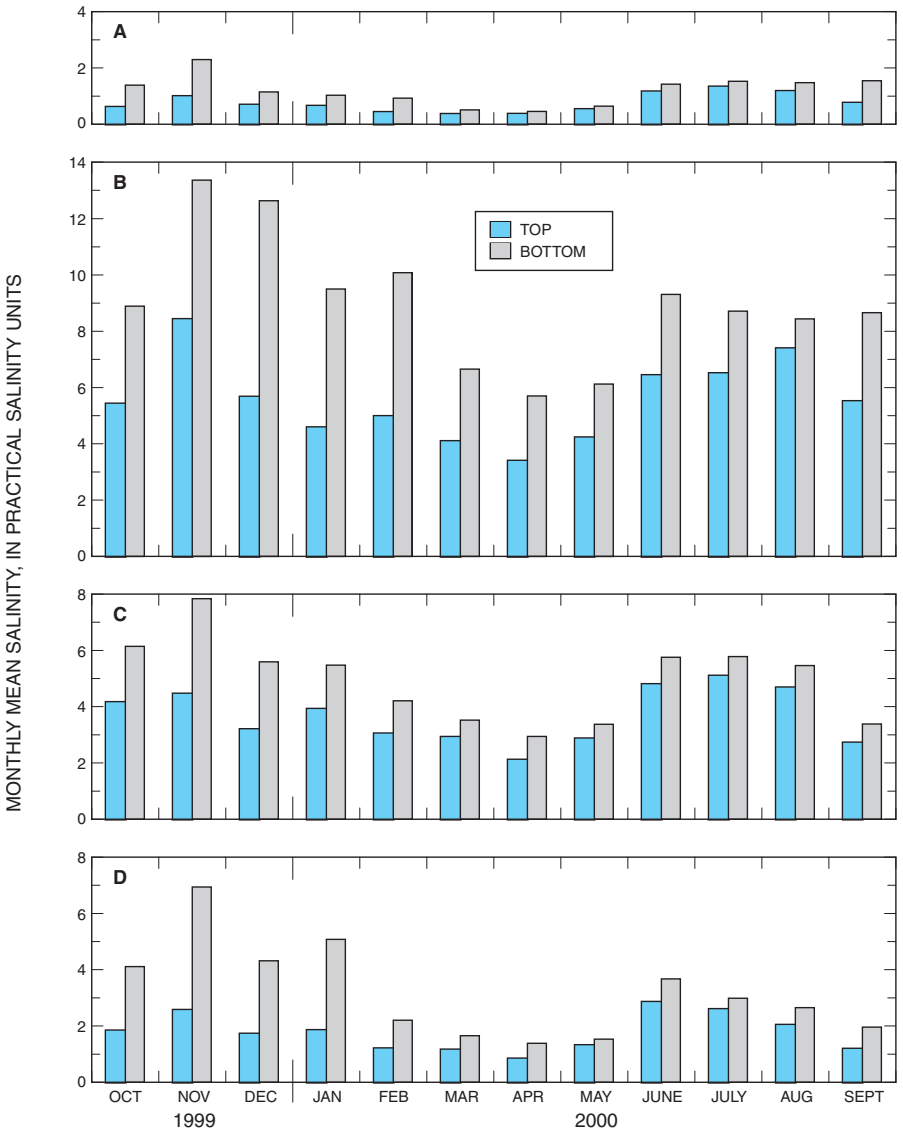

Figure 28. Monthly mean top and bottom salinity for (A) East Pass, (B) East Mouth, (C) West Pass, and (D) West Mouth salinity gages, October 1999–September 2000.

Both inter- and intra-annual variability in salinity was evident at both sites, with salinity ranging from 3–35 psu at site 214 and from 10–35 psu at site 245 during 1995–2003. Although site 245 is closer to the mouth of the Suwannee River, the minimum salinity was lower at site 214 than at 245. This could be the result of the random nature of the salinity measurements (although salinity at site 245 was about 10 psu higher than at site 214 on the day the minimum salinity was measured at site 214; fig. 32), or an indication of the influence of other freshwater sources north of the mouth of the Suwannee. Mean annual streamflow at Wilcox in 1998, which was the year with the lowest salinities as sites 214 and 245, was at the 90th percentile for 62 years of record.

Intra-annual salinity variations were typically 10–15 psu at sites 214 and 245. Salinity at RB during October 1999–September 2003 ranged from 19.6–36.8 psu. At the northwestern cluster of FIM sites (5 sites, fig. 32), salinity during 1999–2000 ranged from 30–37 psu. Even though only one measurement was made at each site during this period, results from measurements made on five different days indicate that fairly large salinity fluctuations exist in the Gulf of Mexico as far as 16 km from the mouth of Wadley Pass.

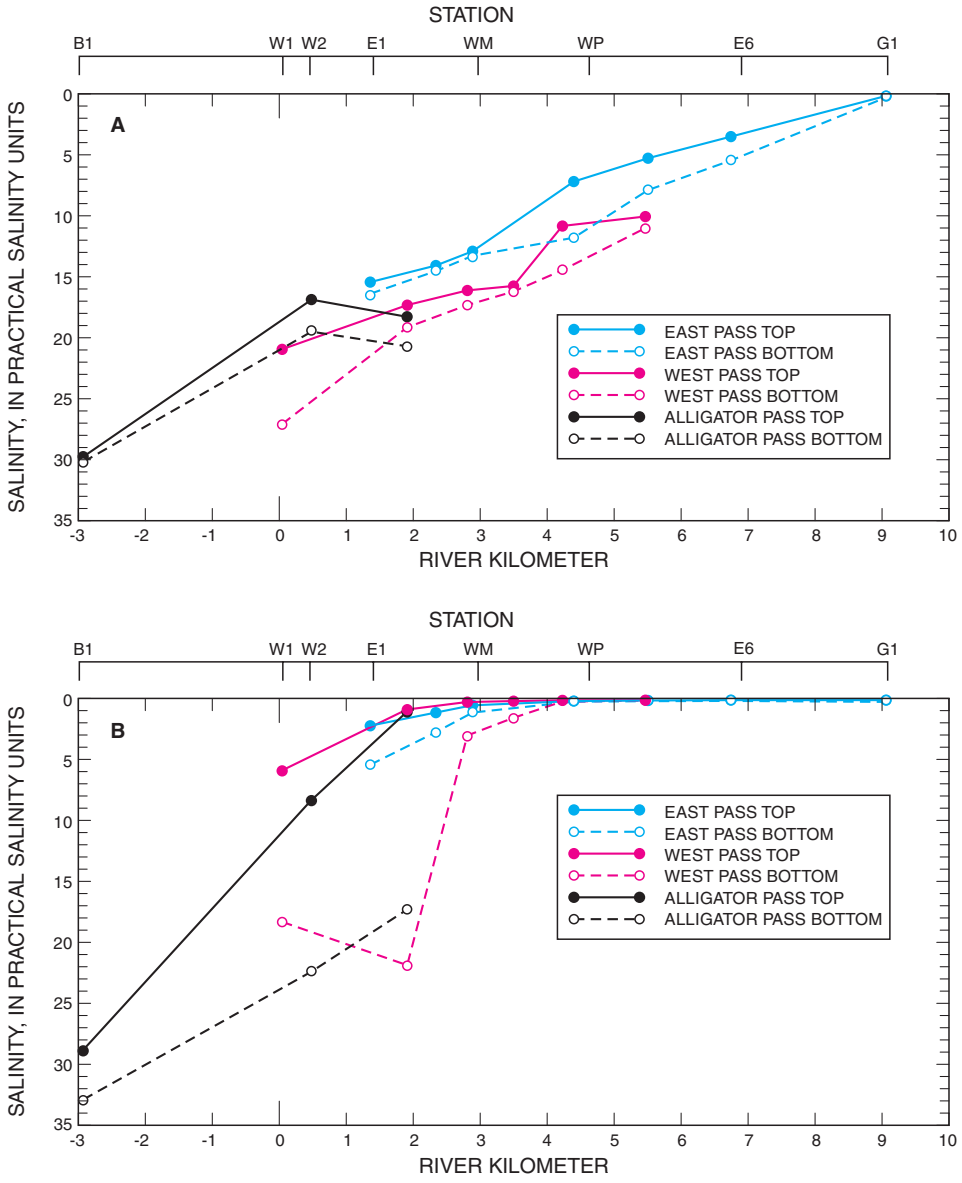

Figure 29. Top and bottom salinity distribution along East Pass, West Pass, and Alligator Pass for (A) high tide conditions and (B) low tide conditions, May 17, 2000.

Simulation of Hydrodynamics and Salt Transport

A three-dimensional, unsteady flow and transport model was constructed for the downstream-most 12 km of the Suwannee River and adjoining parts of the Gulf of Mexico. The numerical modeling code known as EFDC was configured for the Suwannee River study area. The model was calibrated and tested using data collected primarily during October 1999–September 2000. Although some data were collected during October 1998–September 1999, water year 2000 data were more complete than those collected during water year 1999. Time-varying water levels, currents, discharge, and salinity were simulated by the model.

Application of EFDC to the Suwannee River Estuary

The general form of EFDC was applied to the Suwannee River study area by (1) developing a computational grid that provides a realistic approximation of the bathymetry of the estuary; (2) specifying boundary conditions, which are primarily exchanges of mass and momentum at the upstream, Gulf of Mexico, water-surface, and bottom (riverbed and ocean floor) boundaries; and (3) defining model parameters.

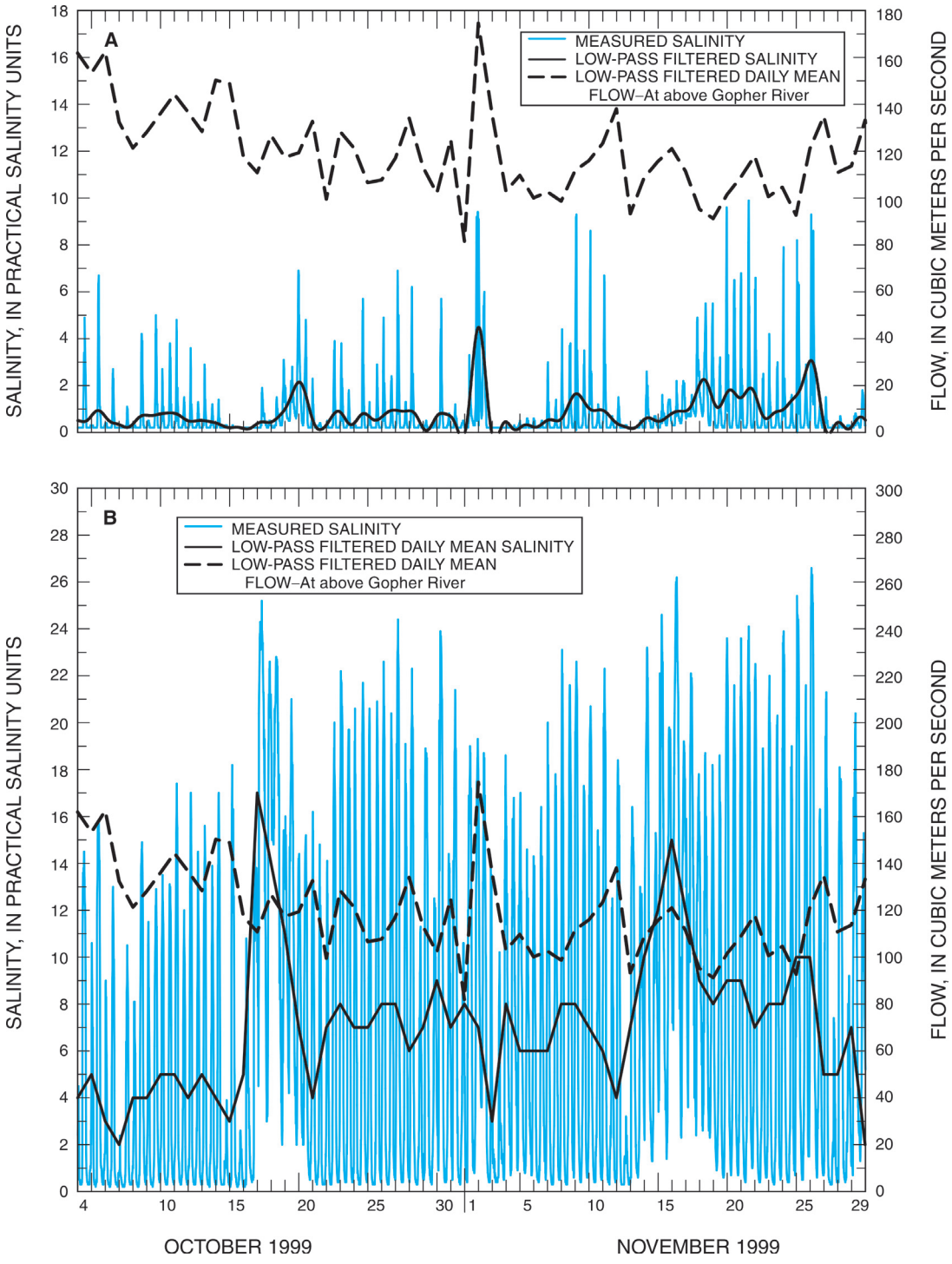

Figure 30. Measured salinity, net flow at above Gopher River, and low-pass filtered salinity for (A) East Pass top salinities and (B) West Pass bottom salinities, October 4–November 30, 1999.

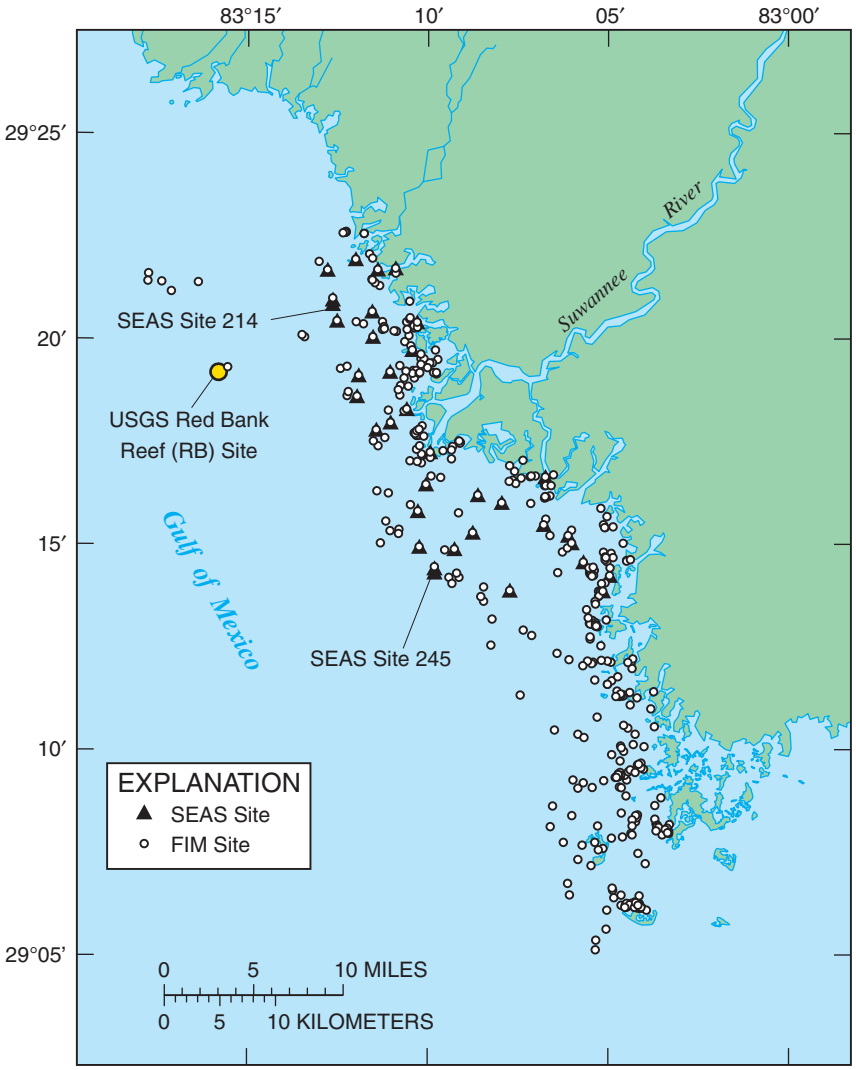

Figure 31. Locations of Shellfish Environmental Assessment Section (SEAS) and Fisheries-Independent Monitoring (FIM) program salinity measurement sites and the RB site, seaward of the mouths of creeks and rivers and in Suwannee Sound and adjacent areas.

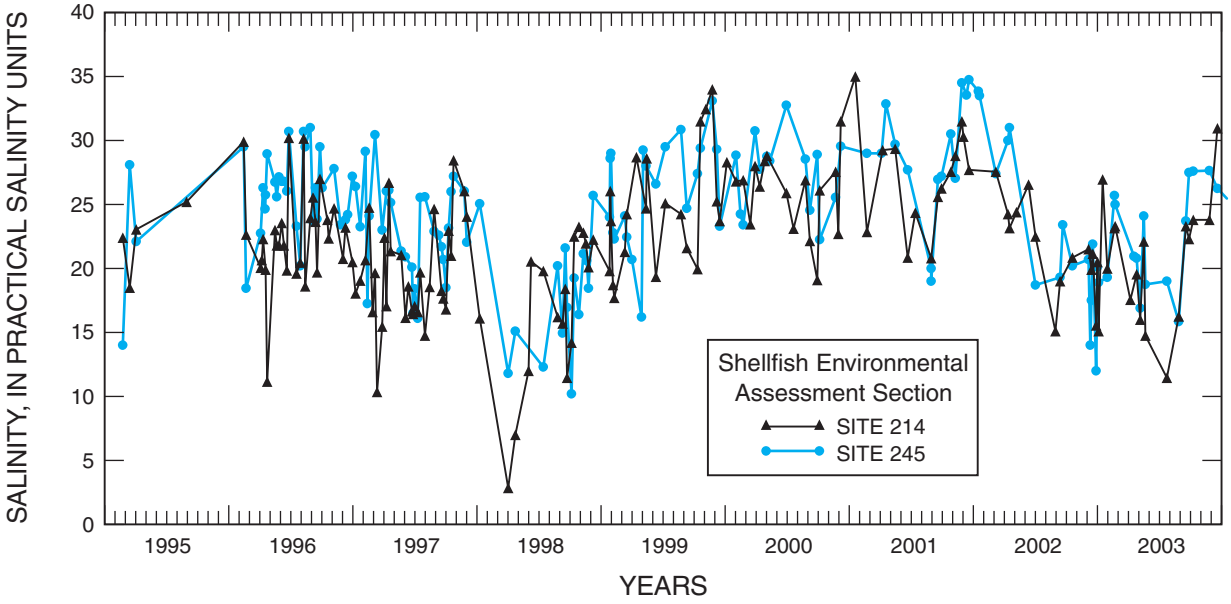

Figure 32. Salinity measured at Shellfish Environmental Assessment Section sites 214 and 245, 1995–2003 (fig. 31).

Computational Grid

The physical domain of the Suwannee River estuary model extends from the AGR streamgage, which is about 12 km from the mouth of the river, out into the Gulf of Mexico (figs. 33 and 34). Along the shore, the model domain extends northward to Horseshoe Point and southward to Cedar Key. The Gulf of Mexico boundary of the model domain is about 27.5 km due west of the mouth of East Pass, and 21 km due west of the mouth of Alligator Pass. The total area encompassed by the model is 1,038.6 km^2.

An orthogonal curvilinear computational grid was used to allow boundaries of the model to closely follow the natural boundaries of the river and the shore and to allow for greater spatial resolution in the river. The model domain contains 2,385 computational cells in each of 6 horizontal layers, giving a total of 14,310 computational cells. Computational cell dimensions range from 22–1,602 m in the x-direction, and from 39–2,492 m in the y-direction, and the area of the cells ranges from 2,100–1.62 km^2. The Cartesian representation of the computational grid, although distorted in scale, clearly illustrates the connections among cells (fig. 35).

EFDC uses the so-called sigma coordinate system (or bottom-following scheme) in the vertical direction. With sigma coordinates, the number of vertical layers in the model is the same, regardless of the water depth (fig. 36), although the relative proportion of total depth represented by each layer need not be the same. Application of the sigma coordinate system requires careful attention to ensure that horizontal gradients in pressure, current, and transported constituents are propagated correctly (Paul, 1993; Mellor and others, 1998). Six sigma layers of uniform thickness were used in the Suwannee model.

Bottom elevation, or depth below NAVD 88, were assigned to each computational cell using the approach described in "Methods." Bottom elevations in the model ranged from 1.50–9.2 m below NAVD 88. As a result, the thickness of the sigma layers in the model ranged from 0.25–1.53 m. A total of 22 percent of the computational cells, representing 16 percent of the model area, had a bottom elevation of -2.0 m or less, and 50 percent of the cells, representing 32 percent of the model area, were at an elevation of -4.0 m or less. These statistics demonstrate that (1) depths in the study area are relatively shallow, and (2) the greatest spatial resolution in the computational grid is for the shallow depths.

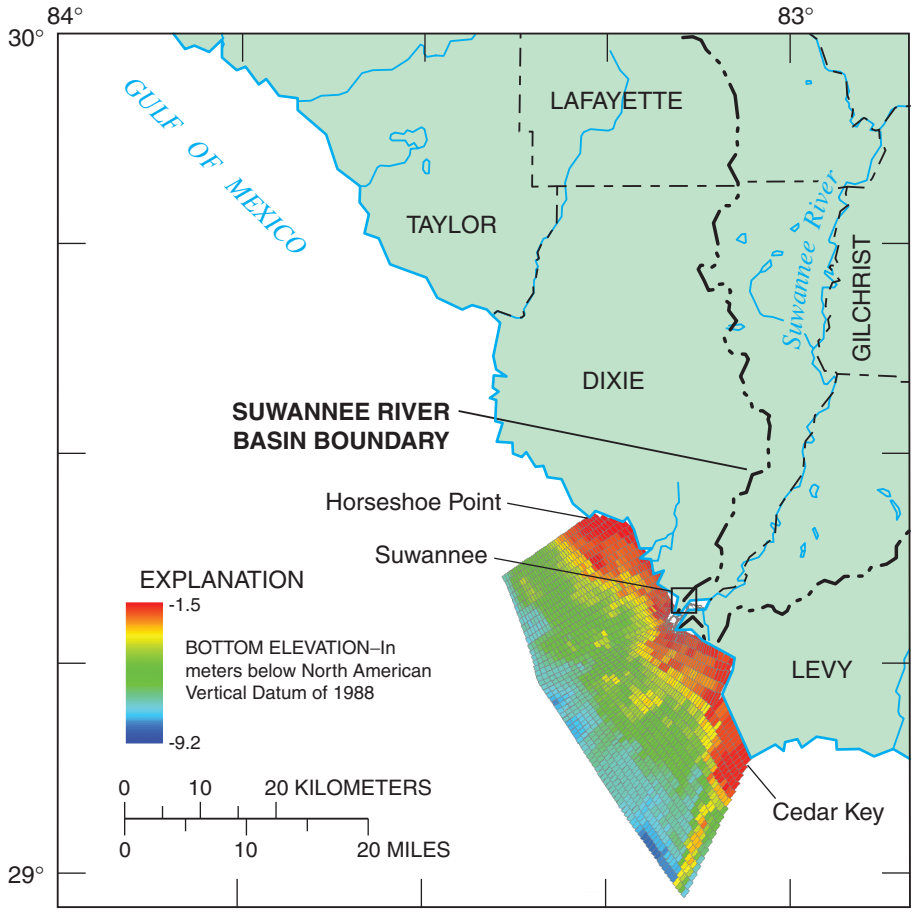

Figure 33. Computational grid for entire Suwannee River estuary model domain.

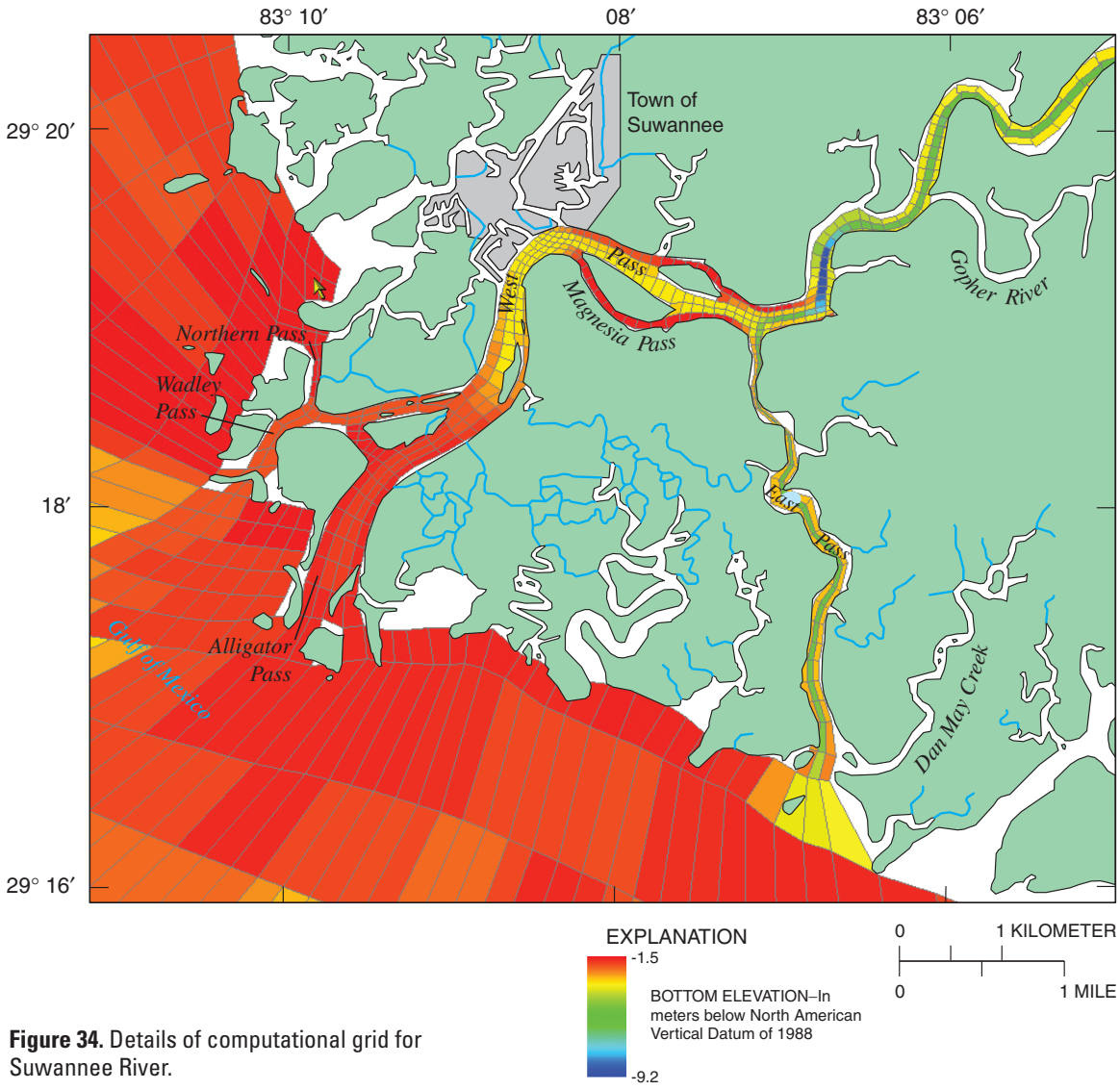

Figure 34. Details of computational grid for Suwannee River.

Boundary Conditions

Boundary conditions for the Suwannee River estuary model are a time series of data that define inflows of mass and momentum to the model domain. Outflows of mass (water and salt) are simulated by the model. Boundary conditions for the Suwannee model are described in this section.

Flow. Measured streamflow at AGR was used as the upstream boundary condition for the model. The boundary was specified at cells (58,91), (59,91), and (60,91) (fig. 35). Boundary data were provided at the 15-minute measurement interval. Streamflows at the computational time interval (5 seconds) were linearly interpolated from the 15-minute measurements.

The computational grid is 3 cells wide and 6 layers deep at the upstream boundary (fig. 36), and the total cross-sectional area at a water level of 0.0 m is 1,211.5 m^2. About 47 percent of the total area is in the center column of cells. Consequently, measured streamflow was distributed within the cross section such that 50 percent of the measured flow was in the center of the channel and 25 percent of the measured flow was in each of the two outer columns of cells. Within each column of cells, flow was distributed uniformly with depth, so that, for example, each computational cell in the center of the channel carried 8.3 percent of the measured flow.

At least 14 submarine springs have been identified along the Gulf Coast of Florida (Rosenau and others, 1998), with most of the springs located either near Tampa Bay or Apalachee Bay. Discharge from submarine springs is usually a combination of submarine fresh ground water and recirculated saline ground water (Taniguchi and others, 2002). Measurements of submarine spring discharge in the northeast Gulf of Mexico ranged from 0.2–710 m^3/s (Cable and others, 1996; 1997).

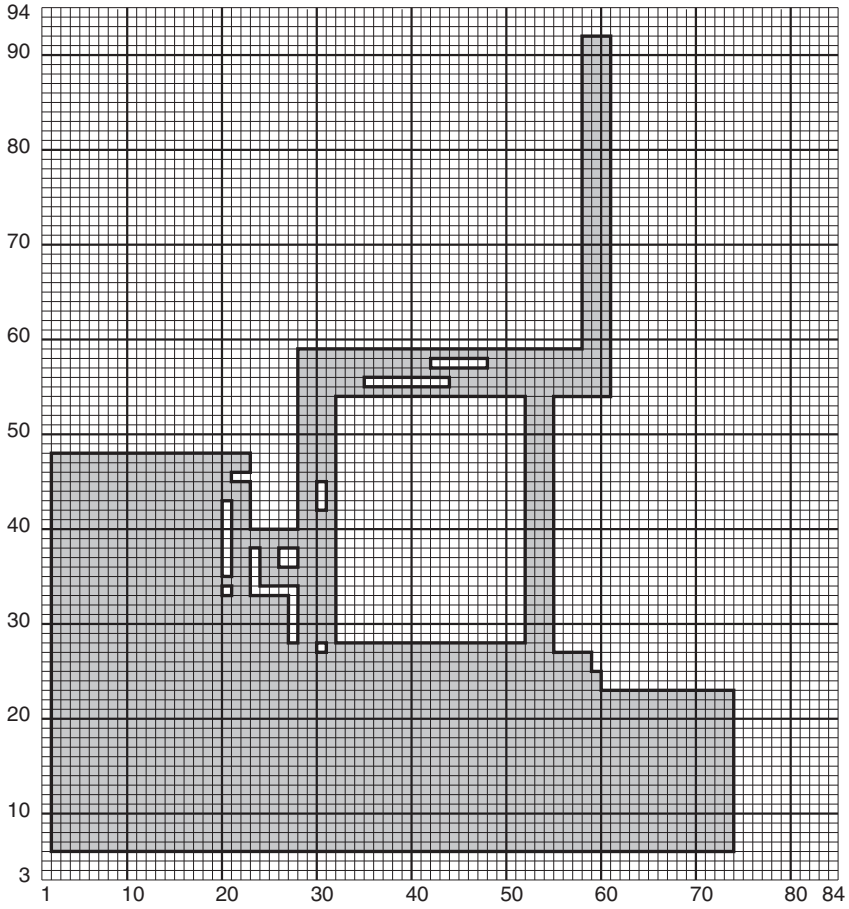

Figure 35. Cartesian representation of computational grid.

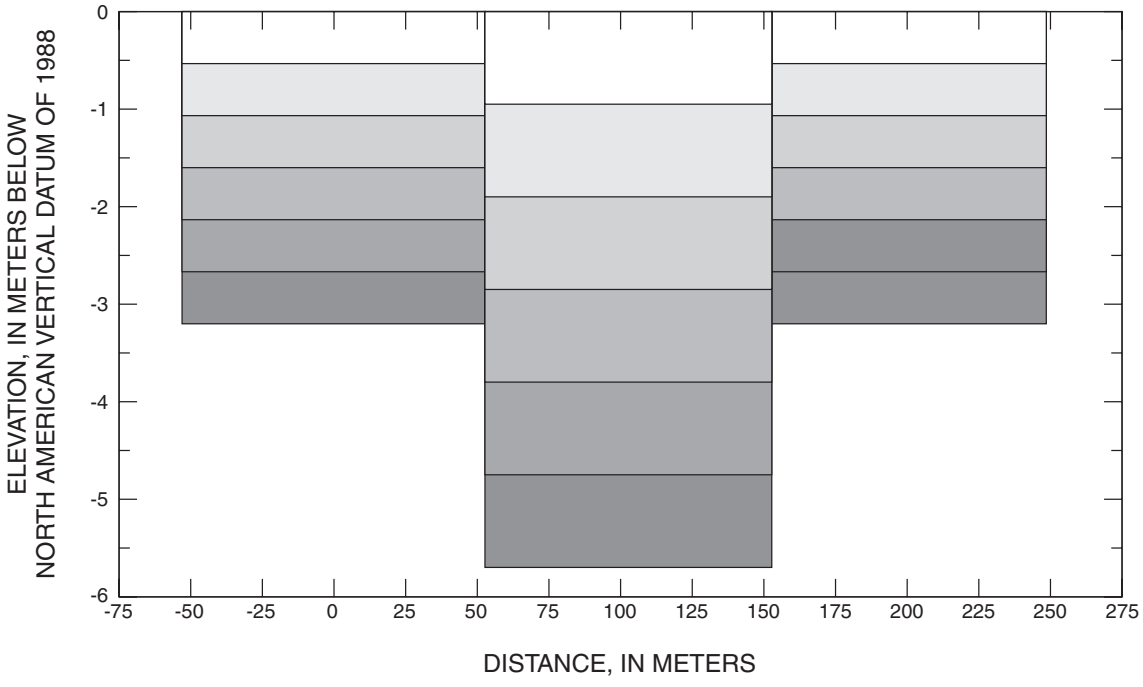

Figure 36. Elevation view of computational grid at above Gopher River streamgage site.

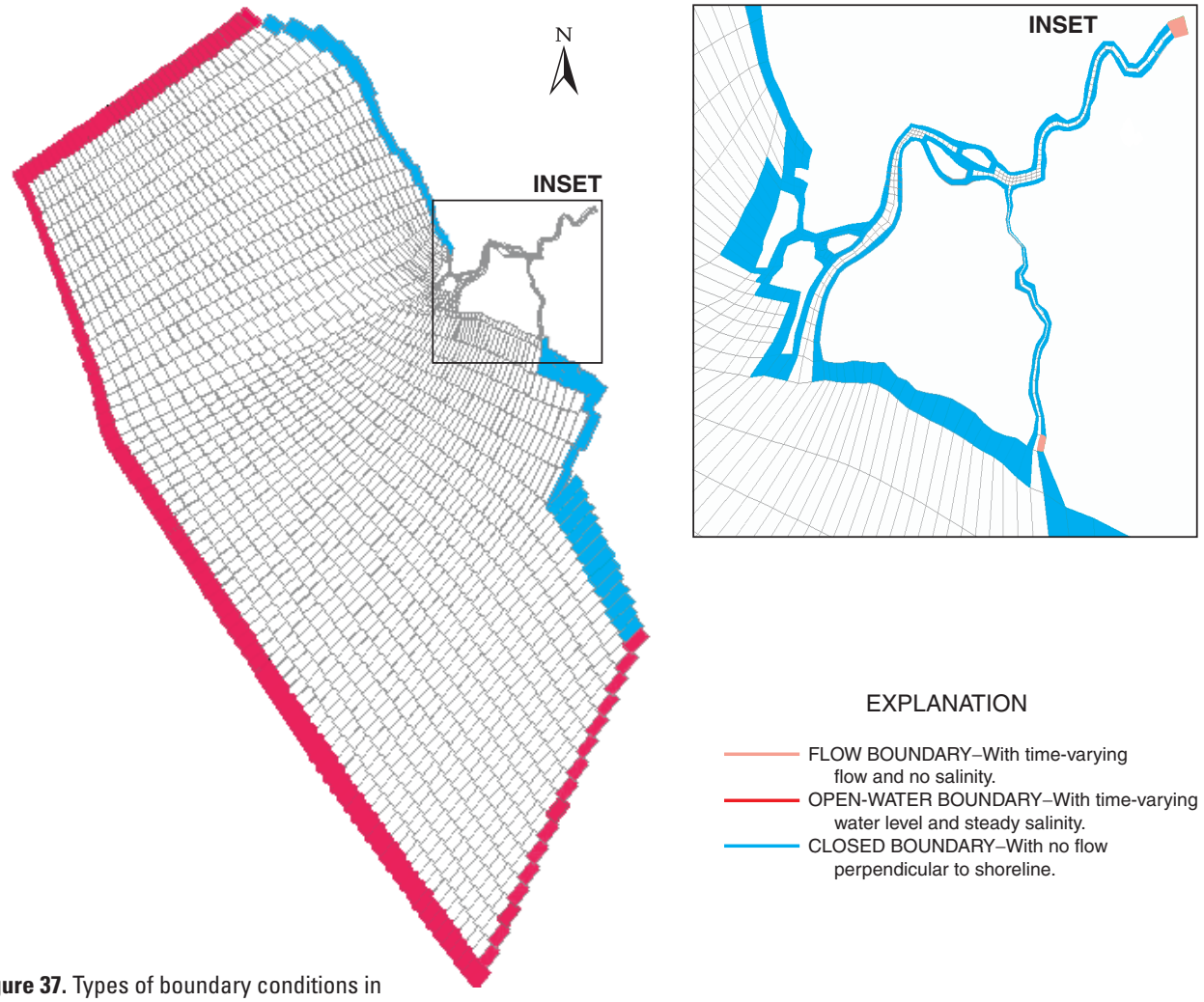

Figure 37. Types of boundary conditions in the Suwannee River estuary model.

Some studies indicate submarine springs may have an effect on seagrass health and distribution (Johannes and Hearn, 1985; Rutkowski and others, 1999).

Sources of ground-water discharge can be included as a boundary in the EFDC model. There are, however, no documented springs in the Suwannee River estuary model domain, although it seems likely that some springs or seeps could be present. Therefore, submarine ground-water discharge was not included as a boundary condition.

There also are a number of tidal creeks having small, but undetermined, catchment areas that drain to the model domain between Horseshoe Point and Cedar Key. Based solely on information from 1:24,000 and 1:100,000 topographic maps, it appears that well-defined channels extend only 2–4 km inland for the tidal creeks south of East Pass and north of Cedar Key. A few discharge measurements were made in Dan May Creek in May 2000 (fig. 11), but insufficient data exist to determine how much of the measured flow was net freshwater flow to the Gulf of Mexico.

North of Alligator Pass and south of Horseshoe Point, several tidal creeks are present that, based on mapped hydrography, appear to have stream networks that extend 10–20 km inland, indicating that these streams might be sources of freshwater to the study area. The largest of the streams is Sanders Creek (fig. 2), which may have a drainage area in excess of 1,200 km^2; Amason and Butler Creeks also appear to have somewhat extensive stream networks. Because no data is available on the amount of net freshwater flow in these creeks, the creeks initially were not included as sources of freshwater to the model domain. Sensitivity tests were subsequently performed to determine the effects of additions of freshwater from selected sources on simulated salinity.

Tides. Tidal boundary conditions were specified for all open-water boundary computational cells. The open-water boundary along the southeastern boundary (fig. 37) is about 20 km long and contains 16 computational cells. The Gulf of Mexico boundary is 49 km long and contains 72 computational cells, and the northwestern open-water boundary is about 15 km long and contains 41 computational cells, giving a total of 129 open-water boundary computational cells.

Several sources of tidal data for the study area were available, including the NOS tide gage at Cedar Key (table 1); the five USGS water-level gages within the Suwannee River (table 1); the water-level gage at RB; and estimated tides in the Gulf from numerical models. Each of these sources offers some advantages and disadvantages for providing boundary tidal data for the Suwannee River model.

Tidal conditions vary continuously throughout the Gulf and the model domain. For example, information from NOS tide tables (National Ocean Service, 2004) indicates that, on average, high water at Cedar Key occurs 3 minutes before high water at the mouth of the Suwannee River, and 9 minutes before high water at Pepperfish Keys (about 9 km north, measured along the shoreline, of Horseshoe Point, and about 30 km northwest of the mouth of Wadley Pass). Low water at Cedar Key occurs, on average, 14 minutes before low water at the mouth of the Suwannee River. This means that, in general, during falling tides, the water surface is higher at the mouth of the Suwannee River than at Cedar Key, thereby indicating that Suwannee River freshwater should generally flow to the south on falling tides (Siegal and others, 1996). There also is about a 0.02 m difference between high-water elevation at the mouth of the Suwannee River and at Cedar Key, and about a 0.03 m difference between low-water elevation at the two locations.

ADCIRC is a barotropic hydrodynamic model with a domain that includes the North Atlantic Ocean from the 60 degree west meridian east to the eastern shore of the United States and Canada, the Gulf of Mexico, and the Caribbean Sea (Luettich and others, 1992; Westerink and others, 1994). The model was used to develop a database of tidal elevation and velocity harmonic constituents for this region (Mukai and others, 2001). Information from the database was subsequently used in this study to estimate astronomical tides at selected locations around the Suwannee River model domain (fig. 38).

The advantage of using the ADCIRC-generated tidal constituent database for defining tidal boundary conditions is that very detailed information on the spatial and temporal variations in tides along the model boundary can be estimated with some certainty. For example, results from tides computed from ADCIRC tidal constituents indicate the tidal amplitude is greater near the shore than along the Gulf boundaries of the model domain (fig. 38), which is information that is not available from tide tables or measured tides. The disadvantage of using the tidal constituent database is that water levels in the Suwannee River model domain are forced by synoptic-scale winds and barometric pressure gradients as well as by astronomical tides, so the astronomical tides predicted from harmonic constituents do not always capture the actual water-level variations (fig. 39).

As previously discussed, water levels measured at the five USGS Suwannee River water-level gages do not accurately reflect tidal conditions in the Gulf of Mexico. Tidal fluctuations in the river are affected substantially by frictional effects near the shore where the water is quite shallow, and by river channel morphometry. The USGS water-level recorder at site RB was set to an arbitrary datum (which varied during the data-collection period) because land surveys could not be run to the site, so data from that site could not be used to provide a tidal boundary condition. The record at the RB site also was less complete than at the other USGS sites.

Tide levels have been measured by NOS at Cedar Key since 1914; hourly and 6-minute tide data are available beginning in 1997 (National Oceanic and Atmospheric Administration, 2003). Verified tidal harmonic constituents also are available for this station so that astronomical tides can be predicted for unmeasured time periods.

Because of the potential difficulties associated with using astronomical tides predicted from ADCIRC-generated harmonic constituents (wind setup not included) and the USGS Suwannee River data (not representative of Gulf conditions), data from the Cedar Key tidal gage were used to construct the tidal boundary conditions. Hourly tide data were retrieved for Cedar Key, and water levels were adjusted to NAVD 88 elevation. (Data may be retrieved as elevation above mean lower low water, which is 0.687 m below NAVD 88 datum, or as elevation above mean sea level, which is 0.066 m below NAVD 88 datum.) Tide data at the computational time interval was interpolated from the hourly boundary-condition data.

Cedar Key tide data were missing for a 13-hour period between December 31, 1999, and January 1, 2000, and between June 23, 2000, at 5:00 p.m. and August 2, 2000, at 10:00 a.m. Astronomical tides predicted for Cedar Key were examined near the periods of missing data and were found to represent measured tides reasonably well (fig. 39). As a result, the predicted astronomical tides were assumed to be a reliable estimate of Cedar Key tides during the periods of missing data. This assumption means that model performance as measured by differences between simulated and measured water levels may not be as good for the periods when measured tide data are missing. Applications of the model for comparing different scenarios, however, will not be affected by the assumption.

Options are available within EFDC to adjust boundary water levels. Time may be adjusted by adding a constant value (positive or negative) to all of the observation times. This option was used to adjust Cedar Key measured tides to tides around the model boundary. High (low) water at the northern boundary of the model domain occurs about 6 (22) minutes after high (low) water at Cedar Key. Determination of the correct time adjustments for tides in each of the boundary computational cells was part of the model calibration process. Adjustments also can be made to measured water levels used for boundary by adding a constant value to each measurement. This adjustment, in effect, modifies the tidal datum and also was part of the calibration process.

Salinity. Salinity-boundary conditions are required for each open-water boundary computational cell, and for each of the 6 vertical layers in these cells (fig. 37). Based on measurements during the study (see previous section) salinity at AGR was always assumed to be zero. Salinity data that could be used to construct the seaward boundary conditions are very limited, and most data were collected landward of Suwannee Reef (fig. 31).

Orlando and others (1993) cite unpublished Florida Department of Natural Resources data collected landward of Suwannee Reef in October–December 1984 and February–April 1988. During the 1984 period, monthly mean streamflow at Wilcox was about 10 percent lower than normal for the time of year. Surface salinity near the shore and about 7 km north of the mouth of Northern Pass was 25 psu, and bottom salinity at that location was 30 psu. Surface and bottom salinity 4 km south of the mouth of East Pass and near the shore averaged 20 psu. Streamflow during the 1988 period was near normal during February and April and about 50 percent greater than normal during March. In general, salinity during the 1988 period was about 10 psu less than average salinity during the 1984 lower flow conditions.

Salinity was monitored more or less continuously during November 1991–November 1992 at locations about 1 km seaward of the mouths of Wadley Pass, Alligator Pass, and East Pass, respectively, at one location adjacent to and landward of Suwannee Reef, and at one location about 1 km seaward of the reef (Siegal and others, 1996). Streamflow at Wilcox during this period was generally lower than normal. Monthly mean flows for 8 of the 13 months during the data-collection period were lower than normal (78–94 percent of normal), and flows during 4 of the other months were no more than 105 percent of normal. Salinity landward of Suwannee Reef was almost always 30 psu or less, ranging from near 0 psu at low tide to as much as 30 psu at high tide. At the site seaward of the reef, salinity typically ranged from 15–30 psu.

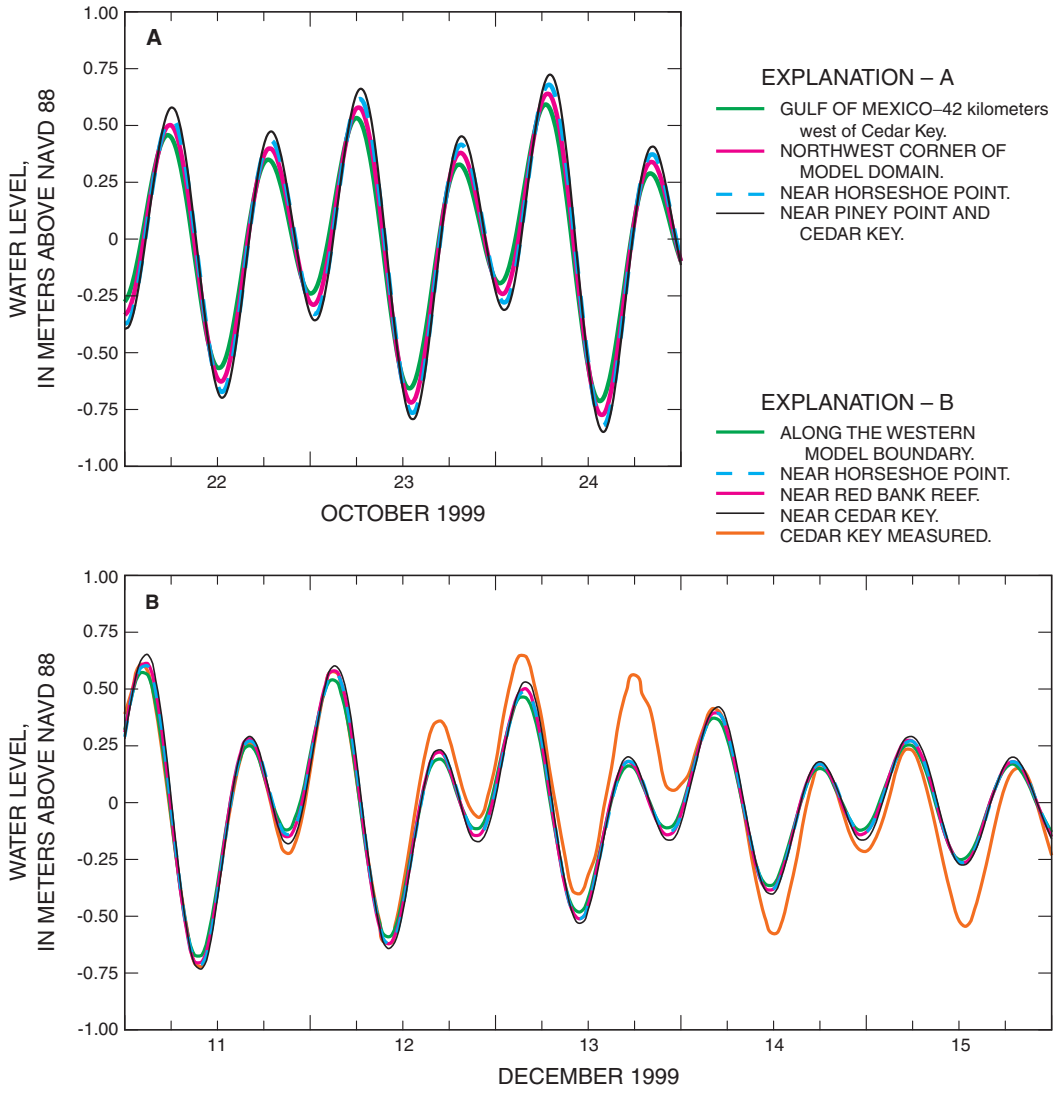

Figure 38. Estimated astronomical tides at selected locations in the Suwannee River model domain for (A) October 22–24, 1999, and (B) December 11–15, 1999, along with measured water level at Cedar Key.

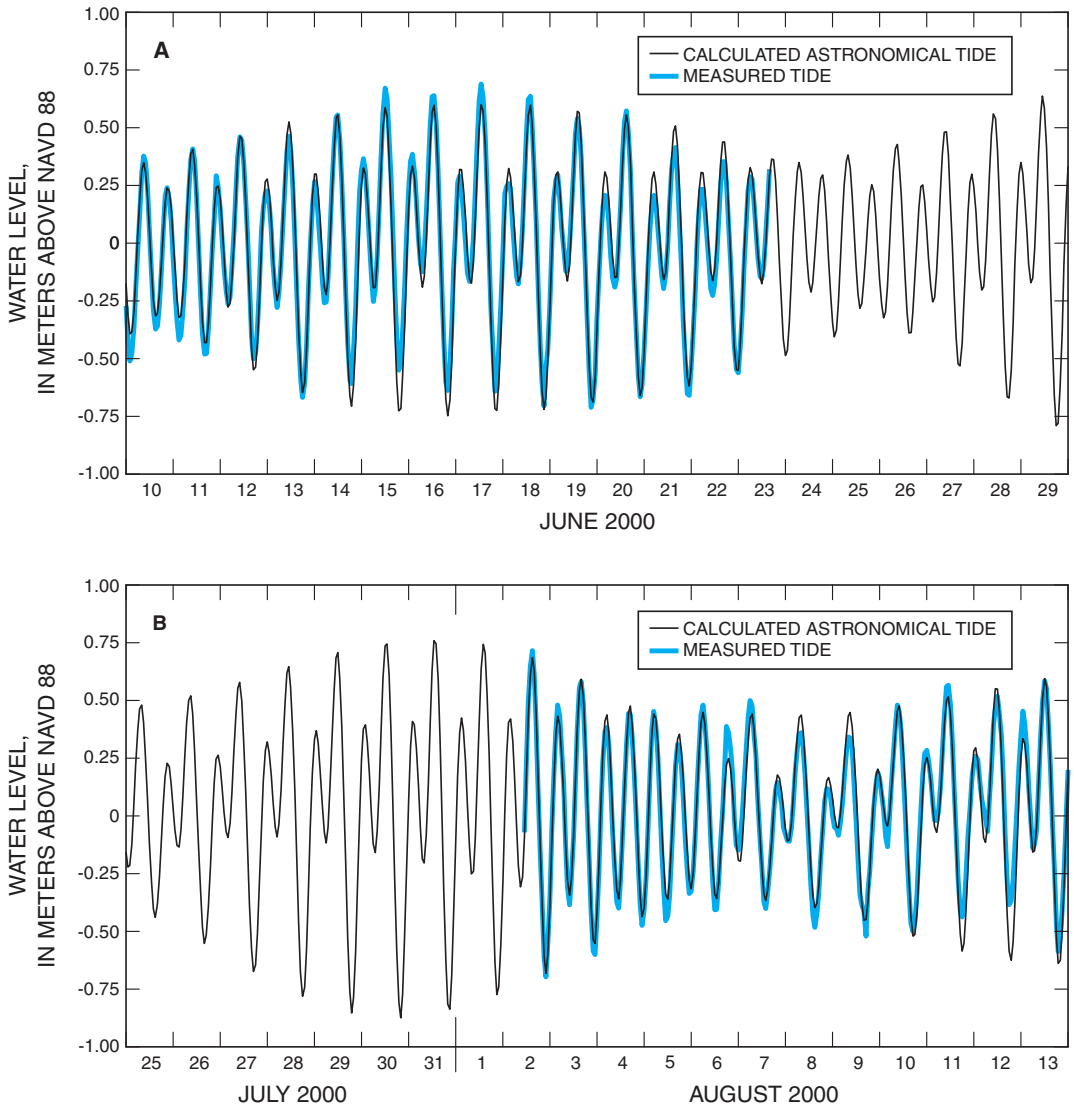

Figure 39. Water levels for measured tides and calculated astronomical tides for Cedar Key tidal gage, (A) June 10–30, 2000, and (B) July 25–August 14, 2000.

A total of 40 percent of the salinity variation was due to tidal fluctuations and 20 percent of the salinity variation was due to nontidal sea-level fluctuations occurring at the 3–10 day period and typically associated with frontal passage. Siegal and others (1996) also concluded that salinity seaward of Suwannee Reef exhibited little seasonal variability, although data from the five FIM sites previously discussed suggest otherwise.

During 1999–2000, 382 salinity measurements were recorded by FIM at 382 sites in the study area (fig. 31). Most of the measurements were made at distinct sites, although many of the measurements were made at locations that were within 250 m of other measurement locations. Salinity values in the northwest group of sites and at sites located in the vicinity of Cedar Key were all greater than 25 psu, and most were greater than 30 psu (fig. 40). Salinity was more variable at the locations near the shore, although all salinities less than 10 psu were within 1.5 km of the shore, and all salinities less than 15 psu were within 3 km of the shore. Nevertheless, salinities as high as 30 psu also were measured very near the shore.

Salinity and water temperature were recorded at one depth at RB during October 1999–June 2000 (fig. 41). The sensor was placed about mid-depth at high tide, but the water depth was shallow and the sensor occasionally was not fully submerged at low tide. Salinity was typically 30–36 psu and exhibited no tidal variation.

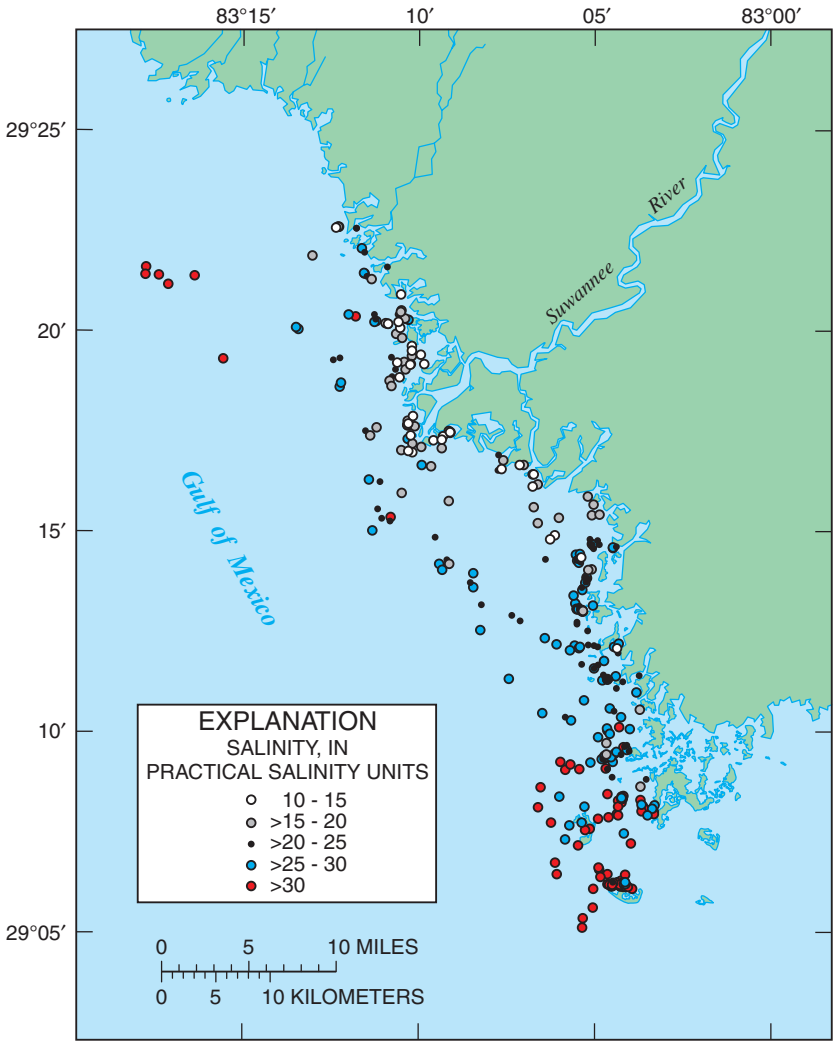

Figure 40. Range of salinities measured at Fisheries-Independent Monitoring program sites near the Suwannee River mouth, 1999–2000.

The seaward-most salinity readings in the study area were reported by Bledsoe (1998). Surface and bottom measurements were made monthly during September–November 1996 (flow at Wilcox was 35–90 percent of average monthly mean flow) and March 1997 (flow at Wilcox was about equal to long-term average monthly mean). Nine stations along a transect that ran approximately west-southwest from the mouth of Wadley Pass were sampled; stations were about 3.7 km apart. The two seaward-most stations were probably outside of the Suwannee River estuary model domain. With the exception of a surface reading in March (34 psu), salinity at these two stations was always 35 psu. Salinity was always 30 psu or greater at the four stations located 20 km or more from the shore.

Information from these studies provide insight into establishment of the salinity-boundary conditions. More quantitative data for establishing the salinity-boundary conditions during the study period, such as was available for the tidal boundary conditions, were not available. Based on the previous studies reported here, it is reasonable to establish a constant 35 psu salinity for all surface boundary cells on the seaward boundary, 36 psu for all bottom boundary cells, and salinity linearly interpolated for the intermediate 4 computational layers. In the absence of any other information, salinity was assumed to be constant in time all along the boundary.

Boundary conditions along the northwest and southeast (fig. 37) are more difficult to establish. Salinity near the shore probably varies periodically with the tides (Siegel and others, 1996). Salinity variations in response to changes in regional streamflow patterns are also probably present near the shore (Orlando and others, 1993; Siegal and others, 1996; fig. 40), but the seaward extent of those variations and the seaward gradient in lag between streamflow and salinity response is not known. In the absence of any information on temporal salinity variations along or near the model boundaries, salinity-boundary conditions along the northwestern and southeastern boundaries were assumed to be time-invariant. Salinity along these boundaries did vary horizontally (from the shore seaward) and vertically, as subsequently described.

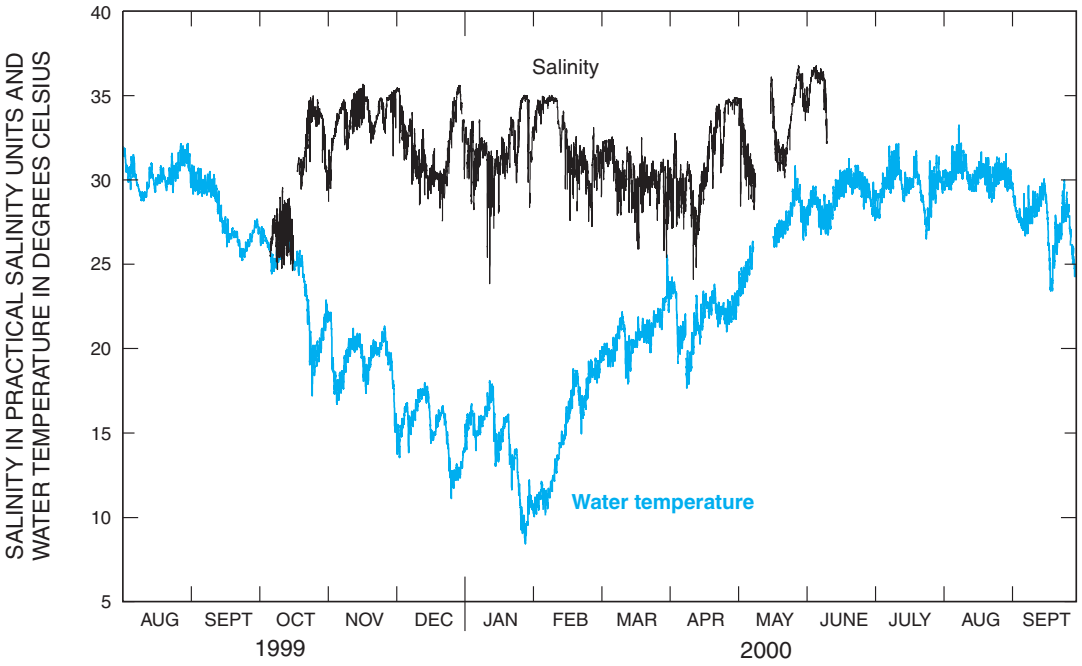

Figure 41. Salinity and water temperature measured at 15-minute intervals at Red Bank Reef during October 1999–September 2000.

Salinity values used for the boundary conditions along the northwestern and southeastern boundary were determined as part of model calibration. Nevertheless, salinity along the boundaries cannot be expected to match actual conditions on any given date during the study period. As a result, good agreement between measured and simulated salinity may be difficult to attain during certain periods, particularly in areas seaward of the mouth of the Suwannee River. The model boundaries, particularly the western boundary, should be sufficiently far from the primary area of interest (Suwannee River) that the effect of these boundary conditions on salinity in the area landward of Suwannee Reef should be moderated. This approach for establishment of the salinity-boundary conditions will allow the Suwannee River model to be used to evaluate salinity changes in the model domain in response to factors other than changes in Gulf of Mexico salinity.

Wind. Wind data were available from three sites in or near the study area: the USGS WP wind gage, and the NOS KB and CK sites (table 1). The effects of synoptic, or regional, winds on water level in the study area are reflected in the Cedar Key tide data. West Pass wind data were used in the model to account for local wind effects on velocity and mixing in the river channel.

Other Model Options and Coefficients

A constant computational timestep of 5 seconds was used for all simulations. The Courant numbers were highest in cell (54,59), which is in the center of the channel just upstream from the East Pass-West Pass split, and were never more than 0.62, well below the threshold of 1.0.

Several different options for numerical solution of the governing equations are available within EFDC. The upwind finite difference scheme was used to solve the horizontal momentum equations. Coriolis and buoyancy forcing are included in the model.

Smoothing of bottom topography can be done automatically by EFDC to improve the stability of the solution and to reduce pressure gradient errors associated with the sigma coordinate system. No depth smoothing was done for the Suwannee model.

Bottom roughness height, which is the logarithmic boundary layer height, can be assigned globally for all cells, or on a cell-by-cell basis. The cell-by-cell approach was initially used for the Suwannee model, although as a result of model calibration, roughness height was assumed to be uniform throughout the model domain. Bank roughness, bed irregularities within computational cells, and channel morphology were the primary factors affecting roughness within the river. Bottom roughness was one of the main calibration parameters.

Turbulent diffusion parameters included:

- 0.001 m^2/s constant horizontal momentum and mass diffusivity coefficient;
- 0.005 dimensionless horizontal momentum diffusivity:
- $1x10^{-6}$ m^2/s molecular kinematic viscosity;
- $1x10^{-9}$ m^2/s molecular diffusivity;
- $1x10^{-6}$ m^2/s minimum kinematic eddy viscosity;
- $1x10^{-8}$ minimum eddy diffusivity; and
- 0.01 m bottom roughness height.

Vertical mixing parameters (eddy diffusivity and kinematic viscosity) are calculated in EFDC using the Mellor-Yamada (Mellor and Yamada, 1982) turbulence closure scheme, as modified by Galperin and others (1988). The scheme uses nine parameters, which were derived from laboratory studies. These parameters were not adjusted for the Suwannee model.

Calibration and Testing

Selected boundary conditions, model parameters, and bathymetry were adjusted to achieve the best agreement between model simulations and data. This section describes the calibration process, selected results, and limited testing. Comparisons between measurements and simulations are made for November–December 1999 and June–July 2000. October 1999 and May 2000 were used as model spin-up periods.

Tides. As previously noted, CK tides were used to describe tidal conditions around boundaries of the model domain, and tides vary in phase and amplitude around the model boundary, so some adjustments to CK tides were made during model calibration to represent these variations.

The final tidal boundary conditions were as follows. Tides at the southeast corner of the model domain (near Cedar Key) were equal to CK tides. Tides at the northeast corner of the model domain (near Horseshoe Point) were equal to CK tides minus 15 minutes. In other words, in this model, tides (both high and low) were always assumed to arrive at Horseshoe Point 15 minutes after arriving at CK. The time difference at boundary cells between CK and Horseshoe Point gradually varied from 0–15 minutes.

This assumption about tidal boundary conditions is somewhat consistent with observations, except that data indicate that the phase difference (time of arrival of a given tide) varies from high tide to low tide. In addition, data indicate a slight variation in tidal amplitude around the model boundary, but these boundary conditions assume the amplitude is spatially constant on the boundary.

As a part of the model calibration process, Cedar Key tides were adjusted by -0.05 m to improve agreement between measured and simulated water levels. A constant resistance coefficient of 0.01 m was used throughout the model domain.

Monthly mean differences between measured and simulated water levels (table 5) were computed as the monthly mean of the hourly differences between measured and simulated water levels (measured water level minus simulated). A negative monthly mean difference indicates that, on average, simulated water levels were greater than measured values. Monthly mean differences generally were positive, except at EM, and less than 0.1 m (table 5). Monthly mean absolute differences between measured and simulated water levels were calculated as the monthly mean of the absolute value of the hourly differences between measured and simulated values. Root mean square (RMS) differences were computed by (1) calculating the difference between measured and simulated values, (2) squaring each of the hourly differences, (3) computing the monthly mean of the squared differences, and (4) calculating the square root of the monthly mean of the squared differences. With the exception of EM, where water levels were low relative to the other sites (fig. 14), RMS differences ranged between 7–28 cm.

High water levels at WP (fig. 42A) and WM were overpredicted by about 5–20 cm, although simulated tidal amplitudes generally agreed with measured values. Differences between measured and simulated water levels at EP (fig. 42B) were smaller than at WP; errors at EP were typically greater for neap tides than spring tides. Tidal amplitudes at EM were greater than measured values.

Table 5. Measured and simulated water-level statistics for East Pass, East Mouth, West Pass, and West Mouth.

[Water-level differences, in meters]

Month	East Pass			East Mouth			West Pass			West Mouth		
	Monthly mean difference	Monthly mean absolute difference	Root mean squared difference	Monthly mean difference	Monthly mean absolute difference	Root mean squared difference	Monthly mean difference	Monthly mean absolute difference	Root mean squared difference	Monthly mean difference	Monthly mean absolute difference	Root mean squared difference
Oct. 1999	0.08	0.10	0.13	-0.07	0.09	0.11	0.01	0.07	0.09	-0.01	0.06	0.08
Nov. 1999	-0.02	0.07	0.08	-0.07	0.09	0.10	0.02	0.06	0.07	0.0	0.05	0.07
Dec. 1999	-0.03	0.08	0.11	-0.05	0.08	0.09	0.03	0.07	0.08	0.01	0.06	0.08
May 2000	0.03	0.20	0.23	-0.02	0.28	0.31	0.04	0.22	0.25	0.02	0.23	0.26
June 2000	0.05	0.20	0.23	-0.02	0.27	0.31	0.05	0.21	0.25	0.04	0.23	0.26
July 2000	0.08	0.21	0.25	-0.01	0.29	0.34	0.08	0.23	0.28	0.04	0.23	0.28

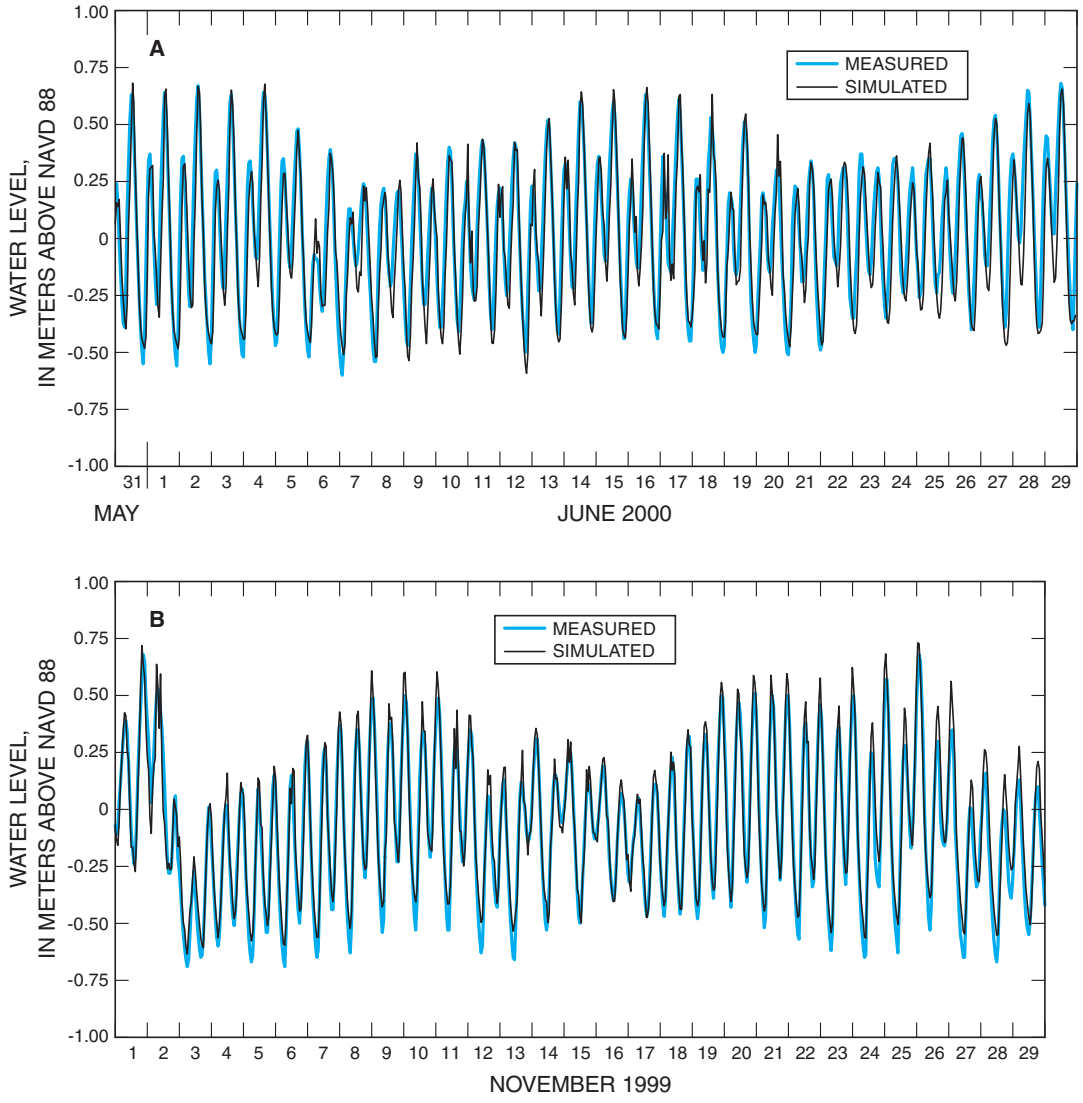

Figure 42. Measured and simulated water levels at (A) West Pass, May 31–June 29, 2000, and (B) East Pass, November 1–29, 1999.

Harmonic analysis was performed on measured and simulated water levels from AGR, EP, EM, WP, and WM for October–December, 1999 (table 6). Measured and simulated amplitudes of the principal diurnal (O1 and K1) and semidiurnal (M2 and S2) harmonics differed by no more than 6 cm, and most differed by less than 2 cm.

Flow. Measured 15-minute flows at AGR were used as the upstream flow boundary condition. During the calibration process, testing was conducted to determine the effect of additional streamflow boundaries on model performance. Possibilities for these additional inflows included the small streams draining directly to the coast north and south of the Suwannee River, including Sanders Creek (fig. 2) to the north and Dan May Creek (fig. 4) to the south.

A total of 36 discharge measurements were made in Dan May Creek during May 30–June 2, 2000 (fig. 26), with 15 of those measurements made during ebb flow. Ebb flows ranged from 1–92 m^3/s and flood flows ranged from 1–144 m^3/s. Insufficient data were available, however, to determine net freshwater flows in Dan May Creek, and no streamflow data were available for the other tidal creeks draining to the model domain. A single salinity measurement was made by FIM near the mouth of Dan May Creek on September 12, 2000. Near-surface salinity was 3.2 psu and near-bottom salinity was 15.3 psu. The high degree of stratification and relatively low surface salinity indicate that freshwater could be flowing down the creek, although the source of the freshwater is unknown.

Table 6. Differences (measured minus simulated) between measured and simulated tidal amplitude for selected harmonic constituents at above Gopher River, East Pass, East Mouth, West Pass, and West Mouth water-level gages, October–December 1999.

Name	Symbol	Difference between measured and simulated amplitude (meters)				
		Above Gopher River	East Pass	East Mouth	West Pass	West Mouth
Principle lunar semidiurnal	M2	-0.006	-0.001	-0.064	-0.002	0.013
Principle solar semidiurnal	S2	0.006	0.008	-0.024	0.002	0.015
Luni-solar diurnal	K1	0.015	0.018	-0.004	0.022	0.024
M2 overtide, quarter diurnal	M4	-0.025	-0.023	-0.006	-0.018	-0.016
Principle lunar diurnal	O1	0.015	0.021	-0.002	0.023	0.021

As previously noted, the average net flow at AGR was about 13 m^3/s less than the average of the sum of the net flows at EP and WP during October 1999–September 2000. Some of the flow measured at AGR could have bypassed the streamgages at EP and WP by flowing across the marshes south of AGR and east of East Pass, although no data are available to confirm or refute this. The inclusion of more extensive tidal marsh areas, including wetting and drying of marsh computational cells, in the model domain might provide insight into whether this possible short-circuiting of the flow is an important process.

Model testing indicated that salinity simulations in East Pass were improved by the addition of a freshwater boundary condition at Dan May Creek (fig. 37), but no improvements in simulated salinity were noted by the addition of freshwater sources to the north of West Pass. As a result, a constant freshwater inflow boundary of 15 m^3/s was added at the computational cell (54,28), which is on the east side of East Pass at its mouth.

This assumed freshwater inflow from Dan May Creek in the model does not represent the total tidal flow in Dan May Creek at any given time, as indicated by the discharge measurements made in May–June 2000. The constant 15-m^3/s freshwater input, however, could be a reasonable approximation to freshwater additions to Suwannee Sound in the vicinity of East Pass, and these inflows do appear to have an effect on East Pass salinity. The assumed flow of 15 m^3/s is likely near the minimum amount of freshwater flow draining to the coast directly east of East Pass, because flows in the Suwannee River were at record lows during the study period. At higher river stages and ground-water levels, freshwater flows directly to the coast probably would be higher than during the study period. Moreover, because net flows in the Suwannee River were relatively constant during the study period (fig. 12), the assumption of a constant net flow from Dan May Creek is reasonable, although some seasonal variation might be expected because of greater evapotranspiration in the spring and summer. During more typical flow years when streamflows are highest in the late spring (fig. 13), seasonal variation in freshwater inputs directly to the coast probably also vary.

Simulated flows at EP and WP generally were less than measured flows (fig. 43). The streamflow amplitude (difference between maximum flood flow and maximum ebb flow) generally was simulated accurately at EP, but simulated ebb flows were less than measured flows and simulated flood flows were greater (more negative) than measured (fig. 43A). The mean difference between measured and simulated flows was 21 m^3/s for November–December at EP, which is less than 5 percent of the total flow range at EP during October 1999–September 2000, and the mean absolute difference was 34 m^3/s. The mean difference between measured and simulated flows for June–July 2000 was 30 m^3/s, and the mean absolute difference was 62 m^3/s. As previously noted, including more tidal marsh areas in the model domain might improve flow simulations by allowing more water to be stored in the marshes during flood flows and released during ebb flows.

Simulated streamflows at WP were less than measured values for both ebb and flood flows (fig. 43B). The mean absolute difference between measured and simulated flows was 88 m^3/s for November–December at WP, which is about 6 percent of the total flow range during October 1999–September 2000. The mean absolute difference between measured and simulated flows for June–July 2000 was 134 m^3/s, or about 10 percent of the flow range. Simulated streamflows at WP were fairly insensitive to CK tidal datum and to changes in channel bathymetry in West Pass between the WP site and the mouths of Alligator, Wadley, and Northern Passes.

Streamflows were simulated quite accurately at site E6, located just upstream from the East Pass-West Pass split (fig. 44). The measured values in figure 44 represent an average of one or more discharge measurements made within an hour or less. Simulated data points were estimated from simulated flows, interpolating between simulated hourly values to estimate simulated flows during the same time the discharge measurements were made. At site E6, there was no tendency to over- or under-simulate flows, and most of the simulations

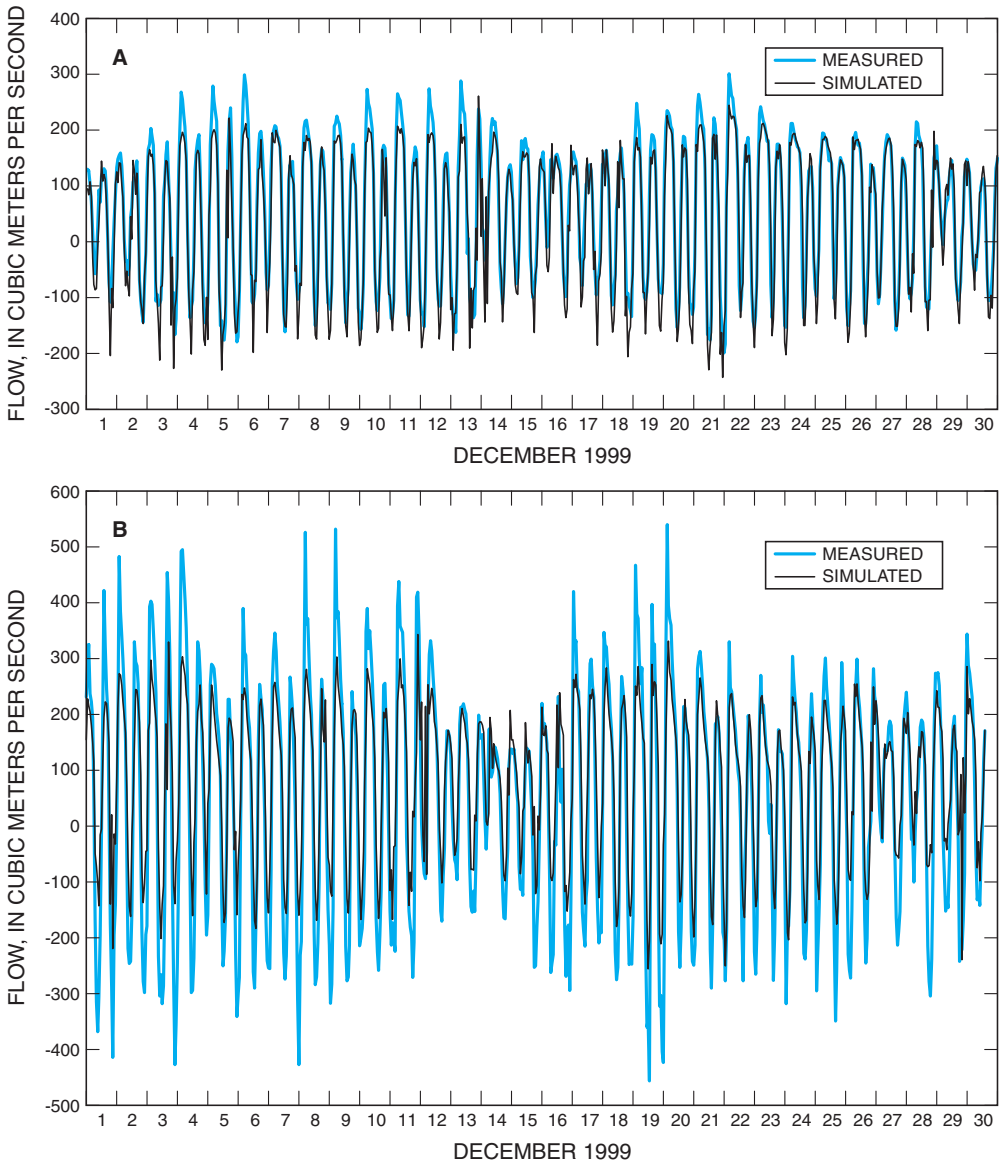

Figure 43. Measured and simulated streamflow at (A) East Pass and (B) West Pass streamgages, December 1–30, 1999.

closely matched measured values. There also was good agreement between measured and simulated flows at Wadley Pass (W4) and Northern Pass (Q7), with a slight tendency toward lower simulations relative to measurements at Wadley Pass, and lower simulations relative to measurements on flood flows at Northern Pass (fig. 44). Ebb and flood flow simulations at Alligator Pass (Q9) were less than measured values, whereas simulated flood flows in the cut downstream from the Wadley-Alligator Pass split (Q5) were greater than measured values and simulated ebb flows were less than measured values. Errors may be the result of inadequate representation of bathymetry in an area with a highly mobile channel.

Simulated ebb flows in Alligator Pass were greater than simulated ebb flows in Wadley Pass, and simulated ebb flows in Wadley Pass were greater than simulated ebb flows in Northern Pass. In fact, flows in Northern Pass often were near zero or flooding during ebb flows in the other two passes. Simulated flood flows in Wadley and Northern Passes were about equal to simulated flood flows in Northern Pass (fig. 45). These patterns correspond with the general patterns observed during the discharge measurements in December 1999 and May–June 2000 (fig. 25A, Wadley and Northern Pass flood flows are approximately equal; fig. 25B, Wadley Pass ebb flows exceed Northern Pass ebb flows).

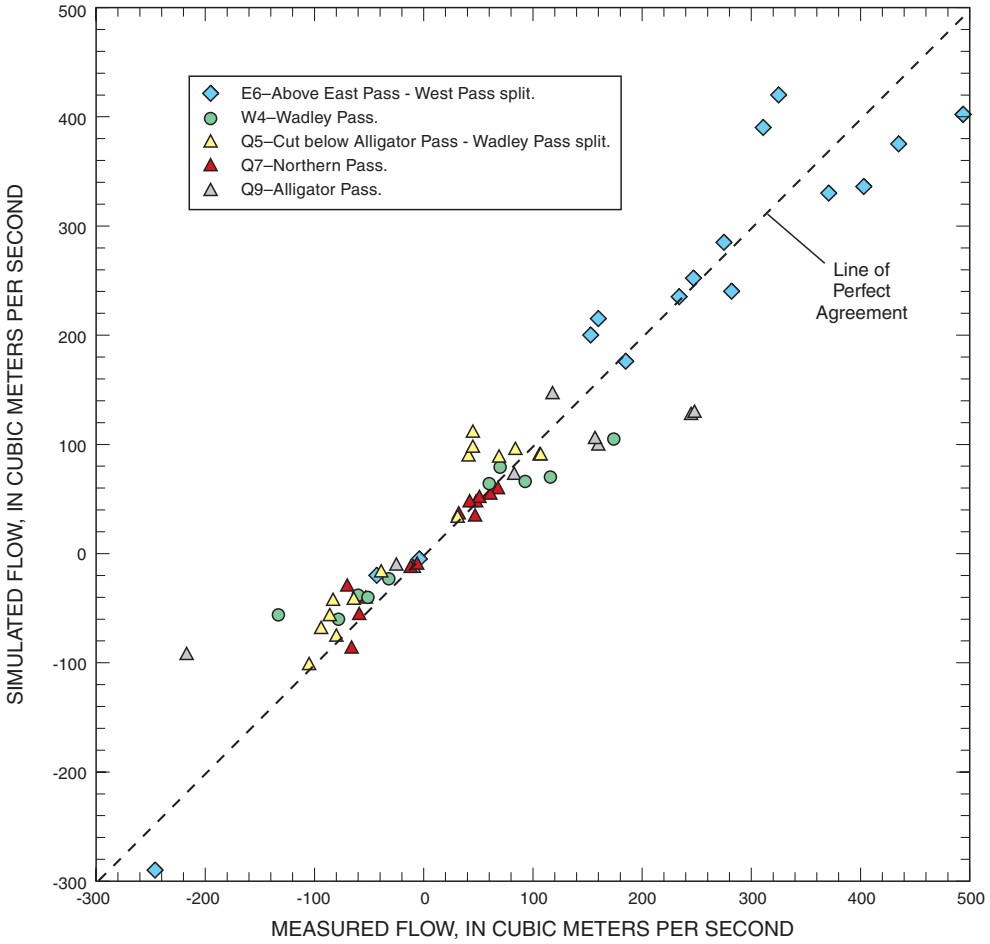

Figure 44. Discharge measurements and corresponding simulated streamflows at Wadley Pass, upstream from the East Pass-West Pass split, Northern Pass, Alligator Pass, and the cut below Alligator Pass-Wadley Pass split for selected times during December 14–16, 1999, and May 30–June 2, 2000.

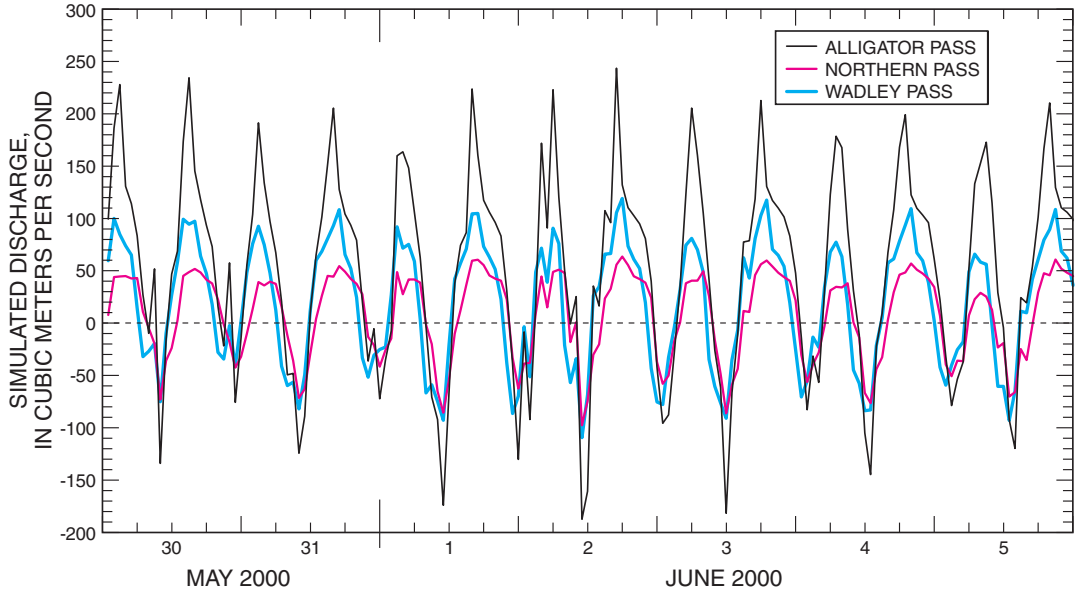

Figure 45. Simulated streamflow at Alligator Pass, Wadley Pass, and Northern Pass, May 30–June 5, 2000.

Simulated flows, particularly for Alligator Pass, exhibit some oscillations that are likely a numerical artifact (fig. 45) resulting from waves reflecting at the tidal boundary. These oscillations would be reduced by increasing the friction coefficient, but this would be at the expense of lower simulated flows at WP.

Salinity. As discussed previously, in the absence of additional data, salinity was assumed to be time invariant along the Gulf of Mexico boundaries of the model domain. Final salinity-boundary conditions on the northwestern and southeastern model boundaries were established as part of the calibration process. Bottom layer salinities ranged from 36 (western) to 25 psu (eastern) on the northwestern boundary and from 36 (western) to 27 psu (eastern) on the southeastern boundary (fig. 46). Surface layer salinities ranged from 35 to 20 psu on both the northwest and the southeast boundaries.

The quality of the salinity simulations, as indicated by differences between measured and simulated salinity at EP, EM, WP, and WM, varied with time at a particular site and among sites (table 7). At EP, simulated monthly mean salinities typically were greater than measured values, with larger differences evident in the summer months (June and July 2000) than during November–December 1999, and top simulated salinities agreed more closely with measured values than did bottom salinities, particularly for June–July 2000 (table 7). Simulated monthly mean salinities at EM agreed very closely with measured values, except for bottom salinities in June–July 2000 (fig. 47, table 7). Other than June–July 2000, the largest difference between monthly mean measured at simulated salinities at EP and EM was 1.9 psu, and most of the differences were less than 1 psu.

This seasonal pattern in simulated salinities—the poorest agreement for bottom salinities in June–July 2000—also was evident at WM (fig. 48; table 7). June–July 2000 bottom monthly mean simulated salinities at WM were about 5 psu greater than measured values, whereas measured and simulated top monthly mean salinities differed by less than 2 psu. Top and bottom simulated maximum salinities occurring during a tidal cycle were typically less than measured values at both WM (fig. 48) and WP. Top simulated minimum tidal-cycle salinities at these sites, however, were typically greater than measured values.

Because there was only one salinity sensor at the RB site and because the water depth at the site was shallow, simulated depth-averaged salinities were compared to measured values at RB (fig. 49, table 7). Differences between monthly mean measured and simulated salinities were 1 psu or less for November–December 1999, and less than 3 psu for June–July 2000 (table 7). Measured salinities were typically bounded by simulated top and bottom layer salinities (fig. 49A), except for July 2000, when measured values were generally less than all simulated salinities in all of the model computational layers (fig. 49B).

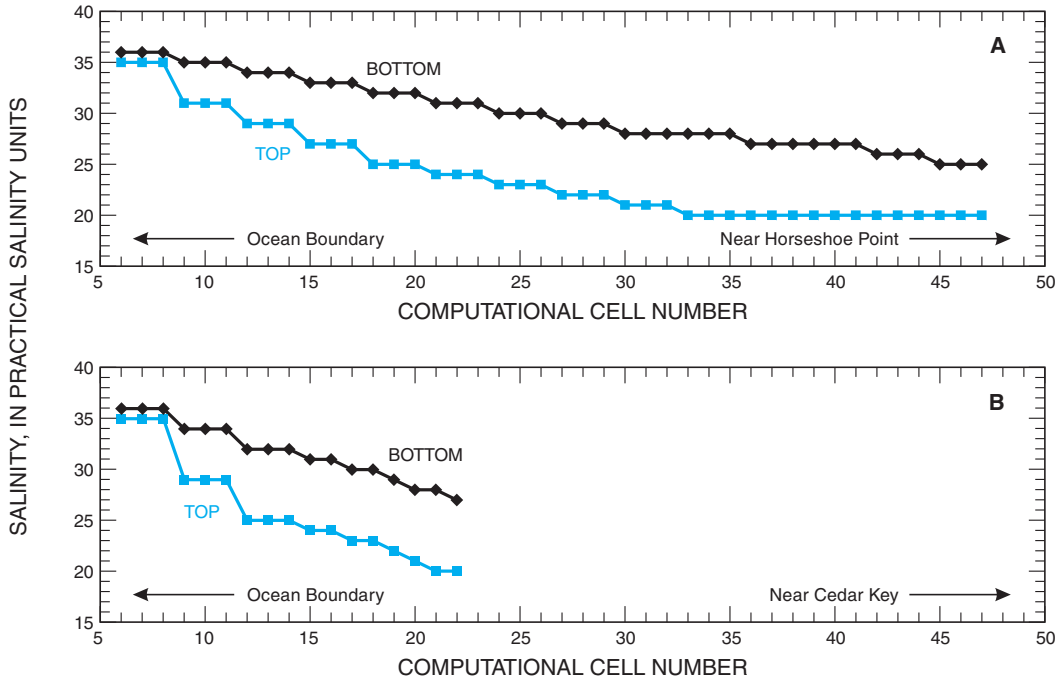

Figure 46. Bottom and surface layer salinity-boundary conditions along the (A) northwestern and (B) southeastern boundaries.

Table 7. Salinity simulation results for East Pass, East Mouth, West Pass, West Mouth, and Red Bank Reef for November–December 1999 and June–July 2000.

Month	Top salinity (in practical salinity units)			Bottom salilnity (in practical salinity units)		
	Monthly mean of difference between measured and simulated salinity	Measured monthly mean salinity	Simulated monthly mean salinity	Monthly mean of difference between measured and simulated salinity	Measured monthly mean salinity	Simulated monthly mean salinity
East Pass						
Nov. 1999	-0.7	1.0	1.7	-1.1	2.3	3.2
Dec. 1999	-0.9	0.7	1.6	-1.9	1.2	3.1
June 2000	-1.2	1.2	2.4	-1.2	1.4	5.1
July 2000	-0.7	1.3	2.0	-0.7	1.5	4.9
East Mouth						
Nov. 1999	1.8	8.3	6.5	0	13.2	13.3
Dec. 1999	-0.1	5.7	5.8	0.6	12.6	12.0
June 2000	-0.2	6.5	6.6	-0.2	9.4	14.6
July 2000	0.3	6.5	6.2	0.3	8.7	15.0
West Pass						
Nov. 1999	1.4	2.6	1.1	2.3	4.3	1.8
Dec. 1999	0.8	1.7	0.9	2.9	4.4	1.5
June 2000	0.9	2.8	1.8	0.9	3.6	3.6
July 2000	1.2	2.6	1.4	1.2	3.0	2.9
West Mouth						
Nov. 1999	2.1	4.4	2.4	-0.6	7.8	8.2
Dec. 1999	0.8	3.2	2.3	-2.3	5.6	8.7
June 2000	1.4	4.8	3.4	1.4	5.7	10.7
July 2000	2.1	5.1	3.0	2.1	5.8	10.5
Red Bank Reef [1]						
Nov. 1999	0.4	33.7	33.3	--	--	--
Dec. 1999	-1.3	32.1	33.1	--	--	--
June 2000	-1.7	31.6	33.4	--	--	--
July 2000	-3.0	30.4	33.3	--	--	--

[1]Salinity measured at only one depth; simulated values are depth averaged.

A total of 38 FIM salinity measurements were made within the model domain during November–December 1999 and June–July 2000. Measurement locations are a subset of all 1999–2000 FIM measurement sites shown in figure 40. Most of the FIM measurements were noted as "surface salinity," although a few sites reported surface and bottom salinities. Mean depth of all the measurements was 0.7 m.

Measured and simulated salinities were compared for the FIM sites (fig. 50). Because there was no clock time reported for the FIM measurements, all simulated salinities are reported for 12:00 p.m. on the date of the FIM measurement. Because most measurements were reported as "surface salinity," measured values are compared to simulated salinities from computational layer 5 (fifth layer up from the bottom).

Simulated salinities tended to be greater than measured values for salinities less than about 25 psu, but measured salinities were generally greater than measured values for salinities greater than 25 psu (fig. 50A). The average difference between measured and simulated salinity for the 38 FIM sites was -0.1 psu, indicating that there was no tendency to over- or under-simulate salinities at the FIM sites. However, the mean absolute difference between measured and simulated salinities was

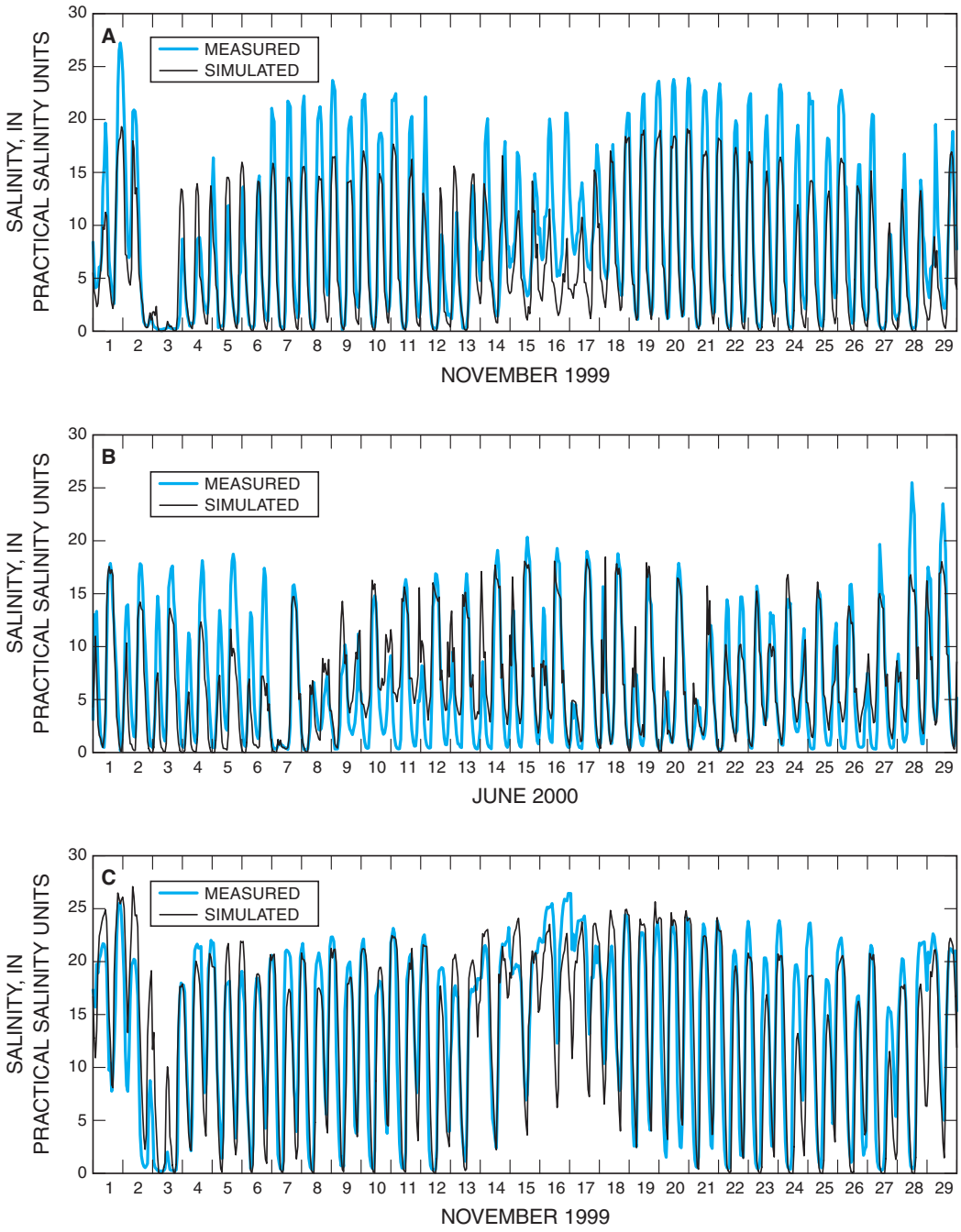

Figure 47. Measured and simulated salinity at East Mouth, (A) top, November 1999; (B) top, June 2000; and (C) bottom, November 1999.

larger, at 3.8 psu. Some of the largest errors were at the lower salinities measured at stations near the shore; salinities at these sites are affected more by tidal fluctuations than those further offshore, so errors associated with an assumed measurement time of 12:00 p.m. would be greater at these sites.

The exact vertical location and water depth of the FIM salinity measurements are unknown. The measured salinity should, however, be bounded by the simulated surface (layer 6) and near-bottom (layer 2) salinities in most cases. This was indeed true (fig. 50B). A total of 14 of the 18 June–July 2000 FIM salinity measurements were bounded by the simulated near-surface and near-bottom salinities, as indicated by the 1:1 line passing between the simulated layer 2 and simulated layer 6 salinity (fig. 50B). Simulated salinities at 12:00 p.m. were again assumed to represent measured conditions.

The daily range in simulated depth-averaged salinities at the FIM sites on the date of the FIM measurements was between 0.8–13.6 psu during June–July 2000. Hence, the assumed FIM measurement time of 12:00 p.m. likely has an effect on the comparison between simulated and measured salinities, particularly at sites with the largest range in daily salinity.

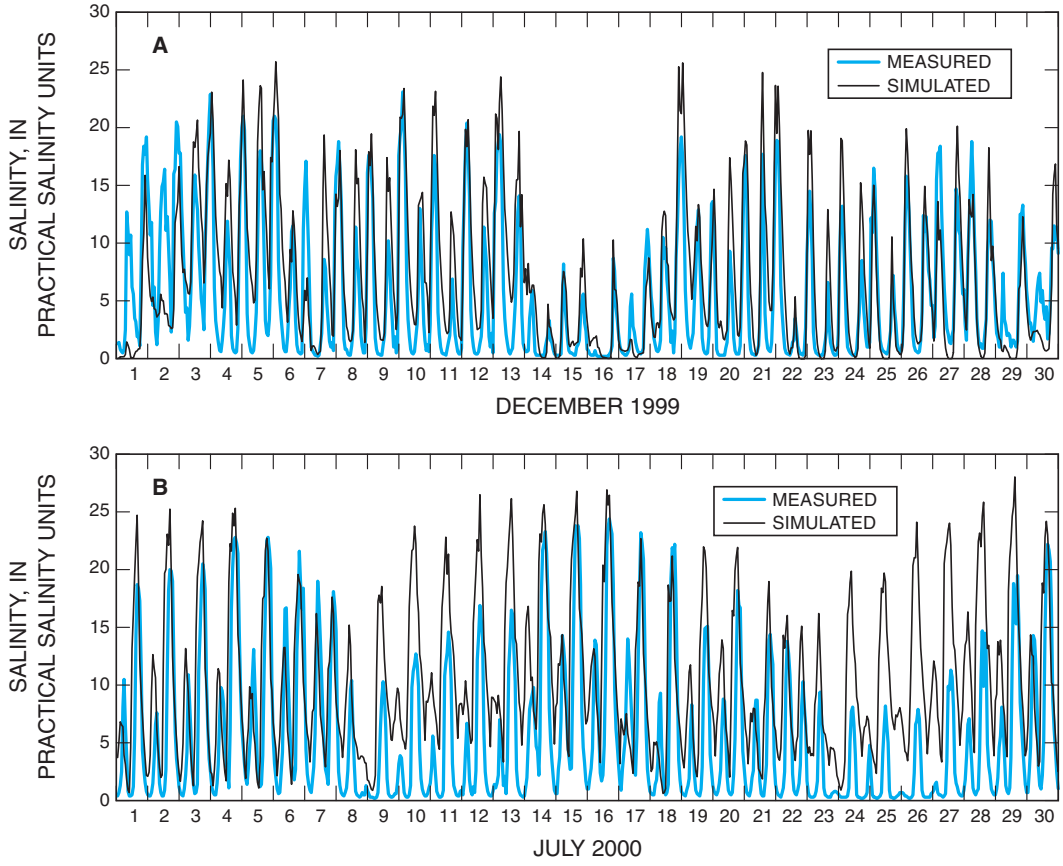

Figure 48. Measured and simulated bottom salinity at West Mouth, (A) December 1999 and (B) July 2000.

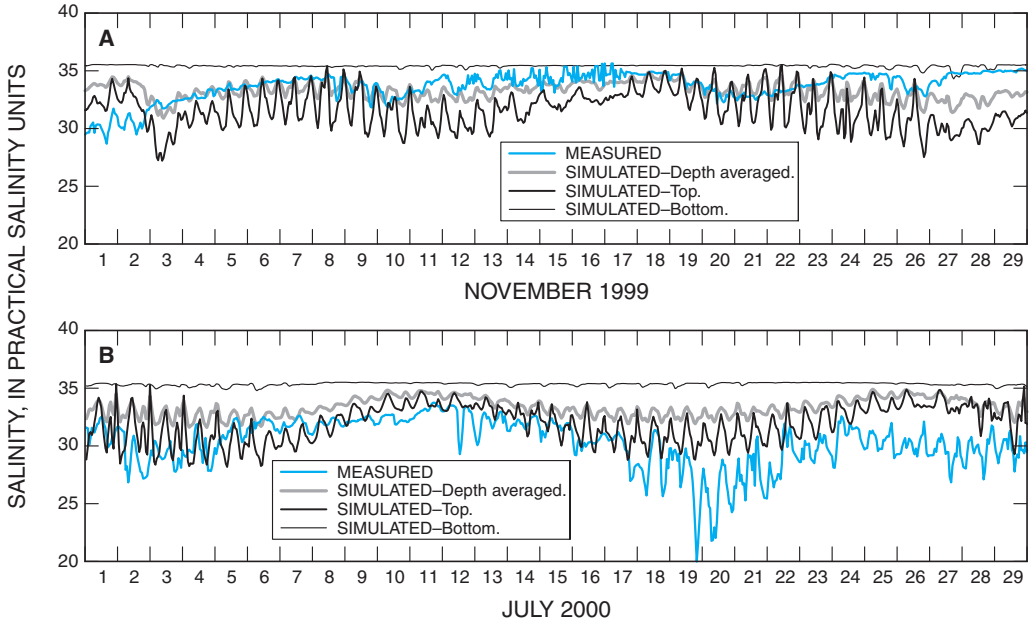

Figure 49. Measured salinity and top, bottom, and depth-averaged simulated salinity at Red Bank Reef, (A) November 1999 and (B) July 2000.

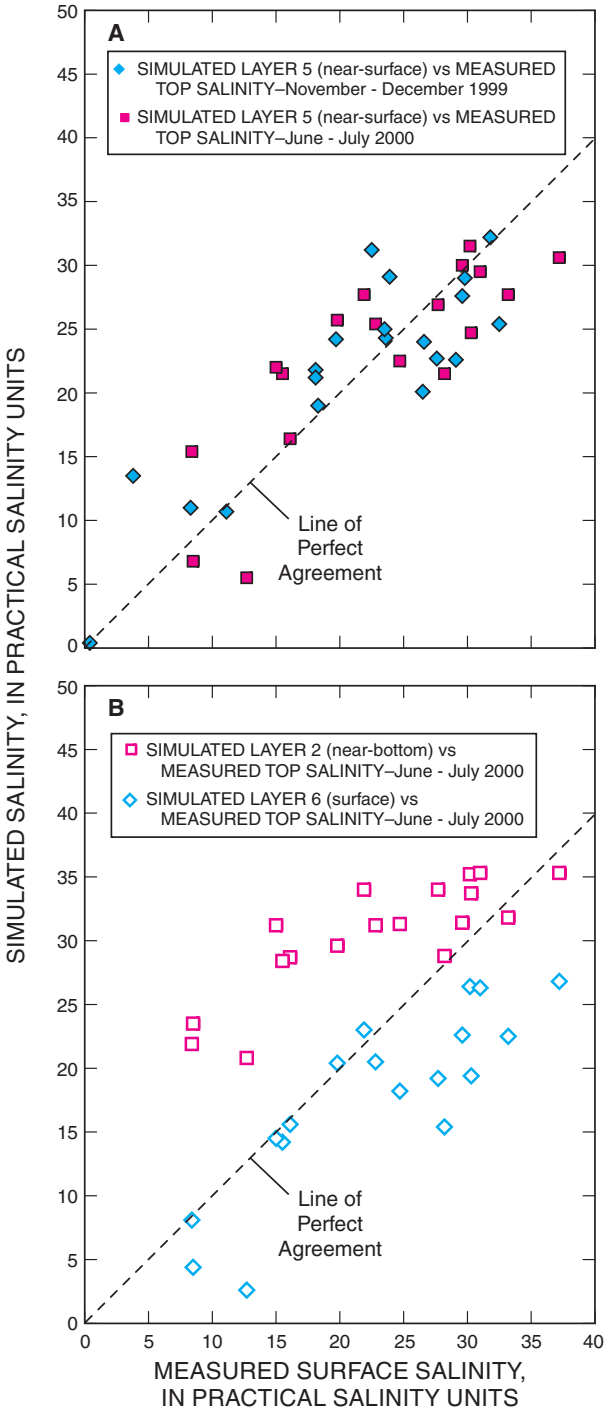

Figure 50. Salinity from Fisheries-Independent Monitoring program measurements and (A) simulated near-surface salinity for November–December 1999 and June–July 2000, and (B) simulated surface and near-bottom salinity for June–July 2000.

Differences between measured and simulated salinities can be attributed to three factors: errors in flow simulations, the assumption of a time-invariant salinity-boundary condition, and fixed sensor depths in a system with a fluctuating water level and variable thickness computational layers. Differences between measured and simulated flows were greater at WP than at EP; correspondingly, differences in measured and simulated salinities were slightly greater at the West Pass sites than at the East Pass sites. Differences between measured and simulated flows at WP were greater in the summer months than the winter months, which corresponded to the pattern in the simulated salinities at WM, but not at WP (table 7).

Seasonal variations in Gulf of Mexico salinity have been observed (fig. 41, and Bledsoe (1998). The seaward-most model boundary is sufficiently far from the mouth of the Suwannee River that the salinity-boundary can reasonably be assumed to be constant. Salinity along the northwestern and southeastern model boundaries, however, certainly varies with season and regional streamflow patterns, particularly near the shore. Salinity-boundary conditions were established along these boundaries during model calibration to provide a reasonable fit to measurements in the Suwannee River while maintaining general patterns established from limited data. As observed during model calibration, changes in salinity-boundary conditions were reflected in simulated salinities. As a result, some of the differences between measured and simulated salinities can be attributed to these assumed boundary conditions.

The third factor affecting the agreement between measured and simulated salinities is related to the position in the vertical where comparisons are made. The field salinity sensors were mounted at fixed depths or distances from the channel bottom. Because of tidal fluctuations of approximately 1 m, the locations of the sensors relative to the water surface varied over a tidal cycle, making identification of the "top" layer difficult. The sigma coordinate system used for the Suwannee River computational grid further complicates comparison of measured and simulated values. Because the number of vertical layers is constant, regardless of the water depth, a sensor located at a fixed depth could be in one computational layer during part of the tidal cycle, and in another layer subsequently. For example, at a location with a mean low water depth of 5 m and a tidal amplitude of 1 m, each computational layer would range between 0.83 and 1.0 m in thickness, and the location of the layer relative to the channel bottom would vary with tidal phase. Top salinities reported herein (unless otherwise noted) were for computational layer 5 (the fifth layer up from the bottom), and bottom salinities were reported for layer 2.

Sensitivity Tests

The sensitivity of model simulations to changes in selected boundary conditions and model parameters was evaluated by using simulation results from November–December 1999 (with a 1-month spin-up period). Ten individual cases were evaluated:

- The calibrated model as described above.
- An increase in bottom elevation—the bottom elevation was raised by 0.3 m in all computational cells.
- The decrease in bottom elevation—the bottom elevation was lowered by 0.3 m in all computational cells.
- A higher salinity-boundary condition along the northwest boundary—all salinity values less than 33 psu for the original boundary condition (fig. 46A) were increased by 3 psu.
- A lower salinity-boundary condition along the northwest boundary—all salinity values less than 35 psu for the original boundary condition (fig. 46A) were decreased by 2–3 psu.
- A higher salinity-boundary condition along the southeast boundary—all salinity values less than 33 psu for the original boundary condition (fig. 46B) were increased by 3 psu.
- A lower salinity-boundary condition along the southeast boundary—all salinity values less than 35 psu for the original boundary condition (fig. 46B) were decreased by 2–3 psu.
- No wind—wind speed was assumed to be zero at all times.
- A higher resistance coefficient—the resistance coefficient was assumed to be 0.02 m (compared to the calibrated value of 0.01 m) throughout the model domain.
- A lower resistance coefficient throughout the model domain—the resistance coefficient was assumed to be 0.005 throughout the model domain.

Monthly mean differences and RMS differences between measured and simulated flows at EP and WP were unaffected by changes in salinity and wind boundary conditions. Errors in simulated flows (monthly mean difference and RMS differences) changed about 5 percent or less in response to doubling and halving the resistance coefficient. Simulated flows were most sensitive to changes in the bed elevation. A decrease in the bottom elevation increased the monthly mean differences between measured and simulated flows at EP and WP by 34–55 percent. RMS differences increased by 2–25 percent. Simulated flows were much lower than measured flows, with simulated peak flood and ebb flows about half of measured values, when the bottom elevation was increased by 0.3 m.

As previously noted, bottom elevations for the computational grid near the shore were estimated from navigation charts because digital data were unavailable for these shallow areas. The results of these sensitivity tests indicate the need for accurate bathymetric data, particularly in these shallow nearshore regions where tides, flow, and salinity are strongly affected by bathymetry.

Simulated salinities also were strongly affected by changes in bathymetry, particularly in the bottom layers at EM and WM (table 8). The absence of wind had no effect on simulated salinity in the river and only a slight effect at the RB site. Changes in the resistance coefficient had fairly strong effects on simulated salinities, with a higher resistance coefficient generally resulting in a decrease in salinity relative to the calibrated model, and a lower resistance coefficient generally resulting in increased salinities (table 8).

Simulated salinities at RB, EM, and WM were affected by changes in the time-invariant salinity-boundary conditions along the northwest and southeast boundaries of the model. Changes in the salinity-boundary conditions did not, however, affect simulated salinities as much as changes in the resistance coefficient or changes in bathymetry. Adjustments to the salinity-boundary conditions only slightly increased or decreased simulated salinities at RB; there was no change in the longer term temporal patterns (fig. 51). This suggests that (1) simulations within the model domain are relatively insensitive to reasonable adjustments in the time-invariant salinity-boundary conditions and (2) improvements in salinity simulations, particularly seaward of the shoreline, require data on temporal variations in salinity along the model boundary.

Example Applications

Each 15-minute value of net streamflow at AGR was reduced by 5 percent, and these reduced net flows were added back to the tidal flows (difference between measured flow and net flow) to create a new boundary condition at AGR. Otherwise, the same boundary conditions used for model calibration were applied. Salinities were subsequently simulated for June 2000 (following a 1-month model spin-up period, or the period in which the initial conditions are transported out of the model domain, and simulation results are subsequently controlled by boundary conditions rather than initial conditions) and compared with salinities simulated using the measured flow AGR boundary condition. A 5-percent net flow reduction for June 2000 amounted to an average decrease in flow of 5 m^3/s. Compared with the original simulation, top and bottom salinities at EP and EM were increased by an average of 0.4 psu for June 2000; WP top and WM bottom salinities increased by 0.5 psu, and the increase in the difference between the top and bottom salinity ranged from 0.1 psu (EM) to 0.6 psu (WP).

Table 8. Results of model sensitivity tests on simulated salinty at the Red Bank Reef, East Mouth, and West Mouth sites, November–December, 1999.

Simulation Description	Change in simulated monthly mean salinity between calibrated model and sensitivity test (positive values indicate monthly mean salinity for test case is greater than monthly mean salinity for calibrated model), in practical salinity units									
	Red Bank Reef (depth-averaged simulated salinity)		East Mouth				West Mouth			
			Top		Bottom		Top		Bottom	
	Nov.	Dec.	Nov.	Dec.	Nov.	Dec.	Nov.	Dec.	Nov.	Dec.
Bottom elevation minus 0.3 meters	-0.9	-0.7	-1.8	-1.8	-5.0	-3.7	-1.4	-0.9	-4.2	-3.7
Bottom elevation plus 0.3 meters	1.9	-0.9	5.4	5.0	13.4	11.8	2.2	1.6	7.8	6.9
Higher northwest salinity boundary condition	0.3	0.2	-0.4	-0.3	-0.6	-0.6	-0.3	-0.2	-1.2	-0.6
Lower northwest salinity boundary condition	0.3	0	-0.3	-0.2	-0.4	-0.5	-0.2	-0.1	-0.5	-0.5
Higher southeast salinity boundary condition	0.2	0.1	-0.3	-0.1	-0.3	-0.3	-0.2	-0.2	-0.9	-0.7
Lower southeast salinity boundary condition	0.2	0	-0.3	-0.2	-0.3	-0.3	-0.2	-0.1	3.5	4.3
No wind	0.3	0.1	0	0	0	0	0	0	0	0
Higher resistance coefficient	0.2	-0.5	0.4	-0.6	-0.9	-2.4	-0.4	-0.6	-2.8	-1.8
Lower resistance coefficient	0.3	-0.4	0.3	0.1	1.0	-0.4	0.5	0.3	1.7	1.5

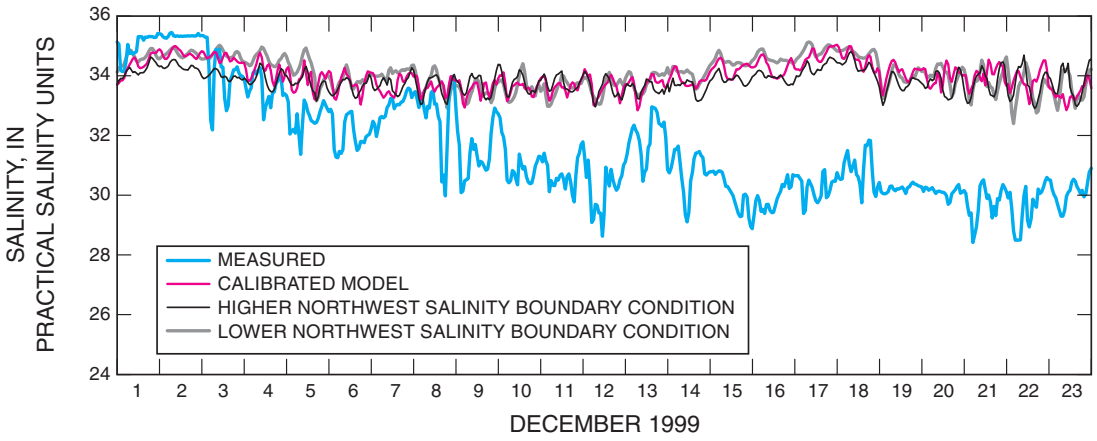

Figure 51. Measured and depth averaged simulated salinities at Red Bank Reef for three different sets of salinity-boundary conditions along the northwest boundary of the model domain.

The Suwannee River estuary model can be used to simulate the transport of neutrally buoyant conservative tracers, as well as salt. As a simple example of such a simulation, a conservative tracer was hypothetically released over a 1-hour period, beginning at 3:00 a.m. on February 5, 2000, during ebb flow at AGR. The material was released uniformly over the depth of flow in the center of the channel, and the initial concentration of the material was 1,000 parts per thousand. Boundary conditions were the same as for the calibrated model.

According to the simulations, the tracer had mixed sufficiently so that the depth-averaged concentration just upstream from the East Pass-West Pass split was about 3 percent that of the initial concentration (fig. 52). The travel time from AGR to EP was about one-half day, but was several hours longer to WP. Concentrations in East Pass were reduced to less than 0.5 percent of the initial concentration within 1 day of the release, but concentrations remained elevated longer in West Pass. Virtually all of the material was flushed through the system within 3 days of release for this low-flow condition.

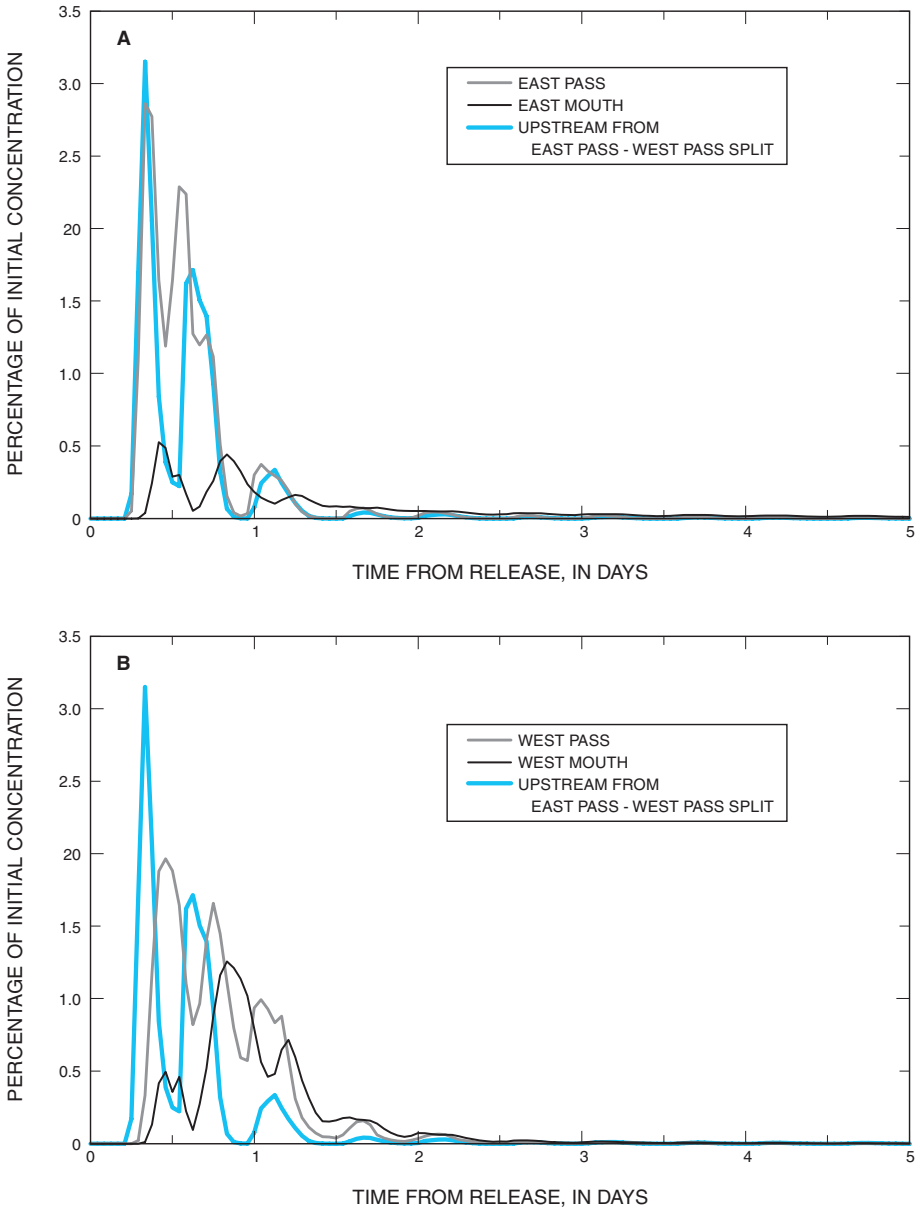

Figure 52. Simulated depth-averaged concentrations of conservative, neutrally buoyant tracer hypothetically released at above Gopher River site at (A) the East Pass and East Mouth sites, and upstream from East Pass-West Pass split, and (B) the West Pass and West Mouth sites, and upstream from East Pass-West Pass split.

Summary and Conclusions

A three-dimensional numerical model was developed to assist in the evaluation of the effects of changes in freshwater flow on the salinity regime of the lower Suwannee River, estuary, and Suwannee Sound. Hydrodynamic and salt-transport modeling were supported by data from a fairly comprehensive data-collection network operated in the lower Suwannee River during 1998–2000.

The study area included all of the downstream-most 10 km of the Suwannee River, Suwannee Sound, and part of the Gulf of Mexico. Data collected during the October 1998–September 2000 were used to characterize hydrologic and salinity conditions in the Suwannee River estuary. Development, calibration, and application of the hydrodynamic and salt-transport model were completed by using data primarily collected during October 1999–September 2000.

Streamflows at Wilcox, Florida, during much of the study period were at record low levels. New record low monthly mean streamflows were established during 11 months of the 24-month data-collection period, with April being the only calendar month for which a new record low was not set. Monthly mean flow was above average only during the first 2 months of the study. During water year 2000, monthly mean flows averaged 35 percent of normal, or about 191 m^3/s lower than normal.

The Suwannee River estuary experiences mixed semidiurnal tides, typified by two unequal high and two unequal low tides each day. Of the Suwannee River gages, EM, the gage nearest the Gulf of Mexico, had the largest total tidal range, and AGR, the most inland gage, had the smallest. Based on previously reported land elevations along the lower Suwannee River, water levels could have been above top-of-bank at selected locations in the lower Suwannee River about 25–30 percent of the time during October 1999–September 2000.

Spectral and harmonic analysis were used to describe tidal conditions at all six USGS water-level gages and at Cedar Key. As expected, most of the tidal energy is associated with diurnal and semidiurnal frequencies (0.042 and 0.083 cycles per hour, respectively. Seaward of the mouth of the Suwannee River, water depth at low tide may be only half the depth at high tide in much of the estuary shoreward of the Suwannee Reef. Hence, frictional effects are relatively greater at low tide than high tide, resulting in tidal distortion and the presence of overtides in the tidal record from the Suwannee River water-level gages.

In general, flood velocities at AGR were about half those at EP and WP. In contrast to flood flows, ebb velocities at EP were somewhat greater than at the other two sites. The median ebb index velocity at EP was 43 cm/s, compared to a median of about 30 cm/s at both AGR and WP (median based on ebb velocities only).

At AGR, measured flows ranged from 558 to -368 m^3/s (negative indicates flood, or upstream flow) during October 1999–September 2000. Maximum ebb flow was 351 m^3/s and maximum flood flow was -315 m^3/s; at WP, maximum ebb flow was 655 m^3/s, almost double the maximum at EP, and maximum flood flow was -711 m^3/s. Flows at AGR were downstream about two-thirds of the time during October 1999–September 2000, a period of extended and record low flows. Flows were in the downstream direction 55 and 58 percent of the time at EP and WP, respectively.

Total flows were consistently greater at WP than EP, probably because West Pass has greater storage than East Pass, thereby resulting in a greater tidal prism in West Pass. During spring tides, the sum of flows measured at EP and WP was almost twice as large as the flow measured at AGR. The difference between flow at AGR and the sum of flows at EP and WP was much smaller during neap tides.

A low-pass digital filter was used to separate the tidal flows from the net (freshwater) flow at the three gaging stations. Net flows were much less variable than total flow; EP net flows were, for example, between 40–70 m^3/s 70 percent of the time during October 1999–September 2000. In contrast to total flows, net flows generally were higher at EP than at WP.

Net freshwater flow increased substantially between Wilcox and AGR, a reach representing only about 3 percent of the total basin drainage area. The average increase in flow between Wilcox and AGR was 30 m^3/s during the study period, and the increase was fairly consistent from month to month. This increase in flow downstream from Wilcox, where the additional contributing drainage area is small, indicates the likely presence of a substantial contribution of ground water to the river in this reach.

The sum of net flows at EP and WP, downstream from AGR, generally was less than the net flow at AGR, with the average difference during the study period equal to 13 m^3/s. Some of the flow at AGR probably bypasses the streamgages at WP and EP; high water that spilled over the banks in the reaches between AGR and the two downstream sites could flow south through the marshes to the Gulf of Mexico, rather than returning to the channel during falling tides.

Additional, specially designed studies could be conducted to determine the source of the apparent increase in flow between Wilcox and AGR and the reason for the apparent loss in flow downstream of AGR. An understanding of ground-water/surface-water coupling in the reach of the river between Wilcox and AGR could lead to improved management of ground-water withdrawals and protection of recharge zones. Flows across the marshlands east of East Pass are likely required to maintain the existing healthy ecosystem. If these marshland flows indeed are the result of diversion of some of the flow measured at AGR, then changes to river flows or channel geometry that subsequently reduce marshland flows could adversely affect the marsh

Salinity near the surface at EP was less than 1 psu 86 percent of the time during October 1999–September 2000, and salinity near the bottom was less than 1 psu 77 percent of the time. In contrast, salinity at EM (both top and bottom) was greater than 1 psu at least 70 percent of the time. Median salinities at EP, WP, and WM were all less than 2 psu, whereas median salinity at EM near the bottom was about 9 psu. There was much less difference in salinity between the WP and WM gages in West Pass than between the EP and EM gages in East Pass. Higher ebb velocities in East Pass, more direct connections between the Gulf and West Pass, and channel geometry all likely contributed to the lower upstream migration of salt in East Pass compared to West Pass.

The Environmental Fluid Dynamic Code (EFDC) three-dimensional hydrodynamic and transport model was applied to the study area. The physical domain of the Suwannee River estuary model extends from the AGR streamgage, which is about 12 km from the mouth of the river, out into the Gulf of Mexico. Along the shore, the model domain extends northward to Horseshoe Point and southward to Cedar Key. The total area encompassed by the model is 1,038.6 km^2. The model domain contains 2,385 computational cells in each of 6 horizontal layers, giving a total of 14,310 computational cells. Computational cell dimensions range from 22–1,602 m in the x-direction, and from 39–2,492 m in the y-direction, and the area of the cells ranges from 2,100–1.62 km^2. Bottom elevations in the model ranged from 1.50–9.2 m below NAVD 88. As a result, the thickness of the sigma layers in the model ranged from 0.25–1.53 m in thickness. A total of 22 percent of the computational cells, representing 16 percent of the model area, had a bottom elevation of -2.0 m or less.

Measured streamflow at AGR was used as the upstream boundary condition for the model. There are no documented springs in the Suwannee River estuary model domain, although it seems likely that some springs or seeps could be present. Therefore, submarine ground-water discharge was not included as a boundary condition. There also are a number of tidal creeks having small, but undetermined, drainage areas that drain to the model domain between Horseshoe Point and Cedar Key. No data were available on the amount of net freshwater flow in these creeks, but model testing indicated that salinity simulations were improved by the addition of a freshwater inflow from Dan May Creek. A constant flow of 15 m^3/s was added at the east side of East Pass to represent inflows from Dan May Creek. This flow was approximately equal to the apparent loss of flow between the AGR gage and the EP and WP gages.

Tidal boundary conditions were specified for all open-water boundary computational cells, and tidal data collected by NOS at Cedar Key were used to construct these boundary conditions. Missing tidal data were estimated by using computed astronomical tides at Cedar Key. Cedar Key tides were shifted in time around the model domain such that the time difference in the arrival of high water at boundary cells between Cedar Key and Horseshoe Point gradually varied from 0–15 minutes. This assumption about tidal boundary conditions is somewhat consistent with observations, except that data indicate that the phase difference (time of arrival of a given tide) varies from high tide to low tide. Insufficient data were available to account for differences in tidal amplitude around the model boundary. Cedar Key tides also were adjusted by -0.05 m to improve agreement between measured and simulated water levels.

Quantitative data for establishing the salinity-boundary conditions during the study period, such as were available for the tidal boundary conditions, were not available. Salinity-boundary conditions along the northwestern and southeastern boundaries were assumed to be time invariant, but did vary horizontally, from 36 psu at the seaward-most computational cell to 20 psu at the shore; vertical variations were typically about 5 psu. Salinity at the seaward boundary was 36 psu at the bottom and 35 psu at the top.

The effects of synoptic, or regional, winds on water level in the study area are reflected in the Cedar Key tide data. West Pass wind data were used in the model to account for local wind effects on velocity and mixing in the river channel. Tests subsequently demonstrated that model results were generally insensitive to changes in local wind boundary conditions.

A constant computational timestep of 5 seconds was used for all simulations. The upwind finite difference scheme was used to solve the horizontal momentum equations, and horizontal momentum diffusion was not activated. Coriolis and buoyancy forcing are included in the model, and no depth smoothing was done for the computational grid. The bottom roughness coefficient was set at 0.01 m.

Monthly mean differences between measured and simulated water levels generally were less than 0.2 m. Root mean square differences, with the exception of EM, were 7–28 cm. Simulated high water levels were slightly higher than measured values at WP and WM. Measured and simulated amplitudes of the principal diurnal (O1 and K1) and semidiurnal (M2 and S2) harmonics differed by no more than 0.065 m, and most differed by less than 0.02 m.

Simulated flows at EP and WP generally were less than measured flows. The streamflow amplitude generally was simulated accurately at EP, but simulated ebb flows were less than measured flows and simulated flood flows were greater than measured flows. The mean difference between measured and simulated flows was 21 m^3/s for November–December at EP, which is less than 5 percent of the total flow range at EP during October 1999–September 2000, and the mean absolute difference was 34 m^3/s. The mean difference between measured and simulated flows for June–July 2000 was 30 m^3/s, and the mean absolute difference was 62 m^3/s.

Simulated streamflows at WP were less than measured values for both ebb and flood flows. The mean absolute difference between measured and simulated flows was 88 m^3/s for November–December at WP, which is about 6 percent of the total flow range at WP during October 1999–September 2000. The mean absolute difference between measured and simulated flows for June–July 2000 was 134 m^3/s, or about 10 percent of the flow range at WP. Simulated streamflows at WP were fairly insensitive to Cedar Key tidal datum and to changes in channel bathymetry in West Pass between the WP site and the mouths of Alligator, Wadley, and Northern Passes.

Streamflows were simulated quite accurately at E6, located just upstream from the East Pass-West Pass split. At E6, unlike EP and WP just downstream, there was no tendency to over- or under-simulate flows, and most of the simulations closely matched measured values. There also was good agreement between measured and simulated flows at Wadley Pass (W4) and Northern Pass (Q7), with a slight tendency toward higher simulations relative to measurements at Wadley Pass, and lower simulations relative to measurements on flood flows at Northern Pass. Simulated flows in Alligator Pass were greater than simulated flows in Wadley Pass, simulated ebb flows in Wadley Pass were greater than simulated ebb flows in Northern Pass, and simulated flood flows in Wadley and Northern Passes were about equal to simulated flood flows in Northern Pass. These patterns of simulated flow reflect measured patterns observed during December 1999 and May–June 2000.

Simulated monthly mean salinities at EP typically were greater than measured values, with larger differences evident in during June and July 2000 than during November–December 1999, and top simulated salinities agreed more closely with measured values than did bottom salinities, particularly for June–July 2000. Simulated monthly mean salinities at EM agreed very closely with measured values, except for bottom

salinities in June–July 2000. This seasonal pattern in simulated salinities—the poorest agreement for bottom salinities in June–July 2000—also was evident at WM. June–July 2000 bottom monthly mean simulated salinities at WM were about 5 psu greater than measured values, whereas measured and simulated top monthly mean salinities differed by less than 2 psu.

Differences between monthly mean measured and simulated salinities at RB were 1 psu or less for November–December 1999, and less than 3 psu for June–July 2000. Measured salinities were typically bounded by simulated top and bottom layer salinities, except for July 2000, when measured values were generally less than all simulated salinities in all of the model computational layers.

Simulated salinities tended to be greater than FIM measured salinities in Suwannee Sound for salinities less than about 25 psu, but measured salinities were generally greater than measured values for salinities greater than 25 psu. The average difference between measured and simulated salinity for the 38 FIM sites was -0.1 psu, indicating that there was no tendency to over- or under-simulate salinities at the FIM sites. The mean absolute difference between measured and simulated salinities, however, was larger, at 3.8 psu. Some of the largest errors were at the lower salinities measured at stations near the shore; salinities at these sites are affected more by tidal fluctuations than those further offshore, so errors associated with an assumed measurement time of 12:00 p.m. would be greater at these sites. The exact vertical location of the FIM salinity measurements was unknown, the measured salinity was bounded by the simulated surface (layer 6) and near-bottom (layer 2) salinities in most cases. The daily range in simulated depth-averaged salinities at the FIM sites on the date of the FIM measurements was between 0.8–13.6 psu during June–July 2000. Hence, the assumed FIM measurement time of 12:00 p.m. likely has an effect on the comparison between simulated and measured salinities, particularly at sites with the largest range in daily salinity.

Seasonal variations in Gulf of Mexico salinity have been observed, so salinity along the northwestern and southeastern model boundaries certainly varies with season and regional streamflow patterns, particularly near the shore. Salinity-boundary conditions were established along these boundaries during model calibration to provide a reasonable fit to measurements in the Suwannee River, while maintaining general patterns established from limited data. As observed during model calibration, changes in salinity-boundary conditions were reflected in simulated salinities. As a result, some of the differences between measured and simulated salinities can be attributed to these assumed boundaries.

Field salinity sensors were mounted at fixed depths, or distances from the channel bottom. Because of tidal fluctuations of approximately 1 m, the locations of the sensors relative to the water surface varied over a tidal cycle, making identification of the "top" layer difficult. The sigma coordinate system used for the Suwannee River computational grid further complicates comparison of measured and simulated values. Because the number of vertical layers is constant, regardless of the water depth, a sensor located at a fixed depth could be in one computational layer during part of the tidal cycle, and in another layer subsequently.

The sensitivity of model simulations to changes in selected boundary conditions and model parameters was evaluated by using simulation results from November–December 1999. Monthly mean differences and RMS differences between measured and simulated flows at EP and WP were unaffected by changes in salinity and wind boundary conditions. Errors in simulated flows (monthly mean difference and RMS differences) changed about 5 percent or less in response to doubling and halving the resistance coefficient. Simulated flows and salinities were most sensitive to changes in the bed elevation. Changes in the salinity-boundary conditions did not, however, affect simulated salinities as much as changes in the resistance coefficient or changes in bathymetry. Adjustments to the salinity-boundary conditions only slightly increased or decreased simulated salinities at RB; there was no change in the longer term temporal patterns. This suggests that (1) simulations within the model domain are relatively insensitive to reasonable adjustments in the time-invariant salinity-boundary conditions; and (2) improvements in salinity simulations, particularly seaward of the shoreline, require data on temporal variations in salinity along the model boundary.

As previously noted, bottom elevations for the computational grid near the shore were estimated from navigation charts, because digital data were unavailable for these shallow areas. The results of these sensitivity tests indicate the need for accurate bathymetric data, particularly in these nearshore shallow regions where tides, flow, and salinity are strongly affected by bathymetry.

As an example of model application, each 15-minute value of net streamflow at AGR was reduced by 5 percent, and these reduced net flows were added back to the tidal flows (difference between measured flow and net flow) to create a new boundary condition at AGR. Salinities were subsequently simulated for June 2000 (following a 1-month model spin-up period) and compared with salinities simulated using the measured flow AGR boundary condition. A 5-percent net flow reduction for June 2000 amounted to an average decrease in flow of 5 m^3/s. Compared to the original simulation, top and bottom salinities at EP and EM were increased by an average of 0.4 psu for June 2000; WP top and WM bottom salinities increased by 0.5 psu, and the increase in the difference between top and bottom salinity ranged from 0.1 psu (EM) to 0.6 psu (WP). Additional simulations for a range of tidal and boundary salinity conditions would be required to develop a clear understanding of the effects of a change in flow on salinity in the Suwannee River estuary.

Some enhancements to the Suwannee River model might further improve simulations of flow and salinity in the lower Suwannee River and Suwannee Sound. Improvements in the quality of bathymetric data for the river and sound are important for accurate simulation of salinity and flow, as tidal fluctuations are strongly affected by bathymetry. The computational grid could be refined to provide greater resolution in Suwannee Sound, but such refinement would depend on better bathymetric data, and computer run times would increase as the number of computational cells increased.

Additional improvements in simulations, particularly in Suwannee Sound, require time-varying data on salinity at several (2–5) locations along the model boundaries. In addition, data on ground-water discharge to the river and freshwater flow from the small tidal creeks draining to the Gulf of Mexico in the model domain would be useful. Finally, inclusion of the saltmarsh area east of East Pass and south of the AGR gage should improve flow and salinity simulations, as well as provide insight into the functioning of the saltmarsh.

References Cited

American Public Health Association, American Water Works Association, and Water Environment Federation, 1992, Standard methods for the examination of water and wastewater (18th ed.): Washington, D.C., American Public Health Association, American Water Works Association, and Water Environment Federation, 981 p.

Berndt, M.P., Hatzell, H.H., Crandall, C.A., Turtora, M., Pittman, J.R., and Oaksford, E.T., 1998, Water quality in the Georgia-Florida Coastal Plain, Georgia and Florida, 1992–96: U.S. Geological Survey Circular 1151, 34 p.

Bledsoe, E.L., 1998, Phytoplankton dynamics and community structure in the Suwannee River estuary, USA: Gainesville, Fla., University of Florida, unpublished M.S. thesis, 77 p.

Boyer, J.N., Gourqurean, J.W., and Jones, R.D., 1999, Seasonal and long-term trends in the water quality of Florida Bay (1989–1997): Estuaries, v. 22, p. 417–430.

Bradley, P.M., Kjerfve, B., and Morris, J.T., 1990, Rediversion salinity change in Cooper River, South Carolina: Ecological implications: Estuaries, v. 13, p. 372–379.

Cable, J.E., Burnett, W.C., Chanton, J.P., and Weatherly, G.L, 1996, Estimating groundwater discharge into the Gulf of Mexico using radon-222: Earth and Planetary Science Letters, v. 144, p. 591–604.

Cable, J.E., Burnett, W.C., and Chanton, J.P, 1997, Magnitude and variations of groundwater seepage along a Florida marine shoreline: Biogeochemistry, v. 38, p. 189–205.

Clewell, A.F., Beaman, R.S., Coultas, C.L., and Lasley, M.E., 1999, Suwannee River tidal marsh vegetation and its response to external variables and endogenous community processes: Quincy, Fla., Report submitted to Suwannee River Water Management District by A.F. Clewell, Inc., 119 p. plus appendices.

Craig, P.M., 2004, User's manual for EFDC_Explorer: A pre/post processor for the Environmental Fluid Dynamics Code: Knoxville, Tenn., Dynamic Solutions, LLC, version 040415.

de Vries, M.P., and Weiss, L.A., 2001, Salt-front movement in the Hudson River estuary, New York—Simulations by one-dimensional flow and solute-transport models: U.S. Geological Survey Water-Resources Investigations Report 99-4024, 69 p.

Dijkzeul, J.C.M., 1984, Tide filters: Journal of Hydraulic Engineering, v. 110, no. 7, p. 981-987.

Friedrichs, C.T., and Aubrey, D.G., 1988, Non-linear tidal distortion in shallow well-mixed estuaries: A synthesis: Estuarine, Coastal and Shelf Science, v. 27, p. 52–545.

Galperin, B., Kantha, L.H., Hassid, S., and Rosati, A., 1988, A quasi-equilibrium turbulent energy model for geophysical flows: Journal of Atmospheric Science, v. 45, p. 55–62.

Godin, G., 1972, The analysis of tides: Toronto, University of Toronto Press, 264 p.

Goodwin, C.R., 1987, Tidal-flow, circulation, and flushing changes caused by dredge and fill in Tampa Bay, Florida: U.S. Geological Survey Water-Supply Paper 2282, 88 p.

Hammett, K.M., 1992, Physical processes, salinity characteristics, and potential salinity changes due to freshwater withdrawals in the tidal Myakka River, Florida: U.S. Geological Survey Water-resources Investigations Report 90-4054, 20 p.

Hamrick, J.M., 1992, A three-dimensional Environmental Fluid Dynamics computer Code: Theoretical and computational aspects: Gloucester, Va., The College of William and Mary, Virginia Institute of Marine Science, Special Report 317, 63 p.

Huang, W., and Foo, S., 2002, Neural network modeling of salinity variation in Apalachicola River: Water Research, v. 36, p. 356–362.

Huang, W., and Spaulding, M., 2002, Modeling residence-time response to freshwater input in Apalachicola Bay, Florida, USA: Hydrological Processes, v. 16, p. 3051–3064.

Ji, Z.-G., Morton, M.R., and Hamrick, J.M., 2001, Wetting and drying simulation of estuarine processes: Estuarine, Coastal and Shelf Science, v. 53, p. 683–700.

Jin, K.-R., Ji, Z.-G., and Hamrick, J.H., 2002, Modeling winter circulation in Lake Okeechobee, Florida: Journal of Waterway, Port, Coastal, and Ocean Engineering, v. 128, no. 3, p. 114–125.

Jin, K.-R., Ji, Z.-G., Hamrick, J.H., and Tisdale, T., 2000, Application of a three-dimensional hydrodynamic model for Lake Okeechobee: Journnal of Hydraulic Engineering, v. 126, no. 10, p. 758–771.

Johannes, R.E., and Hearn, C.J., 1985, The effect of subsurface groundwater discharge on nutrient and salinity regimes in a coastal lagoon off Perth Australia: Estuarine, Coastal, and Shelf Science, v. 21, p. 789–800.

Kjerfve, B., Schettini, C., Knoppers, B., Lessa, G., and Ferreira, H., 1996, Hydrology and salt balance in a large, hypersaline coastal lagoon: Lagoa de Aratuama, Brazil: Estuarine, Coastal, and Shelf Science, v. 42, p. 701–725.

Knowles, N., 2002, Natural and management influences on freshwater inflows and salinity in the San Francisco Estuary at monthly to interannual scales: Water Resources Research, v. 38, no. 12, 1289, doi:10.1029/2001WR000360.

Kurup, G.R., Hamilton, D.P., and Patterson, J.C., 1998, Modeling the effect of seasonal flow variations on the position of salt wedge in a microtidal estuary: Estuarine, Coast, and Shelf Science, v. 47, p. 191–208.

Leadon, C.J., 1979, Environmental effects of river flows and levels in the Suwannee River subbasin below Wilcox and the Suwannee River estuary, Florida: Live Oak, Fla., Suwannee River Water Management District, Interim Report, 152 p.

Lepage, S., and Ingram, R.G., 1986, Salinity intrusion in the Eastmain River estuary following a major reduction of freshwater input: Journal of Geophysical Research, v. 91, p. 909–915.

Light, H.M., Darst, M.R., Lewis, L.J., and Howell, D.A., 2002, Hydrology, vegetation, and soils of riverine and tidal floodplain forests of the lower Suwannee River, Florida, and potential impacts of flow reductions: U.S. Geological Survey Professional Paper 1656-A, 124 p.

Luettich, R.A., Westerink, J.J., and Scheffner, N.W., 1992, ADCIRC: An advanced three-dimensional circulation model for shelves, coasts, and estuaries, Report 1—Theory and methodology of ADCIRC-2DDI and ADCIRC-3DL: Vicksburg, Miss., U.S. Army Engineer Waterways Experiment Station, Technical Report DRP–92–6, 141 p.

Mattson, R.A., and Krummrich, J., 1995, Determination of salinity distributions in the upper Suwannee River estuary: Live Oak, Fla., Florida Game and Fresh Water Fish Commission and Suwannee River Water Management District, 63 p.

Mattson, R.A., and Rowan, M.E., 1989, The Suwannee River estuary: An overview and research and management needs, *in* Davis, F.E., ed., Water: Laws and Management: Betheseda, Md., American Water Resources Association, p. 14B17–14B31.

Mellor, G.L., Oey, L.-Y., and Ezer, T., 1998, Sigma coordinate pressure gradient errors and the seamount problem: Journal of Atmospheric and Oceanic Technology, v. 15, p. 1122–1131.

Mellor, G.L., and Yamada, T., 1982, Development of a turbulence closure model for geophysical fluid problems: Reviews of Geophysics and Space Physics, v. 20, p. 851–875.

Miller, R.L., Bradford, W.L., and Peters, N.E. 1988, Specific conductance: Theoretical considerations and application to analytical quality control: U.S. Geological Survey Water-Supply Paper 2311, 16 p.

Morlock, S.E., Nguyen, H.T., and Ross, J.H., 2002, Feasibility of acoustic Doppler velocity meters for production of discharge records from U.S. Geological Survey streamflow-gaging stations: U.S. Geological Survey Water-Resources Investigations Report 01-4157, 56 p.

Moustafa, M.Z., and Hamrick, J.M., 1993, Modeling circulation and salinity transport in the Indian River Lagoon, *in* Spaulding, M.L., Bedford, K., Blumberg, A., Cheng, R., and Swanson, C., eds., Estuarine and Coastal Modeling III: New York, American Society of Civil Engineers, p. 381–395.

Mukai, A.Y., Westerink, J.J., and Luettich, R.A., 2001, Guidelines for using East Coast 2001 database of tidal constituents within Western North Atlantic Ocean, Gulf of Mexico, and Caribbean: Vicksburg, Miss., U.S. Army Engineer Research and Development Center, Coastal and Hydraulics Engineering Technical Note CHETN-IV-40, 20 p., accessed February 11, 2003, at http://chl.erdc.usace.army.mil/library/publications/chetn/pdf/chetn-iv-40.pdf

National Buoy Data Center, 2003a, Station KTNF1–Keaton Beach, FL: National Oceanic and Atmospheric Administration, accessed May 19, 2003, at http://ndbc.noaa.gov/station_page.phtml?station=KTNF1

National Buoy Data Center, 2003b, Station CDRF1–Cedar Key, FL: National Oceanic and Atmospheric Administration, accessed May 19, 2003, at http://www.ndbc.noaa.gov/station_history.phtml?station=CDRF1

National Geophysical Data Center, 2004, GEODAS Software for Windows, Xwindows and Macintosh OS-X: accessed on August 12, 2004 at http://www.ngdc.noaa.gov/mgg/gdas/gx_announce.html

National Ocean Service, 1985, National estuarine inventory data atlas. Volume 1: Physical and hydrologic characteristics: Washington , D.C., National Oceanic and Atmospheric Administration, variously paged.

National Ocean Service, 2004, Water level tidal predictions: accessed on November 16, 2004, at http://co-ops.nos.noaa.gov/tides04/

National Oceanic and Atmospheric Administration, 1998, Crystal River to Horseshoe Point Navigation Chart: Washington, D.C., National Ocean Service, Chart No. 11408, 1 p.

National Oceanic and Atmospheric Administration, 2001a, National Geophysical Data Center Shoreline/Coastline Data, accessed September 7, 2001, at http://www.ngdc.noaa.gov/mgg/shorelines/shorelines.html

National Oceanic and Atmospheric Administration, 2001b, National Geophysical Data Center Hydrographic Survey Data, accessed September 7, 2001, at http://www.ngdc.noaa.gov/mgg/bathymetry/hydro.html

National Oceanic and Atmospheric Administration, 2003, Station information for Cedar Key, FL: National Ocean Service, Center for Operational Oceanographic Products and Services, accessed May 19, 2003, at http://www.co-ops.nos.noaa.gov/cgi-bin/station_info.cgi?stn=8727520+CEDAR+KEY,+GULF+OF+MEXICO+,+FL

Orlando, S.P., Jr., Rozas, L.P., Ward, G.H., and Klein, C.J., 1993, Salinity characteristics of Gulf of Mexico estuaries: Silver Springs, Md., National Oceanic and Atmospheric Administration, Office of Ocean Resources Conservation and Assessment, 209 p.

Paul, J.F., 1993, Observations related to the use of the sigma coordinate transformation for estuarine and coastal modeling studies, *in* Spaulding, M.L., Bedford, K., Blumberg, A., Cheng, R., and Swanson, C., eds., Estuarine and Coastal Modeling III: New York, American Society of Civil Engineers, p. 336-350.

Pawlowicz, R., Beardsley, B., and Lentz, S., 2002, Classical tidal harmonic analysis including error estimates in MATLAB using T_TIDE: Computers & Geosciences, v. 28, p. 929–937.

Rosenau, J.C., Faulkner, G.L., Hendry, C.W., and Hull, R.W., 1998, Springs of Florida, U.S. Geological Survey Geological Bulletin 31, revised, accessed November 8, 2004, at http://www.flmnh.ufl.edu/springs_of_florida/content.html

Rutkowski, C.M., Burnett, W.C., Iverson, R.L., and Chanton, J.P., 1999, The effects of ground water seepage on nutrient delivery and seagrass distribution in the northeastern Gulf of Mexico: Estuaries, v. 22, p. 1033–1040.

Siegel, E.M., Weisberg, R.H., Donovan, J.C., and Cole, R.D., 1996, Physical factors affecting salinity intrusions in wetlands: The Suwannee River estuary: St. Petersburg, Fla., University of South Florida, Department of Marine Science, 127 p.

Simpson, M., 2002, Discharge measurements using a broadband acoustic Doppler current profiler: U.S. Geological Survey Open-File Report 01-01, 123 p.

Speer, P.E., and Aubrey, D.G., 1985, A study of non-linear tidal propagation in shallow inlet/estuarine systems, part II: Theory: Estuarine, Coastal, and Shelf Science, v. 21, p. 207–234.

Suscy, P., and Morris, F.W., 1998, Proposed discharge limit for Turkey Creek, Brevard County, for maintaining a desirable salinity regime in Indian River Lagoon: Palatka, Fla., St. Johns River Water Management District, Technical Memorandum no. 26, 174 p.

Tanaguchi, M., Burnett, W.C., Cable, J.E., and Turner, J.V., 2002, Investigation of submarine groundwater discharge: Hydrological Processes, v. 16, p. 2115–2129.

Tetra Tech, Inc., 2003, Florida Bay hydrodynamic and salinity model analysis: Fairfax, Va., prepared for South Florida Water Management District, 91 p.

Tillis, G.M., 2000, Flow and salinity characteristics of the upper Suwannee River Estuary, Florida: U.S. Geological Survey Water-Resources Investigations Report 99-4268, 40 p.

U.S. Environmental Protection Agency, 1999, The ecological condition of estuaries in the Gulf of Mexico: Gulf Breeze, Fla., National Health and Environmental Effects Research Laboratory, Report no. EPA 620-R-98-004, 71 p.

U.S. Environmental Protection Agency, 2004, Watershed & water quality modeling technical support center, accessed September 30, 2004, at http://www.epa.gov/athens/wwqtsc/index.html

Wagner, R.J., Mattraw, H.C., Ritz, G.F., and Smith, B.A., 2000, Guidelines and standard procedures for continuous water-quality monitors: Site selection, field operation, calibration, record computation, and reporting: U.S. Geological Survey Water-Resources Investigations Report 00-4252, 53 p.

Walters, R.A., and Heston, C., 1982, Removing tidal-period variations from time-series data using low-pass digital filters: Journal of Physical Oceanography, v. 12, p. 112–115.

Walton, R., Shock, K., and Swarmer, R., 1998, Review of 3-D hydrodynamic and contaminant transport models in Water Resources Engineering 98: New York, American Society of Civil Engineers, p. 1120–1125.

Westerink, J.J., and Luettich, R.A., and Muccino, J.C., 1994, Modeling tides in the western North Atlantic using unstructured graded grids: Tellus, v. 46A, p. 178–199.

Wilde, F.D., Radtke, D.B., Kurklin, J.K., White, A.F., Davis, J.V., Busenberg, E., Nordstrom, D.K., Rounds, S.A., and Gibs, J., 1998, Field measurements, *in* National field manual for the collection of water-quality data: U.S. Geological Survey Techniques of Water-Resources Investigations, book 9, chap. A6, accessed May 19, 2003, at http://pubs.water.usgs.gov/twir9A6